A Generalized Optimal Planning Platform for Microgrids of Remote Communities Considering Frequency and Voltage Regulation Constraints

by

Elham Karimi

A thesis
presented to the University of Waterloo
in fulfillment of the
requirement for the degree of
Doctor of Philosophy
in
Electrical and Computer Engineering

Waterloo, Ontario, Canada

Examining Committee Membership

The following served on the Examining Committee for this thesis. The decision of the Examining Committee is by majority vote.

External Examiner	Bala Venkatesh Professor, Electrical and Computer Engineering
Supervisor	Mehrdad Kazerani Professor, Electrical and Computer Engineering
Internal Member	Claudio Canizares Professor, Electrical and Computer Engineering
Internal Member	Kankar Bhattacharya Professor, Electrical and Computer Engineering
Internal-external Member	Paul Parker Professor, Geography and Environment Management

I hereby declare that I am the sole author of this thesis. This is a true copy of the thesis, including any required final revisions, as accepted by my examiners.

I understand that my thesis may be made electronically available to the public.

Abstract

Access to electricity is a key factor behind development and expansion of modern societies, and electric power systems are the backbone infrastructure for economic growth of nations and communities. However, more than a billion people all over the world have no or limited access to electricity and are deprived of basic services. Furthermore, there are many communities that rely on small-scale isolated microgrids to supply their electric power demands, and many challenges exist in keeping those microgrids operating. The cost of operating isolated microgrids is a major issue which impacts the availability of a proper power network in remote communities. Hence, many organizations, communities and governments around the world are looking into alternative options for electrification of remote communities by considering Renewable Energy (RE) resources, such as wind and solar power, and utilization of Energy Storage Systems (ESS).

This thesis investigates the feasibility of RE deployment in remote communities, by proposing a generalized optimal planning platform and conducting comprehensive simulation studies based on real measured data, and evaluates the impact of economic, technical and operation constraints on the planning of an isolated microgrid involving conventional generation, RE resources and ESS. This work suggests that further investigation should be made on the potential impacts of the integration of RE resource on systems operation constraints, such as frequency and voltage regulation, and the results justify the importance of such investigations. Detailed studies on the impact of operation constraints on the planning and sizing of the microgrid are performed. The impact of ESS on planning studies and its potential role in system operation are analyzed. Furthermore, the impact of RE integration on reduction of diesel generation and thus carbon footprint in remote communities is evaluated. The inclusion of a demand response management strategy in microgrid planning problem is considered and its impact on the integration of RE and ESS in remote communities is analyzed.

The proposed planning platform is applied to the microgrid of Kasabonika Lake First Nation (KLFN), a northern Ontario remote community. The results indicate that RE and ESS integration projects are achievable considering alternative incentives and funding resources. It is also shown that frequency regulation constraints have remarkable impact on the sizing of the RE units and ESS. A sensitivity analysis is also performed in order to study the effect of variable parameters on the optimal design of the microgrid at KLFN.

Acknowledgments

I would like to thank my supervisor Prof. Mehrdad Kazerani for his support during all stages of this research. I cannot thank him enough for his excellent mentorship and encouragement and advice over the past few years. I would also like to thank my PhD examination committee members: Prof. Canizares, Prof. Bhattacharya and Prof. Parker from University of Waterloo and Prof. Venkatesh from Ryerson University for their invaluable comments and feedback on my research. This work was supported by Hatch Ltd. through a Natural Resources Canada ecoEnergy II Project.

This research would not be possible without all the discussions with my colleagues and friends at University of Waterloo. I would like to thank Zuher Al-Nasir, Mariano Arriaga, Marten Pape, Mahmoud Allam, Mauricio Restrepo, Ahmad Abuaish and Talal Alharbi for kindly providing their feedback on various research topics and helping with improvement and advancement of this work.

I am also grateful for the good friends that I met along the way in Waterloo, for having them to share my happiest and darkest moments and for helping me to follow this journey. I would like to thank them all for supporting me endlessly.

Dedication

This thesis is dedicated to my parents, Fatemeh and Rajabali.

Table of Contents

List of Figures

List of Tables

List of Abbreviations

AANDC	Aboriginal Affairs and Northern Development Canada
AGC	Automatic Generation Control
AMPL	A Mathematical Programming Language
AVR	Automatic Voltage Regulator
BARON	Branch-And-Reduce Optimization
CHP	Compressed Heat and Power
DER	Distributed Energy Resources
DFT	Discrete Fourier Transform
DG	Distributed Generation
DICOPT	Discrete and Continuous OPTimizer
DIRECT	DIviding RECTangles
DNLP	Discontinuous Derivative Non-Linear Programming
DRM	Demand Response Management
DSM	Demand Side Management
EA	Evolutionary Algorithm
EENS	Energy Expected Not Supplied
EIR	Index of Reliability
EMS	Energy Management System
ESS	Energy Storage System
EV	Electric Vehicle
GA	Genetic Algorithm
GAMS	General Algebraic Modeling System

GDP	Gross Domestic Product
GHG	GreenHouse Gas
HESS	Hybrid Energy Storage System
HOGA	Hybrid Optimization by Genetic Algorithms
HOMER	Hybrid Optimization Model for Energy Resources
HORCI	Hydro One Remote Communities Inc.
IDFT	Inverse Discrete Fourier Transform
INAC	Indigenous and Northern Affairs Canada
IP	Integer Programming
IPA	Independent Power Authority
IRR	Internal Rate of Return
KLFN	Kasabonika Lake First Nation
LFC	Load Frequency Control
LOC	Loss of Capacity
LP	Linear Programming
LPSP	Loss of Power Supply Probability
LR	Load Restriction
LTRGP	Long-Term Renewable Generation Planning
MATLAB	MATrix LABoratory
MILP	Mixed Integer Linear Programming
MINLP	Mixed Integer Non-Linear Programming
MIP	Mixed Integer Programming
NLP	Non-Linear Programming
NPC	Net Present Cost
NPV	Net Present Value
NSGA-II	Non-dominated Sorting Genetic Algorithm-II
O&M	Operation and Maintenance

OCV	Open Circuit Voltage
OPA	Ontario Power Authority
ORPP	Optimal Reactive Power Planning
PDF	Probability Distribution Function
PEV	Plug-in Electric Vehicle
PLL	Phase Locked Loop
PPA	Power Purchase Agreement
PS	Particle Swarm
PV	PhotoVoltaic
RE	Renewable Energy
RMINLP	Relaxed Mixed Integer Non-Linear Programming
RRRP	Rural or Remote Rate Protection
SMES	Superconducting Magnetic Energy Storage
SOC	State of Charge
SQP	Sequential Quadratic Programming
UC	Unit Commitment
VSI	Voltage Source Inverter

Nomenclature

Indices

h	Index for number of hours in a year
i	Index for customer type
k	Index for RE and ESS equipment type
t	Index for number of years

Parameters

$\Delta\omega_{allowed}$	Accepted frequency deviation
$\Delta\omega_{max}$	Maximum frequency deviation due to RE integration
$\Delta P_{RE,allowed}$	Accepted RE power fluctuation
$\Delta P_{RE,max}$	Maximum RE power fluctuation of optimal RE generation
η_{ch}	Charging efficiency of ESS (%)
η_{dis}	Discharging efficiency of ESS (%)
ω^*	No-load frequency
EPR^{max}	Maximum energy to power ratio of ESS
EPR^{min}	Minimum energy to power ratio of ESS
$M_{pen.}$	Maximum allowed RE penetration level

$N^{n}_{pen.}$	Ratio of the maximum allowed injected power at the point of connection of DERs to the microgrid to the maximum active power injected at each network bus, for every point of connection, n
$P_{rem_{k,t,h}}$	Active output power of each piece of RE equipment (kW)
SOC^{max}	Maximum state of charge of ESS (%)
SOC^{min}	Minimum state of charge of ESS (%)
α_i	Participation factor of i$^{\text{th}}$ DER
β_{fE}	Percentage of the energy capacity of ESS for frequency control (%)
β_{fP}	Percentage of the power capacity of ESS for frequency control (%)
τ_A	Time constant of the amplifier
τ_E	Time constant of the exciter
τ_G	Time constant of the generator
τ_g	Time constant of the governor
τ_R	Time constant of the sensor
τ_T	Time constant of the turbine
b_{cep}	Percentage of available capital contribution at the start of project (%)
b_{CFP_t}	Percentage of the purchased fuel by the utility from the community (%)
b_{efp}	Percentage of available external funding with respect to total project cost (%)
b_{om_t}	Cost variation during equipment's operating lifetime (%)
blt_k	Number of loan payments
C_{d_i}	Savings obtained by replacing fuel ($/kWh)
C_{energy}	ESS energy capacity cost ($/kWh)
C_{FUEL}	Actual price of fuel on-site ($/liter)

cc_d	RE equipment annual cost drop (%)
cce_d	ESS equipment annual cost drop (%)
CPI	Fuel price growth (%)
D	Load damping constant
d_{GS_1}	Nominal diesel generator power minus the spinning reserve when switching to the next bigger generator (%)
d_{GS_2}	Nominal diesel generator power minus the spinning reserve when switching to the next smaller generator (%)
d_{GSa_j}	Linear coefficient for consumption of fuel based on generated power for j^{th} diesel generator (liter/kW)
d_{GSb_j}	Constant coefficient for consumption of fuel based on generated power for j^{th} diesel generator (liter)
d_{GS}^{min}	Lower operation limit of the smallest available generator (%)
d_{gs}^{min}	Diesel generator operation lower limit (%)
$EINC_i$	Incentive for the reserved energy capacity of ESS for frequency control ($/kWh.year)
EXP_i	Power purchase agreement price ($/kWh)
H	Inertia of the rotating mass
INC_i	External energy incentive ($/kWh)
k_A	Amplifier gain
k_E	Exciter gain
k_G	Generator gain
k_I	Integral gain of PI controller
k_P	Proportional gain of PI controller
k_R	Sensor gain

L_k	Lifetime of equipment (years)
$m_{p,i}$	Frequency droop characteristic slope of i$^{\text{th}}$ DER
n_{br}	Total number of buses in the network
$n_{q,i}$	Voltage droop characteristic slope of i$^{\text{th}}$ DER
$p_{j,t}^{max}$	Pre-determined maximum operation set point of the diesel generator j (kW)
$p_{j,t}^{min}$	Pre-determined minimum operation set point of the diesel generator j (kW)
$PD_{i,t,h}$	Power demand of customer i (kW)
$PDG_{red.}$	Percentage of the maximum load demand provided by diesel generator (%)
$PINC_i$	Incentive for the reserved power capacity of ESS for frequency control ($/kW.year)
R	Droop of the governor
r_b	Bank interest rate (%)
r_{d_i}	Discount rate for customer i (%)
r_{FR}	Percentage revenue gained by the community as a result of selling fuel to the utility (%)
r_i	Annual price change (%)
rc_{cap_k}	Present equipment cost ($/kW)
rc_{om_k}	Present O&M cost ($/kW)
RP_j	Nominal power of the diesel generator j (kW)
rp_k	Equipment rated capacity (kW)
RP_t^{min}	Rated power of the smallest diesel generator (kW)
$RSCH$	The percentage of the maximum flexible load (%)
$s_{j,t}$	Binary parameter determining whether diesel generator j is operating in year t

V_i^*	No-load voltage at bus i
$VarOMC_i$	Variable O&M cost of energy storage ($/kWh)
X_s	Synchronous reactance of the synchronous machine

Variables

ω_s	Synchronous speed of synchronous generator (rad/s)
$\Delta\omega$	Synchronous generator speed change
$\Delta\omega_{ss}$	Change in steady state frequency
Δf	Frequency deviation from nominal value
ΔP_e	Deviation in generator electrical power
ΔP_g	Difference between the power set point, ΔP_{ref}, and the power $\frac{1}{R}\Delta\omega$, given by the governor speed characteristics
$\Delta P_{i,p}$	Change in the generation of i$^{\text{th}}$ DER right after primary frequency control takes place
$\Delta P_{i,sche.}$	Scheduled change in the power set point of i$^{\text{th}}$ DER
$\Delta P_{i,s}$	Deviation in the generation of i$^{\text{th}}$ DER right after secondary frequency control takes place
ΔP_{Load}	Non-sensitive load change
ΔP_L	Non-sensitive load change
ΔP_m	Deviation in generator mechanical power
ΔP_{RE}	Renewable output power change
ΔP_V	Change in the valve position
δ	Rotor angle
$\delta_i^{a,b,c}$	Phase angles of the three-phase voltages at bus i
$\phi_i^{a,b,c}$	Phase angles of the internally generated voltages of the synchronous machine

$\theta_{i,j}^{a(ph)}$	Phase angles of the branch admittances
$C_{bpmt_{i,k,t}}$	Bank loan periodic payment amount ($)
$C_{cap_{i,k,t}}$	Capital cost of equipment ($)
$C_{ce_{i,k,t}}$	Initial capital expenses paid by the community ($)
$C_{i,t}$	Project costs ($)
$C_{om_{i,k,t}}$	O&M cost ($)
$C_{rep._{i,k,t}}$	Replacement cost of equipment ($)
$CB_{i,k,t}$	Equipment price drop based on the number of purchased equipment pieces
$D\Delta\omega$	Frequency sensitive load change
$E_i^{a,b,c}$	Magnitudes of the internally generated voltages of the synchronous machine
$EES_{i,t}$	Cumulative ESS energy size
$Energy_{i,t,h}$	Available energy of ESS at each h (kWh)
$EOS_{i,k,t}$	Cumulative number of selected equipment pieces
$EOS_{i,k,t}^{*}$	Optimal sizes of the RE resources
$Esize_{i,t}$	Selected energy sizing of ESS (kWh)
f	System frequency (Hz)
f_{BASE_t}	Fuel consumption of the community before integration of RE resources (liter/year)
f_{max}	Maximum frequency (Hz)
f_{min}	Minimum frequency (Hz)
$f_{nom.}$	Nominal frequency (Hz)
f_{PROJ_t}	Fuel consumption of the community after integration of RE resources (liter/year)
$IS_{i,t}$	Income/Savings ($)

$LR_{i,t}$	Potential loss of opportunity cost ($)
$M_i(s)$	Transfer function of i$^{\text{th}}$ DER
$P_{dg_{j,t,h}}$	Diesel generator j power generation (kW)
$P_{dg_{t,h}}$	Diesel generator power generation (kW)
$P^{a,b,c}_{Gi,spec}$	Specified generated active powers at bus i for three-phases a,b and c
$P^{a,b,c}_{Gi}$	Generated active powers at bus i for three-phases a,b and c
$P^{a,b,c}_{i}$	Calculated injected active powers to bus i for three-phases a,b and c
$P^{a,b,c}_{Li}$	Load active power demand at bus i for three-phases a,b and c
$Pch_{i,t,h}$	Power charged to storage (kW)
$PDflex._{i,t,h}$	Flexible load component of the total load demand (kW)
$Pdis_{i,t,h}$	Power discharged from storage (kW)
$PDresch_{i,t,h}$	Rescheduled load profile after including flexible load (kW)
$Pdump_{t,h}$	Dump load (kW)
$Pex_{i,t,h}$	Power injected to microgrid (kW)
$Pimp_{i,t,h}$	Power purchased from microgrid (kW)
$Prea_{i,k,t,h}$	Available renewable power (kW)
$Prea^{*}_{i,k,t,h}$	Available renewable power, determined from the solution of the optimization problem (kW)
$Preu_{i,t,h}$	Renewable power used to supply the load (kW)
$Pstorage_{i,t,h}$	Power charged/discharged to/from ESS (kW)
$Q^{a,b,c}_{Gi,spec}$	Specified generated injected reactive powers at bus i for three-phases a,b and c
$Q^{a,b,c}_{Gi}$	Generated reactive powers at bus i for three-phases a,b and c

$Q_i^{a,b,c}$	Calculated injected reactive powers to bus i for three-phases a,b and c
$Q_{Li}^{a,b,c}$	Load reactive power demand at bus i for three-phases a,b and c
$V_{i,spec}^{a,b,c}$	Specified magnitudes of the three-phase voltages at bus i
$V_i^{a,b,c}$	Magnitudes of the three-phase voltages at bus i
V_{ref}	Reference voltage
V_t	Terminal voltage
$Wf_{i,t}$	Social welfare ($)
$x_{i,k,t}$	Integer variable representing selected number of equipment pieces
$Y_{i,j}^{a(ph)-n}$	Magnitudes of the branch admittances
$z_{i,t,h}$	Ratio of RE used for different customer types

Chapter 1

Introduction

1.1 Motivation and Relevance

Electricity, as one of the most flexible types of energy, has an important role in development of nations and communities; however, all over the world there are vast population living in communities with no access to electricity or with off-grid microgrids that generate electricity only using fossil fuel-based generators. According to [1], in north America, an off-grid/remote community is defined as: "Any community not currently connected to the North-American electrical grid nor to the piped natural gas network; and is a permanent or long-term (5 years or more) settlement with at least 10 dwellings."

The electric power generation costs in fossil fuel-based power plants are mainly dependent on fuel price, while in remote communities these costs also depend on many factors including the size of the generators, their operating conditions, their performance and efficiency and fuel transportation cost [1]. As a result, the cost of electricity generation from fuel-based generators in remote communities can be multiple times (up to ten times) higher than those on the main grid [1].

Over the past few decades, interest in using locally available Renewable Energy (RE) resources to reduce fuel consumption for electric power generation and increase the power generation capacity to supply the demand of the growing population in remote communities has increased significantly. The reason lies behind the potential economic and environmental benefits these RE resources can provide to the communities. High cost of electricity generation and environmental risks associated with fossil fuel, including local oil spills and greenhouse gas emissions, are among the reasons for expediting the integration

of renewable energy resources into the isolated microgrids of remote communities. The communities are also getting more insight into the potential benefits of renewable energy resources and (in the case of aboriginal people of northern Canada) compatibility of using these resources with their faith and traditional practices concerning preservation of nature and making use of locally available resources. Nevertheless, there exist many challenges and barriers for successful initiation and implementation of RE-based microgrid projects in remote communities.

Although, large-scale on-grid renewable energy projects have been installed successfully worldwide and also in Canada [2–4], remote community projects have been facing many obstacles [5], such as high capital and O&M costs, high technical risks, technology maturity [6], limited understanding of technical feasibility of integration of RE solutions and inadequate confidence in successful deployment of such systems [7].

In order to overcome some of the barriers and deal with the existing challenges, various courses of action can be taken. For example, programs that support the allocation of capital cost grants to help with the project initial investment or production incentives to encourage the operation and maintenance of the installed RE equipment can help to better address the economic challenges of the remote community RE integration projects [6]. The technical challenges involve various aspects of successful operation of the isolated microgrid after incorporation of RE resources, such as scheduling and dispatching the units under supply and demand uncertainty, reliable operation of the microgrid, development and implementation of voltage and frequency control techniques and various power quality and stability issues associated with the integration of distributed generation into the isolated microgrids [8]. In order to conquer some of these challenges, comprehensive studies must be conducted to evaluate the impact of integration of RE resources on technical aspects of the microgrid. These studies can help to better understand and clarify the technical issues of interconnecting distributed generation resources to the isolated microgrids. Consequently, solutions can be proposed to overcome these technical challenges and help to increase the confidence and clear the doubts on technical feasibility of remote community RE projects.

A thorough study on the planning and sizing of a microgrid is the foundation of a successful microgrid project, which investigates the feasibility of establishing a microgrid, determines the required numbers and types of resources, provides an overview of operational conditions of the system and evaluates the project objectives during its lifetime. Microgrid planning in remote communities requires special considerations regarding existing infrastructure, available resources, power system requirements and operation constraints. Thus, a microgrid planning platform that can determine the optimal unit sizes while considering some of the existing challenges and involving the community in the RE integration project is a step towards introducing the cost-effective and environmentally-friendly solutions for

electric power generation in remote communities. This thesis is motivated by the lack of a comprehensive planning model that not only determines the optimal unit sizes, but also includes the operation constraints of the system; i.e., frequency and voltage regulation constraints.

1.2 Literature Review

Over the past two decades, planning and sizing of small-scale microgrids using renewable energy resources have received significant attention from researchers, power industry and governments. The problem of finding the optimal combination of renewable and conventional resources have been the research focus for numerous individuals and organizations all over the world. The planning activities reported in the literature include selecting the planning problem objectives, defining the planning problem constraints, and implementing various problem solving methods.

The main planning objectives considered in the literature are minimizing the cost, minimizing the environmental impact and meeting certain reliability requirements. Depending on the application, each one of those objectives would be assigned a higher priority or a weighted combination of two or all of them would be considered.

Many researchers have used a list of available components and devices, examined the main objective for each of the existing combinations and selected the combination with the best outcome in terms of the desired objective. Another group of researchers have used mathematical optimization programming methods to formulate the planning problem as a linear, non-linear or mixed-integer problem and used different techniques to solve the problem. There has been a great interest in using heuristic algorithms such as Genetic Algorithm (GA), Particle Swarm (PS) and Evolutionary Algorithm (EA) for solving the aforementioned problem. Commercially available software packages such as HOMER, HYBRID2, HOGA and RETScreen, have also been helping researchers develop their planning problem or find a baseline to compare their results with. Furthermore, in some research endeavors, the intermittency issue of renewable resources such as wind and solar and the unpredictable nature of load demand and fuel prices have been considered as a source of uncertainty for developing stochastic or robust optimization problems.

The following literature review highlights some of the research in planning and sizing of isolated microgrids and discusses the methodologies used as well as their major shortcomings.

Microgrid Planning Considering Economic Objective

The economic perspective has been the main priority in most of the existing research with the goal of minimizing the cost of the system. The authors in [9–20] have considered the cost minimization as their main planning and system evaluation objective while considering different types of constraints, resources and different problem solving methods.

A small stand-alone microgrid including photovoltaic modules, wind turbines and battery energy storage system, supplying a residential household is studied in [9]. The number and type of photovoltaic (PV) modules, wind generators, installation height of the wind turbines, PV modules tilt angle and the battery type and nominal capacity are design variables in order to minimize the capital and maintenance cost of the system in a twenty year lifetime period. Genetic Algorithm is used to select the design parameters from a list of commercially available devices by evaluating different combinations that meet the energy balance constraint of the system and selecting the one with the lowest cost. The system operation is simulated for one year with one-hour time resolution and the O&M cost for 20 years are estimated based on the result of the one-year study. *The studied model considers a simple case and has limited applications as it only evaluates a number of different component combinations. The operation of such system in real-time can face various difficulties due to lack of back-up generation in case the operation of RE or storage units is interrupted.*

In [10], the authors investigate the application of Genetic Algorithm in optimization of a hybrid stand-alone system including solar photovoltaic modules, pico-hydro system, wind turbine, diesel generator and batteries. The main goal is to maximize the use of renewable resources and limit the use of diesel generator, while minimizing the net present value of the cost which consists of the capital cost, O&M cost, replacement cost and fuel cost. The optimal operation of system is defined as operating in cycle charging or load following modes. Sensitivity analysis is performed to evaluate the changes in systems design parameters due to considering different price ranges for the components. The mathematical models used in this study are similar to those used by HOMER, and HOMER is used as a baseline to compare the results. *Daily load demand is assumed constant during a year, the considered model is basic and fails to cover meteorological data and load demand variations all year long.*

The authors in [11–13] have developed a solar-wind-battery system to supply a telecommunication relay station by ensuring minimum equivalent annual cost of the system, while making sure that the specified Loss of Power Supply Probability (LPSP) constraint is satisfied. The decision variables defined in a Genetic Algorithm optimization are the PV module number and tilt angle, wind turbine number and installation height, and battery

capacity. *The application is limited to a constant load for a small telecommunication relay station and specific type of equipment.*

Performance of two meta-heuristic methods, Simulated Annealing and Tabu Search, in designing a stand-alone wind-PV-diesel-bio diesel-fuel cell-battery is investigated in [14]. Different types of constraints are considered in this study such as initial cost constraints, unmet load constraints, capacity shortage constraints, fuel consumption constraints, minimum renewable fraction constraint and component size constraints, with load following and cycle charging selected as the operating strategies. Different alternative scenarios are analyzed to study the performance of the designed system in the presence of uncertain variables such as wind speed, load demand and fuel prices. *However, the role and operation scheme of bio-diesel and fuel-cell and their difference with diesel generator and battery are not discussed properly.*

In [15], a diesel generator sizing approach for a stand-alone wind-diesel system is developed and analyzed. The study is done on an existing microgrid in Ramea Island in Newfoundland, Canada, with a peak demand of 1.2 MW. At the time of the study, there were three parallel equal-capacity diesel generators (925 kW each) and six 65 kW wind turbines operating in the island. The goal of the study is to analyze and evaluate the feasibility of installing smaller engines to reduce possibility of partial loading of the generators during light-load conditions in order to maximize total wind contribution of the system and also minimize the number of diesel on/off cycling. The daily and monthly performances of the network under different wind and load profiles are investigated by incorporating an energy flow and dynamic power flow model. *The methodology has limited application as it is focused on one system with fixed RE resources and does not offer a general methodology. Furthermore, the impact of fluctuating and rapid ramping of wind power on the operation of the diesel generators is neglected.*

In [16], a forward-looking dispatch of a microgrid for planning of energy storage and optimal sizing of components is addressed. The study presents a novel approach for solving the optimal design problem and the dispatch strategy using a moving time horizon to couple the operation of the microgrid before and after each window of time. The interaction of Plug-in Electric Vehicles (PEVs) is included by considering time variant connection of components. A hub-based microgrid model is implemented in MATLAB by separating the microgrid into a network of power conversion and storage hubs, where the hubs contain energy storage and conversion devices. The optimal dispatch problem which is formulated as a series of optimization problems solved over a moving-time window is nested within the optimal design problem. The optimal design problem sends a set of design variables to the optimal dispatch problem and the optimal dispatch problem is solved over a 24-hour time horizon and steps forward one hour until the end of the desired time period. The vector of

optimal dispatch solution for the first time step of each time horizon is saved in a matrix and returned to the optimal design problem; the total fuel use and the feasibility information of the optimal dispatch problem are also passed to the design problem. A non-linear programming algorithm, known as Sequential Quadratic Programming (SQP), is used to solve the optimal dispatch problem; the optimal design problem is solved using DIRECT derivative-free algorithm. A case study is implemented to evaluate the proposed approach, in which a PV-diesel-battery-PEV system is considered to supply a small military forward operating base in Afghanistan. The daily load power demand is considered as a base load with an afternoon peak and night time trough; the solar irradiance data is taken from HOMER. The optimization problem aims to find the optimal sizes of Distributed Energy Resource (DER) components, dispatch of DER components and number of vehicles at each time step by minimizing the implementation and operating cost of the microgrid. The results of the simulation are compared with those of HOMER. The authors concluded that the fuel use was reduced by 3-30% by using renewables and storage. *The major shortcoming of the proposed method is that it results in a computationally complicated problem, making it practically impossible to solve for longer periods of time. The optimal dispatch problem is solved only for 3 days in the middle of each month of the year for four different designs and the fuel consumption was estimated based on those simulated days. The study does not consider other types of renewable resources, actual measured data and the uncertainties in load demand and renewables which are very important in military applications and would highly impact the reliability of the system.*

The authors in [17] used the forward-looking strategy introduced in [16] for coupling between sizing and operation and regulation capabilities in microgrids. A stand-alone military base including solar panels and electric vehicles is considered to investigate the impact of battery DC voltage variations on a decentralized regulation scheme. A framework is created in which the sizing, dispatch and regulation problems are optimally solved in a nested manner. The iterative process starts by component sizing with regards to the optimal dispatch and then the solution of the sizing and dispatch problem defines the regulation problem. The solution of the regulation problem adds new design constraints to the optimal component sizing problem. The sizing problem optimizes the sizes of the solar panels, batteries and generators and uses the forward-looking dispatch strategy to define the power dispatch of the components over a one-year period. The objective is to minimize the annual capital and fuel costs. For the regulation problem the system is modeled using the dynamic equations of the inverter by regulating the terminal voltage through adjusting the modulation index; to track the AC voltage waveform, a Phase Locked Loop (PLL) is used. The grid is modeled as a 4-bus network, using the phasor representation of the power flow equations and the loads are considered constant, as they are assumed to be

critical loads and need to be supplied continuously. The battery is modeled as a voltage source with an internal resistance. An instantaneous drop in PV generation is simulated to investigate its impact on regulation; this sudden drop in PV power is compensated for by battery which will cause a big voltage drop across its resistance and will decrease the battery terminal voltage. As a result, even though the battery is capable of providing the required power, it cannot maintain the terminal voltage within specified limits. The conclusion is that regulation problems might happen if the battery is not sized according to the regulatory constraints and the number of battery cells in series and parallel should be revised to keep the battery internal resistance below certain limit. *However, the dynamics of the battery is overlooked in this study, as the terminal voltage is dependent on the battery State of Charge (SOC) as well, and different battery types have different Open Circuit Voltage (OCV)-SOC characteristics. The proposed method considers a very small network for a specific application and can not be expanded to larger-scale applications such as remote communities. The methodology only considers a few instances in time which are assumed to be the worst case, considers a constant load, requires considering a PLL in formulations and does not discuss the impact of sizing on frequency regulation. It has a specific application which is the military, with high reliability requirements which makes the microgrid design very conservative. It also fails to cover some specific issues related to deployment of RE systems in remote locations such as meteorological data uncertainty which seems to be very important for the studied applications (i.e., a military base).*

The authors in [18] have used a method for coordinated sizing of ESS and diesel generators in a stand-alone microgrid using a Discrete Fourier Transform (DFT). Since diesel generator and ESS have different response characteristics, a DFT-based dispatch strategy is used to compensate for the generation demand imbalances at different time scales. In this scheme, the diesel generators can supply the base demand, while ESS compensates for the small and frequent power fluctuations. This method can also be used in the planning of ESS with other types of dispatchable units such as micro-turbines or fuel-cells. In order to consider the fluctuating nature of the RE resources, which the historic data with low resolution is not capable of reflecting, the DFT-based method is proposed to share the power between ESS and diesel generators according to their response characteristics. The proposed method sizes ESS and diesel generators to balance the capital cost and fuel cost, and allocates the power between them by analyzing the spectrum of power. According to the spectrum results, the frequency bands of ESS and diesel generators are determined and the frequency domain results are transformed to time domain signals using the Inverse Discrete Fourier Transform (IDFT) and the assigned powers of diesel generators and ESS are acquired. Since diesel generators have a relatively low response speed, the low-frequency band of the power fluctuation is supplied by diesel generators and the high-frequency com-

ponent is provided by ESS which has a fast response. The proposed method is used to design ESS and diesel generator capacities in a small stand-alone wind-PV-diesel-storage system to supply the load demand of a small island in East-China Sea using the wind power data and load profile with 1-min time resolution. The proposed method is compared with a GA-based optimization technique implementing load following strategy, showing that the proposed method results in a higher ESS capacity and a lower diesel generator capacity. *This method can be very useful in evaluating the impact of renewables in frequency regulation of the microgrid which is not covered in this study. Furthermore, this study only considers the sizing of diesel generator and ESS; however, expansion of this work to include the sizing of various RE resources can add more value to the methodology.*

A long-term renewable generation planning model considering the characteristics of diesel-based remote communities in Canada is presented in [19]. The author implemented a multiple year community planning tool to consider feasible RE solutions in remote communities of Canada using the current operating structure, electricity pricing system, subsidy framework and project funding alternatives. A stand-alone PV-wind-diesel system is designed for supplying the load demand of a remote community in northern Ontario. It is argued that battery energy storage in not a viable option to implement in the studied community due to several challenges such as thermal management, capital cost and O&M costs. In the proposed model, four different stages are recognized: (i) including the input data stage, to gather all the required information such as historical data for natural resources, energy related information and RE equipment specifications; (ii) the forecast stage, to create time series of estimated electric load and RE resources; (iii) the pre-processing stage, to consider the dispatch strategy, pre-set configuration details and overall costs; and (iv) the solution stage, to solve a Mixed Integer Non-Linear Programming (MINLP) problem in MATLAB using the Genetic Algorithm, to maximize the RE planning social welfare for the community. The community's social welfare is defined as the direct income and/or savings from deploying RE equipment minus direct community economic losses as a consequence of RE deployment and the associated project costs through the project planning horizon, such as initial capital cost, loan repayments and O&M costs. Several scenarios are studied and the economic feasibility of each scenario is evaluated by the combined result of Net Present Value (NPV) and the Internal Rate of Return (IRR). Different scenarios consider different schemes, such as funding the project by a single stakeholder, incorporating a loan alternative to finance the project, or using government funding, different discount rates, different annual growth rates and fuel cost growth rates, and increase or decrease in the annual average wind speed and solar irradiation levels. The author concludes that with the proposed model, deploying and operating wind and solar resources could be feasible by obtaining realistic plans, while introducing economic benefits to the community and to the

government agencies that support such projects. *Although the work reported in [19] has valuable contributions, it could be improved by taking into account the integration of ESS and also system operation constraints such as voltage and frequency regulation constraints, as voltage and frequency regulation of the isolated microgrid can be impacted by integration of RE resources.*

A Particle Swarm algorithm is used in [20] to get the optimal configuration of RE and battery units as well as controllable loads in an isolated microgrid. The objective is to maximize the annual profit of the network through maximizing the use of RE resources. The planning model is sub-divided into demand expansion, capacity optimization and operation optimization levels. The maximum possible load demand that can be supplied by the microgrid is determined in the demand expansion level. The optimal capacity of the generation and storage units, as well as the configuration of the controllable loads, are determined in the capacity optimization level. In the operation optimization level, the operation of the microgrid is modeled and solved. A case study on an isolated microgrid in Weizhou Island in Guangxi province, China, is performed to examine the three-level model and also to demonstrate the impact of controllable loads on the objective function. *The operation of such isolated microgrid in the absence of a back-up generation such as diesel generator units can face several challenges including service interruption and poor power quality. Considering these challenges in the planning of the isolated microgrids can help to expand the scope of the work to more realistic cases.*

Microgrid Planning Considering Multiple Objectives

A chance-constrained programming model is presented in [21]. A stand-alone microgrid system with diesel-wind-PV-battery is considered for simultaneously minimizing the total Net Present Cost (NPC) and carbon emission during the systems lifetime. NSGA-II, a multi-objective evolutionary algorithm is adopted to solve the problem by considering a constraint which allows the program to meet LOC (Loss of Capacity, which indicates the ratio of capacity shortage to the load demand) with a certain confidence level. In this study, the probability of having LOC smaller or equal to 0.01 is assumed to be larger than 80%. Since the two objectives, i.e., cost minimization and emission reduction, are in conflict with each other, the authors presented the pareto front of the optimal planning problem and compared the pareto fronts for cases with and without chance-constrained problems. *The solution of the optimal planning model indicates higher RE generation levels compared to diesel generators. The operation of such system in its lifetime could undergo difficulties with regards to regulation of frequency and voltage and should be addressed during planning process.*

The authors in [22] developed an optimal sizing and operating strategy for a stand-alone microgrid in Dongfushan Island, China, including wind, PV, diesel and battery storage units. Genetic Algorithm is used to minimize the system life-cycle cost, maximize the RE penetration and minimize the pollutant emissions. The mentioned microgrid is equipped with a real-time control strategy for the management of the resources in the system. The operation modes of the system are mainly determined according to different levels of battery SOC. The multi-objective optimization is formulated as a single-objective optimization by using a weighted sum of single objectives. The authors conclude that the proposed method improves the RE generation utilization and the operation life of batteries by maximizing RE production. *The method does not consider the impact of RE deployment in remote microgrids such as the impact on frequency of the microgrid.*

The authors in [23] have studied a stand-alone PV-wind-diesel system which supplies two different types of load profiles, a farm load (40.9 kWh in 1 day) and a heavy load (120kWh in 1 day). The objective is to minimize the total cost (capital, maintenance and fuel cost) of the system during planning horizon and the pollutant emission. Genetic Algorithm is used to solve the multi-objective design problem. For the operation of the system, load following and cycle charging strategies are considered. It is evident that the capital cost of the system will be lower when more diesel generation is considered, while the greenhouse gas emissions would be higher; so, in order to solve the problem, a set of RE configurations are introduced and the solution can be selected depending on the trade-off between the objective functions. This study is further expanded in [24] and [25] to include unmet load as an objective and to add battery and hydrogen-fuel-cell units, respectively. *The study considers constant daily load profiles, does not provide a clear solution to the multi-objective design problem and is limited to a specific system.*

A multi-objective optimization model is used in [26] to minimize the system cost, minimize the loss of power supply probability and maximize the utilization of RE resources. The NSGA-II algorithm is applied for solving the optimization problem. A wind-PV-battery-diesel combination is considered to provide the demand of an islanded microgrid on Dong'ao Island in China. The operation of the generation units is controlled based on a dynamic strategy which determines whether the battery or the diesel generator is responsible to track the load fluctuations when the rest of the units only inject power to the microgrid. These decisions are made by a strategy comparing the available power and SOC of the battery with the total load demand and the SOC limits. The solution of the planning model is a set of pareto optimal solutions, that need to be evaluated to select the best combination of the generation units. *The selection criteria between multiple pareto optimal solutions is not discussed properly and the paper fails to address whether the selected unit for following the fluctuations is capable of providing the required amount*

of power and the required ramping rate.

Microgrid Planning Under Uncertainty

A probabilistic approach is presented in [27] to evaluate the performance of a PV-wind microgrid for both grid-connected and stand-alone applications. The long-term meteorological data of wind speed and solar irradiation level is used to characterize the probability distribution of wind speed and daily clearness index. Daily clearness index is defined as the ratio of a particular days total solar irradiation, in kWh/m^2, to the extraterrestrial total solar irradiation for that day, both referred to a horizontal surface. The wind speed and daily clearness index Probability Distribution Functions (PDFs) are convolved to get the probability density function of the combination of the RE resources that will be used for a reliability assessment of the system. The evaluated reliability indices include Energy Index of Reliability (EIR) directly related to Energy Expected Not Supplied (EENS). *The major drawback of this method is that the probability distribution function does not contain the time series information (i.e., time series characteristics and seasonal or diurnal patterns). Furthermore, the operation constraints of the system are limited to the probabilistic demand-supply balance.*

A method for optimal design and planning of a microgrid considering uncertainties is presented in [28]. The expected cost of meeting energy demand is minimized in a recursive deterministic approach. The deterministic optimization problem which is introduced in [29] is solved using a Monte Carlo analysis to calculate the microgrid performance metric; each deterministic optimization is run based on a random draw from a PDF of the input stochastic variables, i.e., energy price and output of wind turbines. After the distribution of the performance metric is known, its expected value is calculated. The recurring deterministic optimization is then repeated for each combination of generators from a defined solution space. The result is determination of a set of probability density functions for each combination of generators. The proposed method is examined on a CHP-boiler-wind-PV-storage-thermal storage system considering both stand-alone and grid-connected modes, adopting a Genetic Algorithm, evaluating metrics such as expected loss or other common risk related metrics. *The study is evaluated using the demand profiles consisting of 12 days of hourly data which limits its scope; also, the study neglects to consider the time series characteristics of the uncertain data such as seasonal or diurnal patterns.*

The authors in [30] considered several type of physical and financial uncertainties in a microgrid. The studied microgrid, which consists of wind, PV and storage units to provide a group of electricity consumers with a peak annual load demand of 8.5 MW, operates in both grid-connected and stand-alone modes and net-metering is considered for power

exchange between the main grid and the microgrid. A robust optimization approach is developed to include forecast errors in load, renewable generation and market prices in the optimization problem, as well as the microgrid islanding which is also treated as a source of uncertainty. The planning problem is decomposed into an investment master problem and an operation sub-problem. The master problem handles the optimal system sizing variables, while the operation sub-problem determines the optimal operation of the microgrid as well as the energy transfer with the main grid. The worst case optimal operation under uncertain conditions is examined based on the optimal sizes determined in the master problem, and optimality cuts are generated and sent to the master problem to govern the subsequent iterations. The solution convergence is examined based on the proximity of a lower bound solution (solution of the master problem) and an upper bound solution (calculated in the operation sub-problem). The iterative process is continued until the convergence criterion is met. The investment master problem is solved annually, while the operation sub-problem is solved hourly for the planning horizon. Data uncertainty is considered by assuming a bound of uncertainty. Each uncertain parameter is expanded in a range around its nominal value obtained from forecasts. The robust optimization problem finds the worst case solution as the uncertain parameters vary in their uncertainty range. The study suggests that in optimal sizing of a microgrid the operation cost plays a more important role than the investment cost. It also shows that the planning solution is more sensitive to market price forecast errors than to other errors. *The study reported in [30] addresses important subjects, but it could benefit from a detailed study on the impact of the renewable resource integration on the operation constraints of the system, such as frequency and voltage regulation limits, in the stand-alone mode.*

A two-stage stochastic model is presented in [31] to minimize the investment and operation costs, and to minimize the investment risks because of resource uncertainty. The first stage of the model determines the sizing of wind-PV-battery-diesel system while the second stage determines the dispatch of generation between diesel generators and batteries. The uncertainty in load demand and wind and solar power are modeled through considering multiple scenarios of uncertain variables. The optimization problem is solved using AMPL programming environment. *Including multiple scenarios significantly increases the size of the problem which makes it difficult to expand the problem to consider the impact of various parameters or consider a large-scale problem. Hence, the scope of the model is limited to small-scale applications.*

1.3 Research Objectives

Based on the past work in the area, comprehensive and inclusive microgrid planning is the best approach to address the barriers to integration of RE resources in remote communities. Although the microgrid optimal planning and operation has been extensively studied in the literature, which could make a strong baseline for the future work, the previous work on microgrid planning often overlook some important factors in the planning process, such as the impact of RE integration on frequency and voltage regulation of the microgrid. Therefore, this thesis proposes a novel multiple-stage planning platform for isolated microgrids considering the operation constraints. The main objectives of this thesis are as follows:

- To develop a multiple-year planning platform that includes the detailed model of isolated RE-based microgrids and considers the operation of the system including system regulation restrictions, such as frequency and voltage regulation requirements. The proposed planning platform can be used to investigate the feasibility of incorporation of RE and ESS in microgrids of remote communities, while taking into account the details of the operation of the system and its frequency and voltage regulation constraints;
- To investigate the impact of renewable energy integration on the quality of the generated power, through conducting simulations and studies on the voltage and frequency profile of the system after addition of RE and ESS unit;
- To evaluate the impact of demand response management on the optimal combination of RE, ESS and diesel generation units, by introducing the flexible load concept to the optimization model;
- To investigate the impact of RE integration on carbon footprint reduction in remote communities and to evaluate the economic requirements for further decreasing the carbon footprint;
- To determine the impact of changing the planning model parameters on the configuration of the system and the planning objective by performing sensitivity analysis.

1.4 Thesis Organization

The rest of this thesis is organized as follows:

Chapter 2 presents a background review of the topics relevant to the proposed planning platform. It includes a general overview of different aspects of microgrids, such as control and regulation. An introduction to Canadian remote communities and the electricity generation in remote communities is presented. Furthermore, an overall view of the microgrid planning model and various optimization techniques are discussed.

The proposed optimal planning platform and its multiple stages are described in Chapter 3. A case study is conducted on Kasabonika Lake First Nation (KLFN) community microgrid to demonstrate the capabilities of the proposed methodology.

Chapter 4 discusses the general methodology for selection of ESS for integration in remote communities. Several ESS technologies are described and compared to identify the most suitable one for incorporation in remote communities. The possibility of integration of a hybrid ESS is also discussed and investigated.

The impact of demand response management on optimal configuration of RE and ESS units is investigated in Chapter 5. Furthermore, the impact of RE and ESS integration on carbon footprint reduction in remote communities is evaluated. A sensitivity analysis is performed to analyze the impact of variations in model parameters on the optimal unit sizes and the economic outcomes.

Finally, Chapter 6 presents a summary of the thesis, highlighting its contributions and possible future research work.

Chapter 2

Background

This Chapter discusses different topics relevant to the proposed research on optimal planning of an isolated RE-based microgrid considering system operation constraints. First, a general overview of different microgrid components, including DERs and loads, and their control and operation is presented, followed by a discussion on Canadian remote community microgrids. Then, planning of RE-based remote community microgrids is addressed. The Chapter ends with description of optimization methodology and algorithms.

2.1 Microgrids

A microgrid is defined as a cluster of Distributed Energy Resources (DERs) and loads, with the capability to operate in connection with the grid or in stand-alone mode [32]. Among the main drivers of emerging microgrid solutions are growing population, which leads to growing energy demand, increasing stress on the main power grid, government incentives to promote DER deployment and the need for reliable and secure power generation resources [32]. The purpose of these systems is to provide reliable and affordable energy to the customers, reduce the stress on the conventional power systems, and alleviate the adverse environmental effects of conventional power generation facilities. The public will also benefit from access to more reliable and higher quality electricity service; Therefore, the on-site generation of electricity will mitigate the risks and losses associated with the centralized power generation systems [32]. However, the microgrids have unique challenges and issues different from those found in traditional power systems, and their success and development depend on how well they are planned and operated [33]. Hence, a robust microgrid planning strategy needs to take several important factors into account.

These include the availability of energy resources in the targeted location, a wide range of available technologies, the costs and investments required for the integration of DERs, operation, control and management strategies, and the uncertain nature of renewable energy resources and loads.

2.1.1 Distributed Energy Resources (DERs)

Distributed energy resources refer to the electric power generation units connected to medium or low voltage distribution systems. They include generation and storage units such as wind turbines, photovoltaic cells, diesel generators, batteries, fuel cells, and flywheels [34]. Widespread use of DER technologies in power systems can provide significant benefits to the power system by helping to mitigate distribution system capacity constraints, providing voltage support, improving system stability, reducing line losses and line congestion, and deferring expansion of distribution and transmission facilities [35]. Integration of DERs also affect remote communities and isolated microgrids by providing alternative generation resource options to help improve the quality of power and reliability of their electricity generation systems as well as offering cost effective solutions to reduce the electricity generation cost. Among DER technologies, wind turbines, solar photovoltaic, diesel generators and energy storage systems have found their way into the research and practical applications more than other available technologies. Hydro power is another major technology which has been deployed in numerous areas depending on the availability of resources. Also, energy storage technologies such as batteries and electrolyzer-hydrogen storage-fuel cell combination are becoming feasible options for integration in microgrids [35].

2.1.2 Microgrid Loads and Demand Management

The main purpose of development of microgrids is to serve the customers' load demands at the highest quality and/or reliability, preferably at the lowest cost. Availability of generation resources on the one hand, and the consumption behavior of the customers on the other hand, impact the success of microgrids in achieving their goals. Different types of customers including residential, commercial and industrial loads have various consumption patterns. Although the consumption behavior of the customers can be independent of availability of the energy resources, it can be shaped and managed in response to the change of the electricity price over time or receiving incentives, to realize the preferred demand patterns of the power system operators.

Customers' response may include changing electricity usage in certain time periods in response to pricing arrangements without changing the consumption in other times, such as temporarily adjusting the settings of the air conditioning or heating systems. Another type of response includes shifting the consumption to a different time, such as using household appliances in off-peak periods [36]. One common way to achieve this is to enforce time-of-use pricing schemes to encourage the customers to shift their electricity usage from periods where electricity price is high to the intervals with lower electricity price. Such schemes are under the category of energy management programs, called Demand Response Management (DRM).

Implementing Demand Response (DR) can improve the utilization of the power generation resources by modifying the demand patterns. It can also decrease the need for power network expansion plans by decreasing the peak load demand. The customers can also gain benefits by participating in DRM programs through receiving incentives and savings on their bills by lowering their consumption in high-price periods [37].

2.1.3 Microgrid Control

Microgrid's control system must be able to establish the reliable and economic operation of the system. The main features of the control system include [38]: controlling the output voltage and currents of the DER units to ensure they track the desired reference values, maintaining the microgrids power balance, keeping the voltage and frequency within their acceptable limits, design and incorporation of Demand Side Management (DSM) mechanisms for controlling the loads if applicable, determining appropriate dispatch of DER units to ensure minimum operation cost and reliable system operation.

In stand-alone mode, the operation and control of the system is much more challenging than in grid-connected mode and requires careful design of strategies for balancing the power. In order to ensure that the load is being supplied at all times, mechanisms should be defined to maintain the power balance within the system by local controllers using local measurements or by a central controller which defines the set points of the local controllers via communication. In a microgrid, three levels of control including primary, secondary and tertiary are implemented through combining the local and central control approaches.

Primary control is the fastest control level which operates based on local measurements. Islanding detection, output voltage and frequency control and power sharing and balancing are the actions specific to this level. The output voltage and frequency control and power sharing in synchronous generators are done by the voltage regulator and governor, under the influence of inertia of the machine. In Voltage Source Inverter (VSI)-based DERs, control

loops are designed to simulate the inertia for frequency regulation and power sharing, and to control the voltage and current [38].

Secondary control level or microgrid Energy Management System (EMS) has the role of ensuring reliable, secure and economic operation of the microgrid. Optimal Unit Commitment (UC) and restoring the nominal voltage and frequency after the action of primary control are the main objectives of this control level. The operation speed in this control level is lower than that in the primary level [38].

Tertiary control, which is the highest control level and is considered part of the main grid, determines the long term optimal set points and coordinates the operations of multiple microgrids that are interacting with one another [38].

As shown in Figure 2.1, in the case of isolated microgrids (i.e., permanently intentionally islanded microgrids), secondary control level is the highest control level and operates in conjunction with primary level to ensure reliable operation of the system.

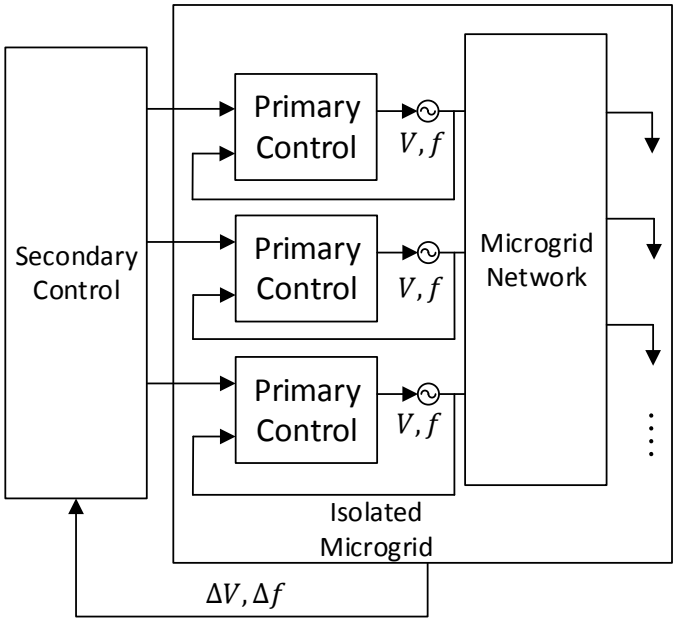

Figure 2.1: Primary and secondary control levels of an isolated microgrid [38].

2.1.4 Frequency and Voltage Regulation in Isolated Microgrids

The main variables participating in the control of operation of a microgrid are voltage, frequency, active and reactive powers [38]. In the isolated microgrids the voltage and frequency of the system are not supported by a large grid; instead, they are controlled by the DER units of the microgrid. Changes in real and reactive powers of the load demand affect the frequency and voltage magnitudes of the microgrid which must be compensated for by generation units to make sure that frequency and voltages are regulated.

Frequency and Voltage Control in Synchronous Machines

In a synchronous machine, the Load Frequency Control (LFC) loop and the Automatic Voltage Regulator (AVR) loop, control the relation between the real power and frequency, and the reactive power and voltage magnitude, respectively. The goal of the LFC and AVR is to maintain the frequency and voltage within a specified range. The schematic diagram of LFC and AVR controls of a synchronous generator is depicted in Figure 2.2.

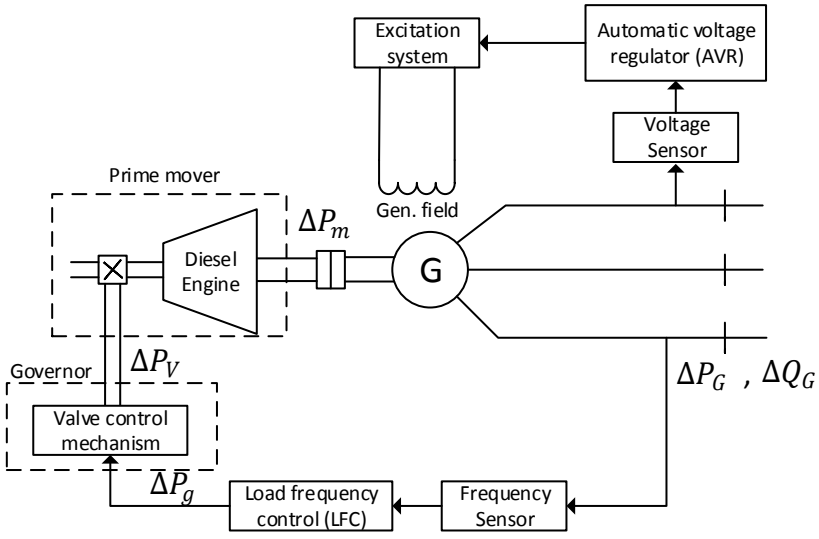

Figure 2.2: Schematic diagram of LFC and AVR of a synchronous generator [39].

According to the scheme shown in Figure 2.2, the change in the frequency is sensed, amplified and sent to the prime mover to request for an increment/decrement in torque. The prime mover changes the generator output power which results in a change in the

frequency. The mathematical models of the generator, load, prime mover and governor are as follows [39]:

- Generator model:

$$\frac{2H}{\omega_s}\frac{d^2\Delta\delta}{dt^2} = \Delta P_m - \Delta P_e \tag{2.1}$$

- Load model:

$$\Delta P_e = \Delta P_L + D\Delta\omega \tag{2.2}$$

- Prime mover model:

$$G_T(s) = \frac{\Delta P_m(s)}{\Delta P_V(s)} = \frac{1}{1+\tau_T s} \tag{2.3}$$

- Governor model:

$$G_g(s) = \frac{\Delta P_V(s)}{\Delta P_g(s)} = \frac{1}{1+\tau_g s} \tag{2.4}$$

In (2.1)-(2.4), ΔP_m and ΔP_e are the deviations in generator mechanical and electrical powers, δ the rotor angle, ω_s the synchronous speed, H the inertia of the rotating mass, ΔP_L the frequency-insensitive load change, $D\Delta\omega$ the frequency-sensitive load change, ΔP_V the change in the valve position and τ_T and τ_g time constants. ΔP_g is the difference between the power set point, ΔP_{ref}, and the power $\frac{1}{R}\Delta\omega$, given by the governor speed characteristics.

$$\Delta P_g = \Delta P_{ref} - \frac{1}{R}\Delta\omega \tag{2.5}$$

R is the droop of the governor defined by:

$$R = \frac{\Delta\omega}{\Delta P} \tag{2.6}$$

Any disturbance in the load active power will result in a change in the frequency according to the system dynamics, as stated by the above equations. In order to restore the frequency to its nominal value, Automatic Generation Control (AGC), which is a

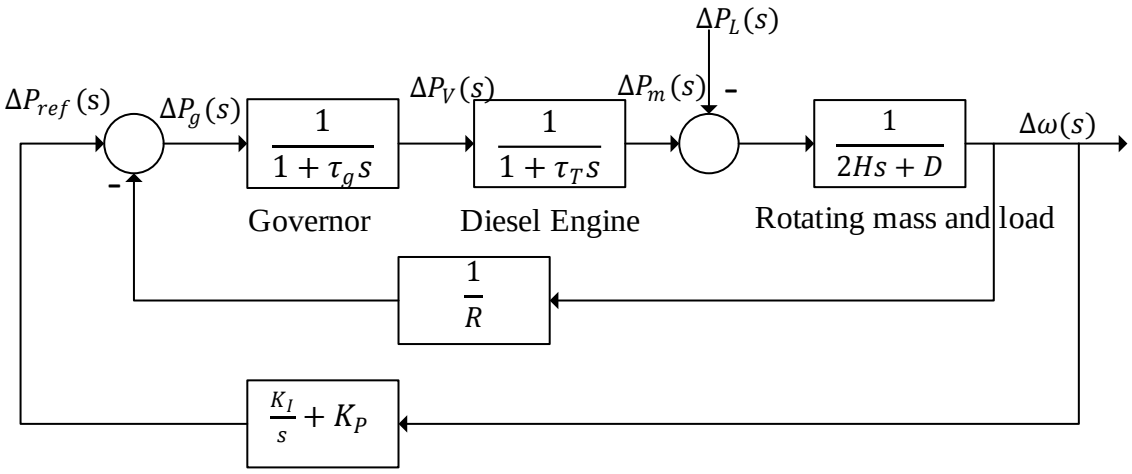

Figure 2.3: The AGC control block diagram of a synchronous machine [39].

closed-loop controller, changes the set point of the active power to eliminate the frequency mismatch. The AGC control block of a synchronous machine is shown in Figure 2.3.

The closed-loop transfer function of the control system shown in Figure 2.3 with ΔP_L as input is [39]:

$$\frac{\Delta\omega(s)}{\Delta P_L(s)} = -\frac{s(1+\tau_g s)(1+\tau_T s)}{s(2Hs+D)(1+\tau_g s)(1+\tau_T s)+K_I+s(K_P+\frac{1}{R})} \tag{2.7}$$

A block diagram can also be derived for Automatic Voltage Regulator (AVR) control loop of a synchronous machine as depicted in Figure 2.4. K_A, K_E, K_G and K_R are the gain values and τ_A, τ_E, τ_G and τ_R are the time constants for amplifier, exciter, generator and sensor, respectively.

The transfer function of the terminal voltage, $V_t(s)$, to the reference voltage, $V_{ref}(s)$ can be derived as:

$$\frac{V_t(s)}{V_{ref}(s)} = \frac{K_A K_E K_G K_R(1+\tau_R s)}{(1+\tau_A s)(1+\tau_E s)(1+\tau_G s)(1+\tau_R s)+K_A K_E K_G K_R} \tag{2.8}$$

Frequency and Voltage Control in Inverters

Inverters are used as an interface to connect the DC output of RE resources such as solar and wind generators and ESS to the AC power grid. The controller units of inverters are

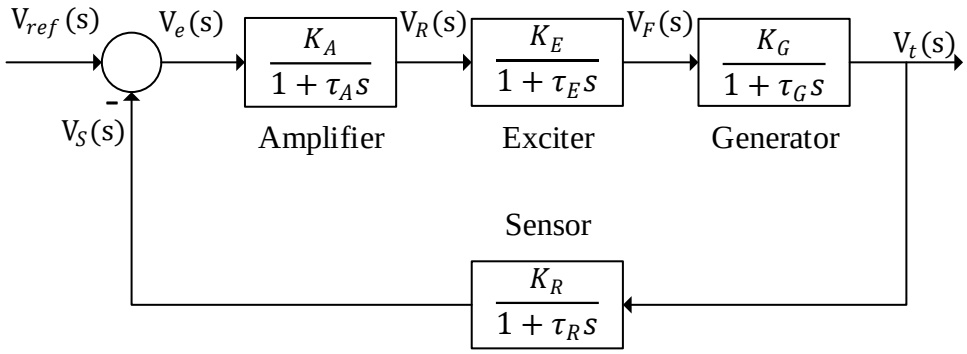

Figure 2.4: A simplified automatic voltage regulator block diagram [39].

able to mimic the behavior of the governor of the synchronous machines by implementing the relationships between active power and frequency as well as reactive power and voltage through droop characteristics. The feedback signals of output voltage and current are transferred to dq frame and the calculation of the power and accordingly voltage and frequency reference is performed based on the received signals.

Inverters can be controlled to operate in three different schemes: grid-forming, grid-supporting and grid-feeding [40]. A grid-forming inverter acts as an ideal voltage source and sets the frequency and voltage of the local grid through a control loop. A grid-supporting inverter acts as an ideal ac-controlled current/voltage source and regulates its output current/voltage. A grid-feeding inverter delivers active and reactive power to contribute in regulation of voltage and frequency.

Figures 2.5-2.7 illustrate the inverter control block diagrams for grid-forming, grid-feeding and grid-supporting three-phase voltage source inverters, respectively.

Frequency Regulation and Load following

Maintaining the balance of supply and demand is a crucial requirement in a power system. This operation becomes even more challenging in isolated RE-based microgrids due to presence of fluctuating and intermittent RE generation.

Frequency regulation and load following are two critical services carried out in power systems to ensure the balance between demand and supply during normal operation of the system. Fast fluctuations in load are tracked by (primary frequency control) and the system frequency is kept within desired limits by utilizing the available generation and/or storage

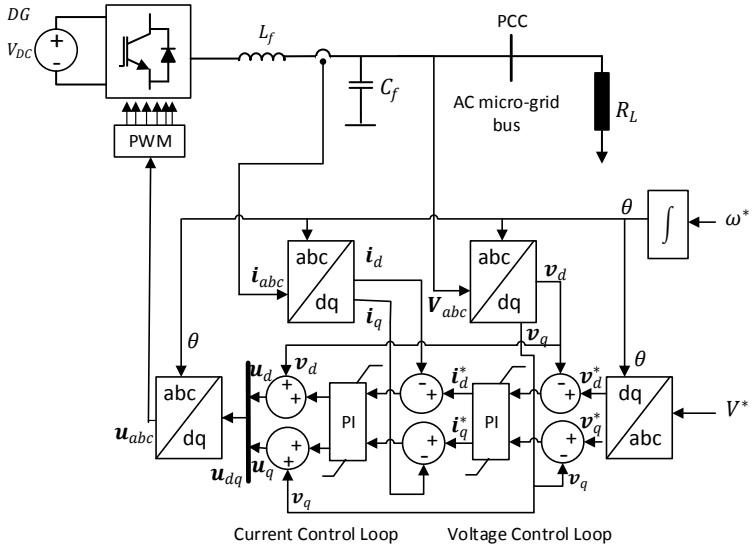

Figure 2.5: Three-phase grid-forming voltage source inverter control block diagram [40].

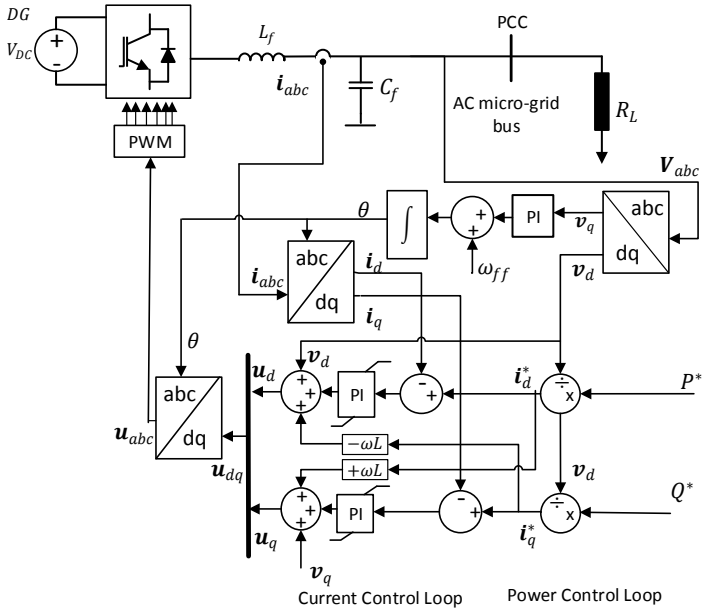

Figure 2.6: Three-phase grid-feeding voltage source inverter control block diagram [40].

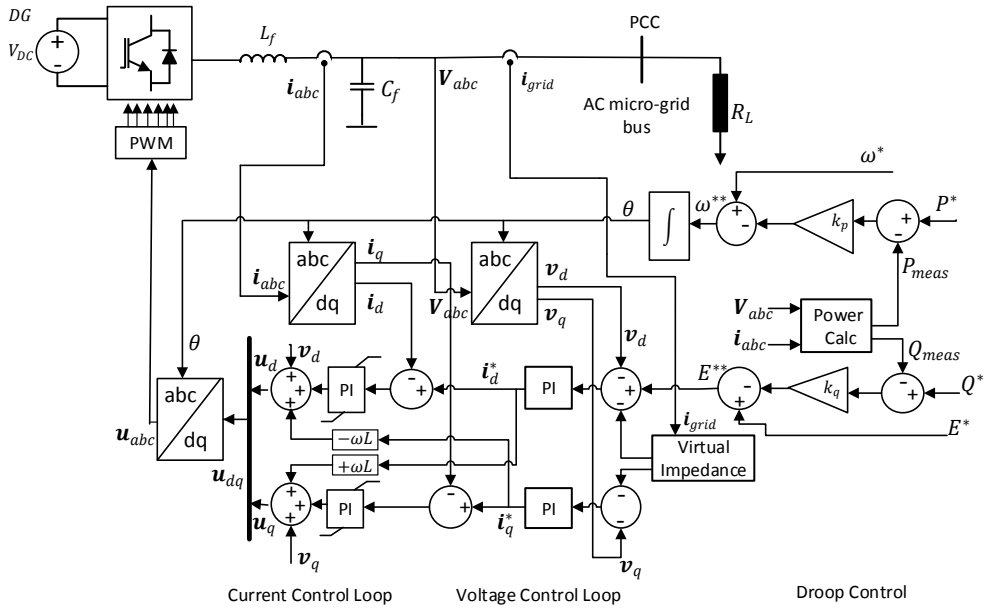

Figure 2.7: Three-phase grid-supporting voltage source inverter control block diagram [40].

resources that are equipped with AGC. Load following (secondary frequency control) is performed using generation, storage and load resources to track the slow fluctuations in load and restore the frequency to nominal value. The ramp rate required for providing primary frequency control as a regulation service is 5-10 times more than that for load following [41]. Frequency regulation operates based on an automated closed loop control on local scale; however, load following operates in centralized system scale and can include human intervention or supervision [42].

The performance of regulation and load following services is greatly impacted by integration of intermittent and highly fluctuating RE resources, especially in isolated microgrids, where due to the characteristics and limited sizes of the DERs the system inertia is often much lower than that of the main power grid [43].

The contribution of conventional generation resources, such as diesel generators, in frequency and load following is rather limited by their sizes and ramping capabilities. Thus, in order to provide reliable regulation and load following services for isolated microgrids with RE resources, adequate reserve capacities, capable of compensating for fast-ramping and intermittent RE generation, must be allocated.

Figure 2.8 shows the distribution of the available capacities of the generation and stor-

age units. In addition to the scheduled power that has to be provided by each unit, there must be some capacity reserved for contribution in primary and secondary frequency control tasks, for the units participating in those actions. The allocated reserve for primary frequency control should be able to act fast and provide the required service within a few seconds after the disturbance, while the secondary control reserve needs to be activated within a few minutes to respond to the changes in load and restore the system frequency.

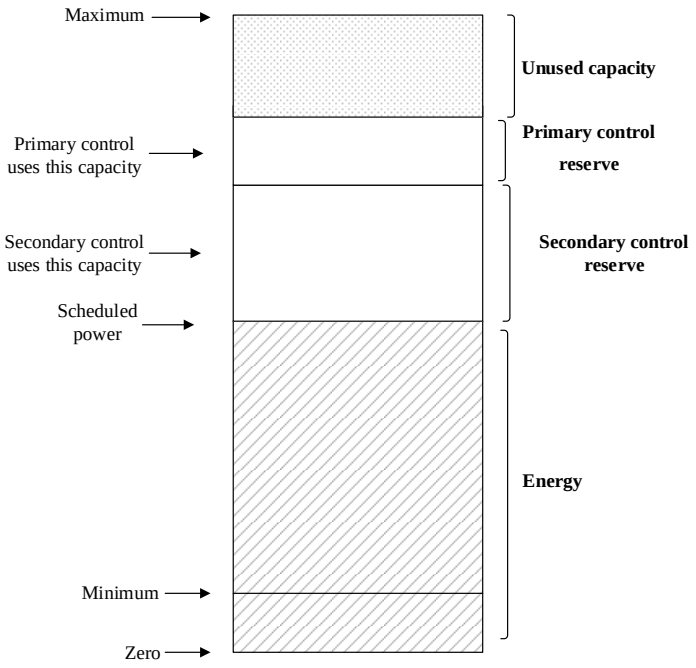

Figure 2.8: Allocation of generation and storage capacities participating in frequency control [44].

The participation of DERs, including RE, ESS and conventional generation resources, that allocate frequency reserve capacity in frequency control takes place according to the schematic shown in Figure 2.9.

In Figure 2.9, ΔP_{Load} is the frequency-insensitive load change, ΔP_{RE} the renewable output power change, $\Delta\omega$ the system angular frequency change, H the inertia of the rotating mass, D the load damping constant, $m_{p,1}$ to $m_{p,n}$ the frequency droop characteristic slopes of DERs participating in primary frequency control actions, α_1 to α_n (where $\sum_{i=1}^{n} \alpha_i = 1$) the participation factors of DERs in secondary control actions, $M_1(s)$ to $M_n(s)$ the transfer functions of DERs, and $K_i(s)$ the PI controller transfer function. $\Delta P_{1,sche.}$ to $\Delta P_{n,sche.}$

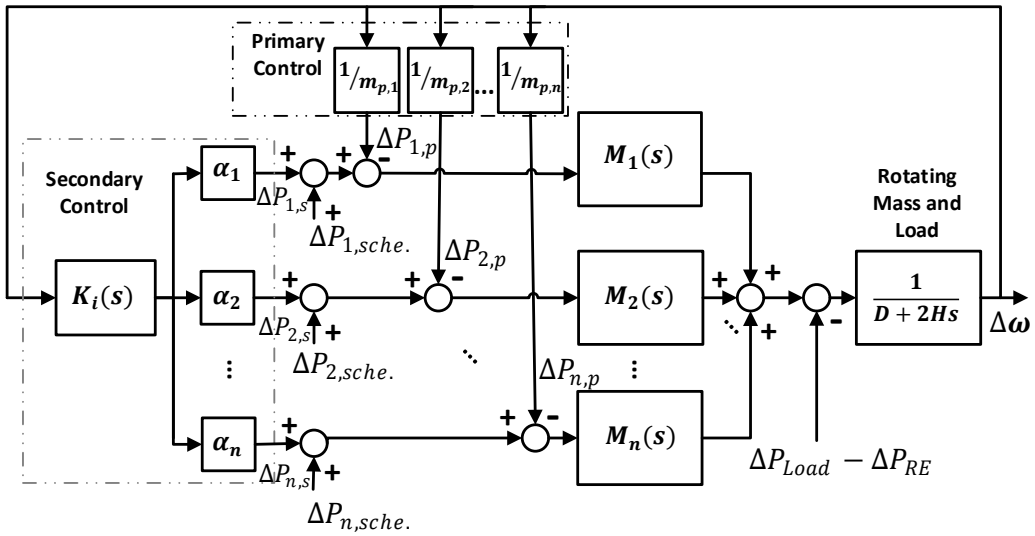

Figure 2.9: Frequency control loops with different generation and storage units participating in frequency control actions [45], [46].

are the scheduled changes in the power set points of the DERs. $\Delta P_{1,p}$ to $\Delta P_{n,p}$ are the changes in the generation right after the primary control takes place. $\Delta P_{1,s}$ to $\Delta P_{n,s}$ are the deviations in the generation after the secondary control operates. The RE units not participating in frequency control actions are represented as negative loads and their output power is deducted from total system load.

Right after a change in load and RE generation, which causes a disturbance to the system, the frequency of the system deviates from the nominal value and the generation units modify their generation to compensate for the lack or excess of power caused by the disturbance and to keep the frequency within acceptable range. Thus, the steady-state frequency of the system changes to a new value, as presented in (2.9) [39].

$$\Delta\omega_{ss} = \frac{-(\Delta P_{Load} - \Delta P_{RE})}{\frac{1}{m_{p,1}} + \frac{1}{m_{p,2}} + ... + \frac{1}{m_{p,n}} + D} \tag{2.9}$$

Generation of the units changes according to the change in frequency as well. Thus, enough primary reserve capacity must be available to accommodate these changes.

$$\Delta P_{1,p} = -\frac{\Delta\omega_{ss}}{m_{p,1}} \tag{2.10}$$

$$\Delta P_{2,p} = -\frac{\Delta\omega_{ss}}{m_{p,2}} \tag{2.11}$$

$$\Delta P_{n,p} = -\frac{\Delta\omega_{ss}}{m_{p,n}} \tag{2.12}$$

The secondary frequency reserves start acting within 1-10 minutes after the disturbance, to restore the nominal value of frequency. After that, the required power to compensate the deviation from pre-disturbance state is supplied by the units participating in secondary frequency control based on their participation factors, α_i $(i = 1, 2, ..., n)$. Hence, the powers generated by different units, deviate from their pre-scheduled values as follows:

$$\Delta P_{1,s} = \alpha_1 \times (\Delta P_{Load} - \Delta P_{RE}) \tag{2.13}$$

$$\Delta P_{2,s} = \alpha_2 \times (\Delta P_{Load} - \Delta P_{RE}) \tag{2.14}$$

$$\Delta P_{n,s} = \alpha_n \times (\Delta P_{Load} - \Delta P_{RE}) \tag{2.15}$$

The secondary reserve capacity must be enough to provide the modified power for the period after the secondary control takes place. Hence, the required energy to be provided by different units also changes from pre-scheduled values:

$$\Delta E_1 = \Delta t \times \Delta P_{1,s} = \Delta t \times (\alpha_1 \times (\Delta P_{Load} - \Delta P_{RE})) \tag{2.16}$$

$$\Delta E_2 = \Delta t \times \Delta P_{2,s} = \Delta t \times (\alpha_2 \times (\Delta P_{Load} - \Delta P_{RE})) \tag{2.17}$$

$$\Delta E_n = \Delta t \times \Delta P_{n,s} = \Delta t \times (\alpha_n \times (\Delta P_{Load} - \Delta P_{RE})) \tag{2.18}$$

In (2.16)-(2.18), Δt is the time period between the secondary frequency control takes place until the next disturbance.

Figure 2.10 demonstrates the participation of the generation/storage units in an arbitrary system of two units after a disturbance and the changes in powers according to (2.13)-(2.18). It can be seen that the primary control reserves are responsible for providing instantaneous power in short time scales right after the disturbance, while secondary control reserves should be able to compensate for the mismatch of the load and generation by providing long-term power to restore the frequency.

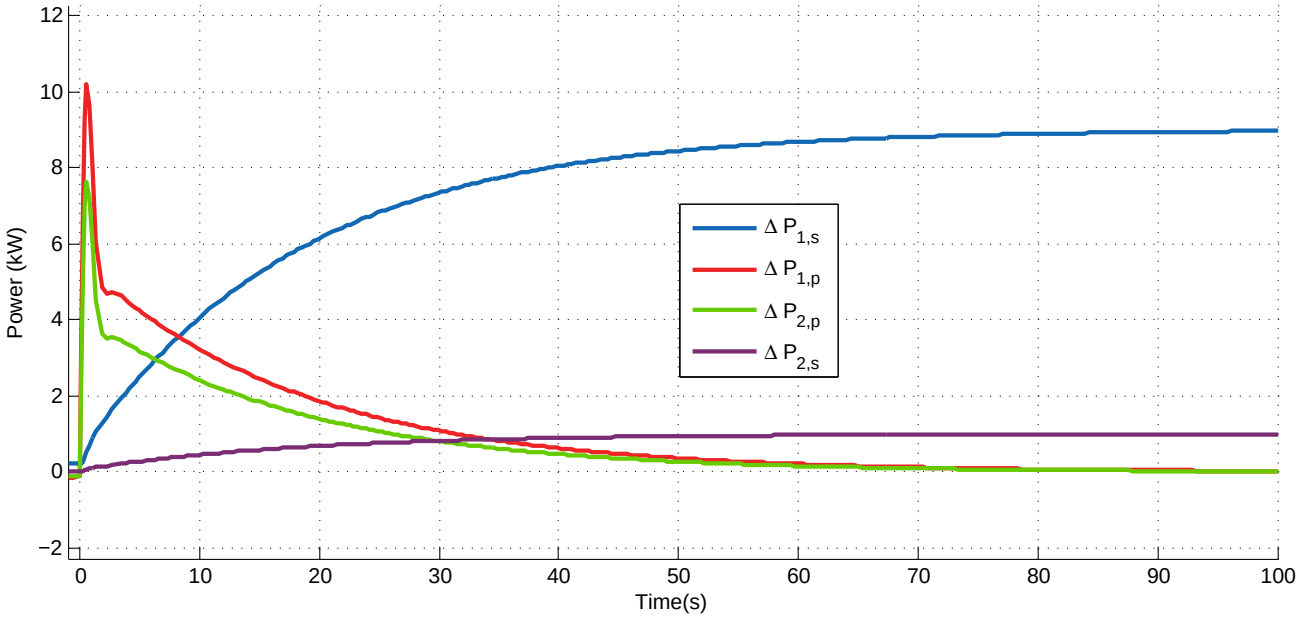

Figure 2.10: Participation of two units in primary and secondary frequency control and their power and energy contributions.

Voltage Regulation

Maintaining the voltage magnitudes within specified limits, called voltage regulation, is one of the most critical operation tasks in the distribution networks. Voltage is a local variable in a power network and its value at each bus of the network depends on the structure of the system and distribution of the loads, contrary to frequency which is a global quantity. Hence, to study the status of system voltages, the structure of the network, the locations of loads and DERs, and values of line impedances must be available.

In order to determine the voltage profile at different network buses, the voltage drop in each feeder, the current and power flows and the losses in steady-state operation, power flow study (load flow study) is performed. Power flow analysis provides the status of the system under given load and generation conditions.

A three-phase power flow model, such as the one presented in [47], can be used to determine the status of an isolated microgrid comprising of DERs under unbalanced load conditions. The power flow algorithm presented in [47] considers the inverter-based DG units operating in droop mode. The frequency of the system is assumed to be a variable that is determined in the solution of the power flow model.

The power flow equations used to determine the voltage profile of the system are as follows:

$$P_{Gi}^{a,b,c} - P_{Li}^{a,b,c}(\omega, \left|V_i^{a,b,c}\right|) - P_i^{a,b,c}(\omega, \left|V_i^{a,b,c}\right|, \left|V_j^{a,b,c}\right|, \delta_i^{a,b,c}, \delta_j^{a,b,c}) = 0 \tag{2.19}$$

$$Q_{Gi}^{a,b,c} - Q_{Li}^{a,b,c}(\omega, \left|V_i^{a,b,c}\right|) - Q_i^{a,b,c}(\omega, \left|V_i^{a,b,c}\right|, \left|V_j^{a,b,c}\right|, \delta_i^{a,b,c}, \delta_j^{a,b,c}) = 0 \tag{2.20}$$

$$P_i^a = \sum_{\substack{i=1 \\ j \neq i}}^{n_{br}} \sum_{ph=a,b,c} [|V_i^a| \left|Y_{i,j}^{a(ph)-n)}\right| \left|V_i^{ph}\right| \cos(\theta_{i,j}^{a(ph)} + \delta_i^{(ph)} - \delta_i^a) - |V_i^a| \left|Y_{i,j}^{a(ph)-n)}\right| \left|V_j^{ph}\right| \cos(\theta_{i,j}^{a(ph)} + \delta_j^{(ph)} - \delta_i^a)] \tag{2.21}$$

$$Q_i^a = \sum_{\substack{i=1 \\ j \neq i}}^{n_{br}} \sum_{ph=a,b,c} [|V_i^a| \left|Y_{i,j}^{a(ph)-n)}\right| \left|V_j^{ph}\right| \sin(\theta_{i,j}^{a(ph)} + \delta_j^{(ph)} - \delta_i^a) - |V_i^a| \left|Y_{i,j}^{a(ph)-n)}\right| \left|V_i^{ph}\right| \sin(\theta_{i,j}^{a(ph)} + \delta_i^{(ph)} - \delta_i^a)] \tag{2.22}$$

Equations (2.19) and (2.20) describe the mismatch equations of bus i in the network, where $P_i^{a,b,c}$ and $Q_i^{a,b,c}$ represent the calculated injected active and reactive powers, $P_{Gi}^{a,b,c}$ and $Q_{Gi}^{a,b,c}$ are the generated active and reactive powers and $P_{Li}^{a,b,c}$ and $Q_{Li}^{a,b,c}$ the load active and reactive power demands at three phases (a, b, c) of bus i. $\left|V_i^{a,b,c}\right|$ represents the magnitudes of the three-phase voltages at bus i, with the corresponding phase angles represented by $\delta_i^{a,b,c}$. ω is the system frequency, n_{br} the total number of buses in the network, and i and j the bus number indices. $\left|Y_{i,j}^{a(ph)-n)}\right|$ and $\theta_{i,j}^{a(ph)}$ represent the magnitudes and phase angles of the branch admittances defined by the following three-phase branch admittance matrix:

$$\left[Y_{ij}^{abc}\right] = \left[Z_{ij}^{abc}\right]^{-1} = \begin{bmatrix} Y_{ij}^{aa-n} & Y_{ij}^{ab-n} & Y_{ij}^{ac-n} \\ Y_{ij}^{ba-n} & Y_{ij}^{bb-n} & Y_{ij}^{bc-n} \\ Y_{ij}^{ca-n} & Y_{ij}^{cb-n} & Y_{ij}^{cc-n} \end{bmatrix} \tag{2.23}$$

There are six unknown variables for each PQ-Bus in the network, $\left|V_i^{a,b,c}\right|$ and $\delta_i^{a,b,c}$, which are determined by solving (2.19) and (2.20). For PQ-Buses, $P_{Gi}^{a,b,c}$ and $Q_{Gi}^{a,b,c}$ are replaced by their pre-specified values $P_{Gi,spec}^{a,b,c}$ and $Q_{Gi,spec}^{a,b,c}$, respectively.

The unknown variables for PV-Buses are the phase angle of the voltages, $\delta_i^{a,b,c}$. For PV-Buses, $P_{Gi}^{a,b,c}$ and $\left|V_i^{a,b,c}\right|$ are replaced by their pre-specified values, $P_{Gi,spec}^{a,b,c}$ and $\left|V_{i,spec}^{a,b,c}\right|$, respectively, to solve the three mismatch equations in (2.19).

The inverter-based Droop-Buses have twelve mismatch equations to solve for twelve unknown variables, $\left|V_i^{a,b,c}\right|$, $\delta_i^{a,b,c}$, $P_{Gi}^{a,b,c}$ and $Q_{Gi}^{a,b,c}$. In addition to the six mismatch equations of (2.19) and (2.20), the following equations are solved to determine the unknown values:

$$|V_i^a| - \left|V_i^b\right| = 0 \tag{2.24}$$

$$|V_i^a| - |V_i^c| = 0 \tag{2.25}$$

$$\delta_i^a - \delta_i^b - \frac{2\pi}{3} = 0 \tag{2.26}$$

$$\delta_i^a - \delta_i^c + \frac{2\pi}{3} = 0 \tag{2.27}$$

$$P_{Gi}^a + P_{Gi}^b + P_{Gi}^c - P_{Gi}(\omega) = 0 \tag{2.28}$$

$$Q_{Gi}^a + Q_{Gi}^b + Q_{Gi}^c - Q_{Gi}(\left|V_i^{a,b,c}\right|) = 0 \tag{2.29}$$

Many isolated microgrids have one or more diesel generators operating in their system. Hence, it is necessary to incorporates the equations of the diesel generator units into the power flow algorithm. For synchronous generator-based units operating in droop mode, eighteen equations can be identified to solve for eighteen unknown variables, $\left|V_i^{a,b,c}\right|$, $\delta_i^{a,b,c}$, $P_{Gi}^{a,b,c}$, $Q_{Gi}^{a,b,c}$, $\left|E_i^{a,b,c}\right|$ and $\varphi_i^{a,b,c}$. The following equations are solved in addition to (2.19) and (2.20) to find the unknown variables:

$$|E_i^a| - \left|E_i^b\right| = 0 \tag{2.30}$$

$$|E_i^a| - |E_i^c| = 0 \tag{2.31}$$

$$\varphi_i^a - \varphi_i^b - \frac{2\pi}{3} = 0 \tag{2.32}$$

$$\varphi_i^a - \varphi_i^c + \frac{2\pi}{3} = 0 \tag{2.33}$$

$$P_{Gi}^a + P_{Gi}^b + P_{Gi}^c - P_{Gi}(\omega) = 0 \tag{2.34}$$

$$Q_{Gi}^a + Q_{Gi}^b + Q_{Gi}^c - Q_{Gi}(\left|V_i^{a,b,c}\right|) = 0 \tag{2.35}$$

$$P_{Gi}^{a,b,c} - \frac{\left|V_i^{a,b,c}\right| \left|E_i^{a,b,c}\right|}{X_s} \sin(\varphi_i^{a,b,c} - \delta_i^{a,b,c}) = 0 \tag{2.36}$$

$$Q_{Gi}^{a,b,c} - \frac{\left|V_i^{a,b,c}\right| (\left|E_i^{a,b,c}\right| \cos(\varphi_i^{a,b,c} - \delta_i^{a,b,c}) - \left|V_i^{a,b,c}\right|)}{X_s} = 0 \tag{2.37}$$

In (2.30)-(2.37), $\left|E_i^{a,b,c}\right|$ and $\varphi_i^{a,b,c}$ are the magnitudes and phase angles of the internally generated voltages, and X_s is the synchronous reactance of the synchronous machine.

In (2.28), (2.29), (2.34) and (2.35), the three-phase active and reactive powers of the droop-controlled DG units are determined as follows:

$$P_{Gi}(\omega) = \frac{1}{m_{p,i}}(\omega^* - \omega) \tag{2.38}$$

$$Q_{Gi}(\left|V_i^{a,b,c}\right|) = \frac{1}{n_{q,i}}(V_i^* - |V_i|) \tag{2.39}$$

where $m_{p,i}$ and $n_{q,i}$ are the droop characteristics slope for frequency and voltage regulation. The no-load frequency and voltage are denoted as ω^* and V_i^*.

Optimal Reactive Power Planning

A common practice in power systems is to reduce transmission losses and improve the voltage levels by allocating reactive power support resources. However, addition of reactive power support requires determination of the size and location of the reactive support resources. Devices such as shunt capacitors are often used in power systems to regulate the voltages at system buses.

The Optimal Reactive Power Planning (ORPP) problem is developed to solve the issue of optimal placement of reactive power support devices and optimal allocation of reactive power resources in power networks. Different objectives considered for ORPP include maintaining the voltages within an acceptable range and minimizing the total investment cost of Var resources and/or power losses of the network. The constraints include the voltage limits at network buses, reactive power limits of generators and Var resources, power flow balance and security constraints [48].

The mathematical model of an ORPP problem can be defined as a multi-objective minimization (or maximization) problem, as represented in (2.40), where $J(X)$, $G(X)$ and $H(X)$ are the vectors of objectives, equality constraints and inequality constraints, respectively.

$$\begin{aligned} Min \quad & J(X) = \begin{bmatrix} J_1(X) & J_2(X) & ... & J_z(X) \end{bmatrix}^T \\ s.t. \quad & G(X) = \begin{bmatrix} g_1(X) & g_2(X) & ... & g_{m_1}(X) \end{bmatrix}^T = 0 \\ & H(X) = \begin{bmatrix} h_1(X) & h_2(X) & ... & h_{m_2}(X) \end{bmatrix}^T \leq 0 \end{aligned} \tag{2.40}$$

The vector of variables, including integer and continuous variables, is defined as:

$$X = \begin{bmatrix} x_1 & x_2 & ... & x_n \end{bmatrix}^T \tag{2.41}$$

In (2.40) and (2.41), z, m_1, m_2 and n are the numbers of objectives, equality constraints, inequality constraints and decision variables, respectively.

The vector of objective functions includes one or more objectives, such as those given by (2.42), that are selected based on the objectives of ORPP problem [49].

$$\begin{bmatrix} J_1 \\ J_2 \\ J_3 \\ ... \\ J_n \end{bmatrix} = \begin{bmatrix} Var\ cost \\ Real\ power\ loss \\ Deviations\ from\ specified\ operating\ points \\ ... \\ -(Static\ voltage\ stability\ margin) \end{bmatrix} \tag{2.42}$$

The constraints of ORPP problem can include the following [49]:

$$\begin{bmatrix} G_1 \\ G_2 \\ ... \\ G_n \end{bmatrix} = \begin{bmatrix} Active\ power\ balance \\ Reactive\ power\ balance \\ ... \\ ... \end{bmatrix} \tag{2.43}$$

$$\begin{bmatrix} H_1 \\ H_2 \\ H_3 \\ H_4 \\ ... \\ H_n \end{bmatrix} = \begin{bmatrix} Active\ power\ generation\ limits \\ Reactive\ power\ generation\ limits \\ Bus\ voltage\ limits \\ Var\ source\ size\ limits \\ ... \\ Line\ flow\ limits \end{bmatrix} \tag{2.44}$$

The variables of ORPP problem may include the following:

$$\begin{bmatrix} x_1 \\ x_2 \\ x_3 \\ ... \\ x_n \end{bmatrix} = \begin{bmatrix} Generator\ active\ power \\ Generator\ reactive\ power \\ Bus\ voltage\ magnitude \\ Bus\ voltage\ phase\ angle \\ ... \\ Var\ resource\ size \end{bmatrix} \tag{2.45}$$

2.2 Canadian Remote Community Microgrids

There are around 290 remote communities (long-term or permanent settlements not connected to the main power grid) across Canada where the installed capacities of isolated microgrids range from 100kW to 150 MW [19]. These isolated microgrids are operated either by provincial/territory-wide utilities or community-owned utilities [19]. The electricity generation energy resources vary in remote communities depending on their location; however, hydro power, diesel fuel, heavy fuel oil, natural gas and very low amount of wind and solar energy are the main energy resources for electricity generation [19]. The access to some of these communities is only by plane or via winter roads, depending on the ice conditions. Hence, fuel transportation is often costly and impacts the cost of electricity generation significantly.

Dependency on fossil fuel for electricity generation, load demands reaching power plant maximum installed capacities, high costs of electricity generation, and environmental impacts of burning fossil fuels are the main energy challenges most of these remote communities are presently facing [19]. In order to overcome some of these energy-related challenges, integration of RE resources is being actively considered.

Providing the electricity demand of the communities with RE resources has many positive impacts including reduced fossil fuel consumption by diversifying the energy resources, reduced environmental impacts and increased social and economic benefits by providing the communities with development opportunities [1]. However, these potential benefits

can be gained only if the existing challenges of incorporation of RE resources, including energy management, microgrid control, developing microgrid standards, determining the ownership status of the microgrid and defining the framework for incentives, subsidies and regulations, are overcome [19]. On the other hand, investigating the feasibility of incorporation of RE resources in remote communities requires access to accurate and on-site measured data of available RE resources, such as wind speed or solar irradiation data, which is highly limited or not available for most of these locations.

2.2.1 Electricity Generation in Northern Ontario Remote Communities

Among many Canadian remote communities, 37 are located in the province of Ontario. These communities' electricity service is supplied by Hydro One Remote Communities Inc. (HORCI) or Independent Power Authorities (IPAs). HORCI is a generation and distribution company that provides electricity to 21 remote communities. The rest of the communities are receiving electric power service through IPAs in the form of community-owned and operated utilities.

The electricity rates vary among different customer groups for both HORCI and IPA-provided communities. There are two electricity rate groups: Standard-A (Unsubsidized) and non-Standard-A (Subsidized) customer groups. Federal, provincial and community buildings pay the Standard-A rate which is equal to the real cost of electricity generation at northern Ontario remote communities (up to 92 cents/kWh in 2013). The non-Standard-A customers which are the residential and commercial customers, pay the same rate as the customers connected to the main grid in Ontario (8-17 cents/kWh in 2013) [50]. The non-Standard-A rate is subsidized by Indigenous and Northern Affairs Canada (INAC), formerly known as Aboriginal Affairs and Northern Development Canada (AANDC), and Ontario's Rural or Remote Rate Protection (RRRP) funding resources [50]. The IPA-operated customers pay slightly higher rates compared to those of HORCI's (approximately 2% higher), but they have similar customer category rates.

Currently, diesel generators are the main source of electricity generation in northern Ontario remote communities. However, with growing population and the increasing energy demand, which is estimated to be at an average rate of 2% annually, most of these communities are reaching their maximum installed capacity and entering a load restriction status, where they can no longer connect new facilities to the electricity grid.

Northern Ontario remote communities are considering direct connection to the provincial transmission grid and also the feasibility of adding RE resources to their existing

isolated microgrids. The development of the Wataynikaneyap Power project and progress of RE integration projects will have positive impacts on reducing dependency of these communities on diesel fuel as well as contributing to growth and development of these communities and creating job opportunities in Canada and northern Ontario [51].

2.3 Planning of RE-based Remote Community Microgrids

In order to develop a microgrid planning model, the stakeholders and their participation in electricity generation activities should be determined first. In northern Ontario remote communities, there are four stakeholders involved in the electricity cost model [19]:

- The provincial government: The government of Ontario provides the communities with funding resources for planning the projects. It is also responsible for setting regulations and the baseline for electricity subsidy allocation under the Rural or Remote Electricity Rate Protection (RRRP).
- The utility: HORCI is a non-for-profit corporation that is responsible for operation and maintenance of the diesel generators, which is a zero-sum process for the utility. These costs are covered by the customer payments and from RRRP budget.
- The local fuel supplier: In some communities, the community is the provider of the fuel to the utility and selling fuel is considered a source of income to the community.
- The customers: The customers are either subsidized, paying the same price as the on-grid customers, or unsubsidized, paying the real cost of electricity generation.

The stakeholders' participation in electricity generation activities is summarized in Figure 2.11.

The planning model used for RE projects in remote communities must take the interest of the stakeholders into account, as well as the composition of customer categories. Hence, a Long-Term Renewable Generation Planning (LTRGP) model has been developed in [19], which aims to maximize the benefits to the remote community considering the customer categories and the stakeholders' contribution in RE planning projects.

The objective of the planning optimization problem is defined to maximize the discounted value of the total social welfare of the community over the planning horizon, as presented in (2.46).

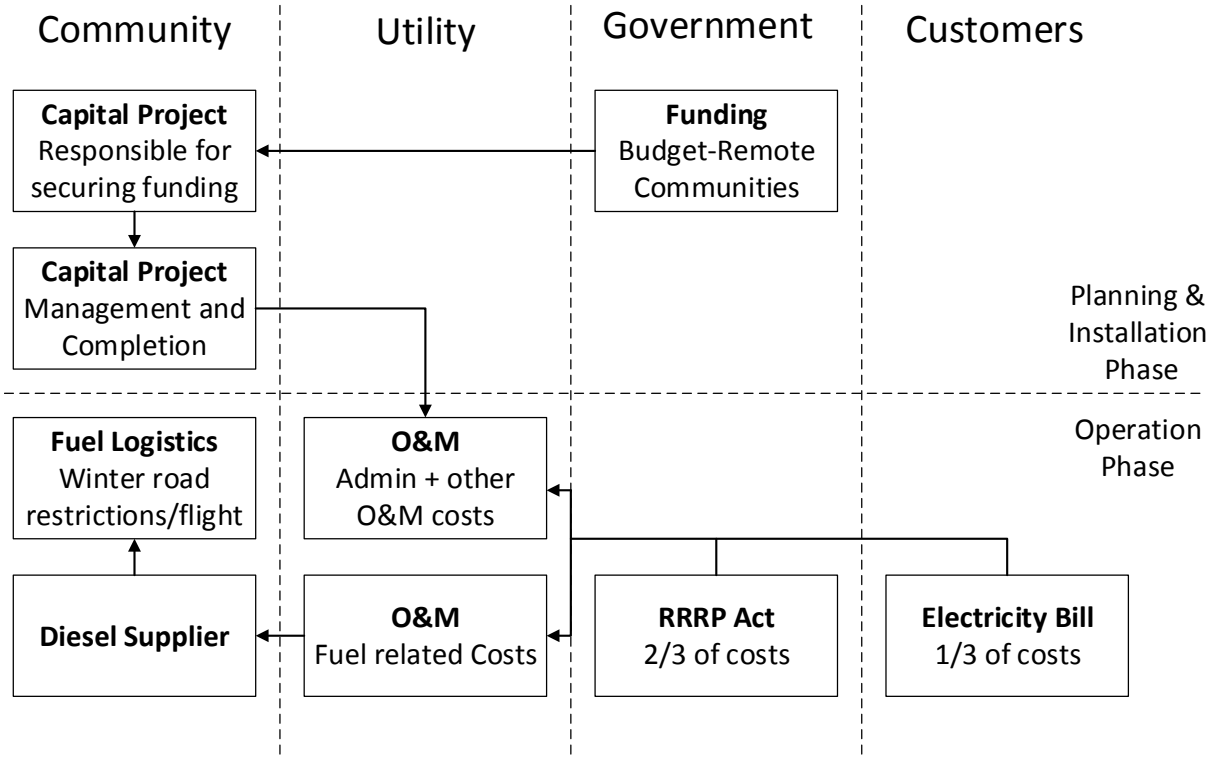

Figure 2.11: Stakeholders' participation in electricity generation activities [19].

$$max \sum_{t=1}^{T} \sum_{i=1}^{I} \frac{Wf_{i,t}}{(1+r_{d_i})^t} \tag{2.46}$$

In (2.46), $Wf_{i,t}$ is the social welfare for different customer types and its discounted value is maximized in the optimization problem. $Wf_{i,t}$ is defined by (2.47) as the sum of project income or savings, $IS_{i,t}$, minus project costs, $C_{i,t}$. r_{d_i} is the discount rate for customer i, t the index for number of years in the planning horizon and I and T the total number of customer groups and total number of years in the planning horizon, respectively.

$$Wf_{i,t} = IS_{i,t} - C_{i,t} \tag{2.47}$$

Total savings, costs and losses constitute the components of the social welfare. The savings depend on the price of the electricity paid by different customers in a community

and the amount of renewable energy used to supply the load demand, $Preu_{i,t,h}$. The savings obtained by different types of customers as a result of fuel replacement, C_{d_i}, and available external energy incentives, INC_i, determine the economic value of the savings according to (2.48). r_i is the annual change in price of electricity, h the index for number of hours and H the total number of hours in a year.

$$IS_{i,t} = [C_{d_i} \cdot (1 + r_i)^t + INC_i] \cdot \sum_{h=1}^{H} Preu_{i,t,h} \tag{2.48}$$

The cost of the project, as described by (2.49), consists of the initial capital expenses paid by the community, $C_{ce_{i,k,t}}$, periodic loan payments to the bank as an external funding resource, $C_{bpmt_{i,k,t}}$, and operation and maintenance (O&M) costs of the equipment, $C_{om_{i,k,t}}$. k is the index for equipment type, including RE resources.

$$C_{i,t} = \sum_{k=1}^{K} C_{ce_{i,k,t}} + C_{bpmt_{i,k,t}} + C_{om_{i,k,t}} \tag{2.49}$$

The initial capital payment to be made by the community is a fraction of the total capital cost of the equipment, $C_{cap_{i,k,t}}$. Part of the capital cost is paid by an external resource, such as government funding, while the other part is provided by a bank loan. In (2.50), b_{cep} and b_{efp} represent the percentage of available capital contribution at the start of the project and the percentage of available external funding with respect to the total project cost, respectively.

$$C_{ce_{i,k,t}} = C_{cap_{i,k,t}} \cdot b_{cep} \cdot (1 - b_{efp}) \tag{2.50}$$

The nominal power ratings of the selected equipment, rp_k, and the corresponding cost per kW, rc_{cap_k}, are used to calculate the total capital cost of the equipment, as given by (2.51). It is also assumed that the equipment cost declines by $cc_d\%$ each year, and the cost decreases linearly with increase in the number of purchased equipment pieces, $CB_{i,k,t}$, until a certain number of equipment pieces is reached (20, in this case), as given by (2.52). In (2.51), $x_{i,k,t}$ is the number of RE units to be deployed.

$$C_{cap_{i,k,t}} = [rc_{cap_k}.rp_k \cdot x_{i,k,t} \cdot CB_{i,k,t}] \cdot (1 - cc_d\% \cdot t) \tag{2.51}$$

$$CB_{i,k,t} = \begin{cases} 1.01 - 0.01 \cdot x_{i,k,t} & x_{i,k,t} \leq 20 \\ 0.8 & x_{i,k,t} > 20 \end{cases} \tag{2.52}$$

The amortization repayment of the bank loan, $C_{bpmt_{i,k,t}}$, is another component of the project's total cost, given by (2.49). It considers the loan interest rate and determines every installment, as given by (2.53). The payment amounts are calculated based on one single payment per year and the payments are made each year after the beginning of the loan term.

$$C_{bpmt_{i,k,t}} = [C_{cap_{i,k,t}} - C_{ce_{i,k,t}} - C_{cap_{i,k,t}} \cdot b_{efp}] \cdot \frac{r_b \cdot (1+r_b)^{blt_k}}{(1+r_b)^{blt_k} - 1} + C_{bpmt_{i,k,t-1}} \tag{2.53}$$

In (2.53), r_b and blt_k are the bank interest rate and total number of loan payments, respectively.

The O&M cost of the equipment, $C_{om_{i,k,t}}$, is determined using the present O&M cost of the units, rc_{om_k}. In (2.54), b_{om_t} represents the O&M cost variation through the equipment's operating lifetime.

$$C_{om_{i,k,t}} = rc_{om_k} \cdot rp_k \cdot (1 + b_{om_t}) \cdot EOS_{i,k,t} \tag{2.54}$$

$EOS_{i,k,t}$ representing the cumulative number of selected equipment rating at investment year t, is given by (2.55).

$$EOS_{i,k,t} = \begin{cases} x_{i,k,t} & t \leq 1 \\ EOS_{i,k,t-1} + x_{i,k,t} & t > 1 \end{cases} \tag{2.55}$$

In some cases where community is the provider of fuel to the utility, there will be a loss component after incorporation of RE resources to the community as a result of reduced fuel consumption. This is given by (2.56) and can be considered as a cost component and added to the total costs of the project.

$$LR_{i,t} = r_{FR} \cdot C_{FUEL} \cdot b_{CFP_t} \cdot (1 + CPI)^t \cdot (f_{BASE_t} - f_{PROJ_t}) \cdot z_{i,t,h} \tag{2.56}$$

In (2.56), $LR_{i,t}$ is the potential loss of opportunity cost, r_{FR} the percentage revenue gained by the community as a result of selling fuel to the utility, C_{FUEL} the actual price of fuel on-site, b_{CFP_t} the percentage of the purchased fuel by the utility from the community, CPI the fuel price growth, f_{BASE_t} and f_{PROJ_t} the fuel consumption of the community

before and after integration of RE resources, respectively, and $z_{i,t,h}$ the ratio of RE used for different customer types, defined by equations (2.57) to (2.59).

$$z_{i,t,h} = \frac{Preu_{i,t,h}}{\sum_{i=1}^{I} Preu_{i,t,h}} \tag{2.57}$$

$$f_{BASE_t} = \sum_{j=1}^{J} \sum_{h=1}^{H} (d_{GSa_j} \cdot P_{FG_{BASE_{j,t,h}}} + d_{GSb_j}) \tag{2.58}$$

$$f_{PROJ_t} = \sum_{j=1}^{J} \sum_{h=1}^{H} (d_{GSa_j} \cdot P_{FG_{proj_{j,t,h}}} + d_{GSb_j}) \tag{2.59}$$

In (2.58) and (2.59), d_{GSa_j} and d_{GSb_j} are the linear and constant coefficients for consumption of fuel based on generated power and j is the index for diesel generator in case of having different generator sizes. $P_{FG_{BASE_{j,t,h}}}$ and $P_{FG_{proj_{j,t,h}}}$ are the j^{th} diesel generator's power generation at hour h in year t for the base case with no RE generation and after RE integration, respectively.

The constraints of the planning problem are presented in (2.60)-(2.67). In (2.60), the power provided by the diesel generator, $P_{dg_{t,h}}$, has been represented by the difference between the the load demand of each customer type, $PD_{i,t,h}$, and the power provided by the deployed RE resources, $Prea_{i,k,t,h}$.

$$P_{dg_{t,h}} = \sum_{i=1}^{I} (PD_{i,t,h} - Prea_{i,k,t,h}) \tag{2.60}$$

Diesel generators have a lower limit for the percentage of rated power that they generate which should not be violated at every hour during their operation. In (2.61), d_{gs}^{min} and RP_t^{min} are the diesel generator lower limit in percent and rated power of the smallest diesel generator (kW), respectively.

$$Pdg_{t,h} \geq d_{gs}^{min} \cdot RP_t^{min} \qquad \forall h = 1, 2, ..., H \tag{2.61}$$

The unit commitment and dispatch of diesel generators is independent of the optimal planning problem. The optimal planning model determines the amount of required power

generated by diesel generation station, $P_{dg_{t,h}}$. However, the dispatch strategy of the various available diesel generators and their corresponding spinning reserves are determined based on a simple strategy, as indicated in [19]. This strategy considers a 15% spinning reserve margin and the commitment of the units is based on available generators' rated capacity and its comparison with the required power from diesel generators. It is assumed that there is enough diesel generation capacity available on-site to fulfill the requirement on diesel generation and reserve capacities.

The unit commitment for dispatch of diesel generators in a single-generator operation scheme can be presented as follows [19]:

$$P_{dg_{j,t,h}} = \begin{cases} P_{dg_{t,h}} & if \quad p_{j,t}^{min} \leq P_{dg_{t,h}} < p_{j,t}^{max} \\ 0 & otherwise \end{cases} \tag{2.62}$$

In(2.62), $P_{dg_{j,t,h}}$ is the power provided by diesel generator j, $P_{dg_{t,h}}$ the power required by diesel generation station, $p_{j,t}^{min}$ the pre-determined minimum operation set point of the diesel generator j and $p_{j,t}^{max}$ the pre-determined maximum operation set point of the diesel generator j. $p_{j,t}^{min}$ and $p_{j,t}^{max}$ are determined according to the following pre-specified constraints:

$$p_{j,t}^{min} = \begin{cases} d_{GS}^{min} \cdot RP_j \cdot s_{j,t} & if \quad j = 1 \\ p_{j-1,t}^{max} \cdot s_{j,t} & if \quad j = 2, ..., J \end{cases} \tag{2.63}$$

$$p_{j,t}^{max} = \begin{cases} d_{GS_1} \cdot RP_j \cdot s_{j,t} & if \quad j \ \ to\ j+1 \ \ turns \ \ on \\ d_{GS_2} \cdot RP_j \cdot s_{j,t} & if \quad j \ \ to\ j-1 \ \ turns \ \ on \end{cases} \tag{2.64}$$

In (2.63), d_{GS}^{min} is the lower operation limit of the smallest available generator, RP_j the nominal power of the diesel generator j, $s_{j,t}$ a pre-specified binary parameter to determine whether diesel generator j is operating in year t.

In (2.64), the nominal diesel generator power minus the spinning reserve is d_{GS_1} when switching to the next bigger generator, and d_{GS_2} when switching to the the next smaller generator, respectively. d_{GS_1} is set to 85% (considering 15% reserve capacity), while d_{GS_2} is set to a lower value compared to d_{GS_1}, i.e. 75%-80%, to reduce the number of generator start-ups by creating a hysteresis model that represents the waiting time until the load falls below the spinning reserve of the next smaller generator.

The power provided by renewable energy resources to supply load demand, $Preu_{i,t,h}$, is calculated in (2.65) based on the total amount of RE power generated by RE equipment. For each customer type, i, if the total generated RE power, $\sum_{k=1}^{K} Prea_{i,k,t,h}$, is higher than

the total load demand of that customer type, $PD_{i,t,h}$, the value of $Preu_{i,t,h}$ is equal to the demand of that group. Otherwise, $Preu_{i,t,h}$ is equal to the total generated RE power, $\sum_{k=1}^{K} Prea_{i,k,t,h}$, as presented in (2.65).

$$Preu_{i,t,h} = \begin{cases} \sum_{k=1}^{K} Prea_{i,k,t,h} & \sum_{k=1}^{K} Prea_{i,k,t,h} < PD_{i,t,h} \\ PD_{i,t,h} & \sum_{k=1}^{K} Prea_{i,k,t,h} > PD_{i,t,h} \end{cases} \tag{2.65}$$

Equation (2.66) calculates the available power from RE resources through multiplication of the output power of one unit of RE equipment, $P_{rem_{k,t,h}}$, by number of pieces of equipment, $EOS_{i,k,t}$.

$$Prea_{i,k,t,h} = P_{rem_{k,t,h}} \cdot EOS_{i,k,t} \tag{2.66}$$

The constraint given by (2.67) is added to make sure that the same equipment type for each customer group is deployed only once during planning horizon.

$$x_{i,k,t} = EOS_{i,k,t} \quad \forall x_{i,k,t} > 0 \tag{2.67}$$

2.4 Optimization of the Planning Model

The optimal planning problem can be solved to get the optimal sizing of the RE units for integration in the isolated microgrid. There exists a collection of optimization algorithms, rather than a universal optimization algorithm, each being appropriate for solving a particular type of optimization problem. Depending on the type of the objective function, constraints and optimization variables, an appropriate optimization algorithm has to be selected. If the objective function and all the constraints are linear functions, the problem is called a Linear Programming (LP) problem; otherwise, it is a Non-Linear Programming (NLP) problem. In some type of optimization problems, the variables only take integer values, such as the number of the generators in a power plant or the decision on whether a certain plan should be implemented or not. The mathematical formulation of these problems includes sets of integers or binary variables, and such problems are known as Integer Programming (IP) problems. If there is no restriction on some of the variables in the problem to be integer or binary variables, and there are some integer or binary variables in the problem, the problem is called a Mixed Integer Programming (MIP) problem.

2.4.1 Optimization with GAMS

The General Algebraic Modeling System (GAMS) has been designed with the capability of modeling different types of optimization problems, including linear, nonlinear and mixed integer. The main features based on which GAMS was mainly developed are providing a high level language for formulating large and complicated models, allowing to make simple and safe changes to the model, stating the problem by algebraic relationships and describing the model independent of solution algorithms [52].

The GAMS language is very similar to commonly-used programming languages and allows the user to enter data and describe the model in algebraic statements. The software takes care of the technical machine-specific problems such as address calculation and storage assignments. GAMS also offers many other desirable features such as portability of the GAMS models, allowing them to be solved on different types of computers, a file oriented system, and an interface providing the capability of the integration of GAMS with other existing and future user environments [52]. GAMS provides access to many solvers which can be run and list the solution without any knowledge of solver options or return codes. These solvers are used for solving different types of problems, depending on their features and the problem solving methods they use [53]. Some of the commonly used solvers are described as follows [53]:

- BARON: The Branch-And-Reduce Optimization Navigator (BARON) is used for solving nonlinear and mixed integer linear problems. It is used to solve deterministic global optimization algorithms using branch and bound type methods. These methods are guaranteed to provide global optimal solutions, if some conditions such as availability of finite lower and upper bounds on the variables are met.

- CONOPT: GAMS uses three families of nonlinear programming algorithms for solving nonlinear models and CONOPT is one of them. CONOPT is available in three versions, CONOPT1, CONOPT2 and CONOPT3 and all of these solvers find the local optimum. CONOPT often has a good performance with very nonlinear constraints; however, it is not easy to find out which algorithm performs better in solving a particular problem. CONOPT is also very good at finding the solution for models with few degrees of freedom and the square systems of equations without an objective function.

- CPLEX: GAMS/CPLEX provides the capability to mix the GAMS power with the power of CPLEX optimizers which are mainly designed for solving large problems in a fast manner. Linear, quadratically constrained and mixed integer programming problems can be solved using CPLEX solution algorithms.

- DICOPT: Discrete and Continuous OPTimizer (DICOPT) implements algorithms for solving mixed integer nonlinear programming problems. These types of problems include binary, integer and continuous variables. The MINLP algorithm inside DICOPT is capable of solving NLP and MIP sub-problems using solvers that are run under GAMS.
- MINOS: GAMS/MINOS is designed to find locally optimal solutions to linear and nonlinear programming problems. However, the first derivative of the nonlinear functions must exist (i.e., the nonlinear function must be smooth) . The global optimum can be found only if the nonlinear objective function and constraints are convex. Otherwise, several local optima may exist. MINOS is capable of solving LP, NLP, DNLP (Non-Linear Programming with Discontinuous Derivative) and RMINLP (Relaxed Mixed Integer Nonlinear Programming) problems.

2.5 Summary

This Chapter presented a background review of microgrids and various aspects related to their planning and operation. Microgrid control levels and frequency and voltage regulation were discussed, as well as the models and diagrams of frequency and voltage regulation in synchronous machines and inverters. The isolated microgrid frequency control block diagram and a three-phase power flow algorithm were presented that can be used for studying the regulation requirements of the isolated microgrids. The optimal reactive power planning problem which is used for improving voltage levels of microgrids was discussed. An introduction to the remote communities in Canada and the structure of electricity generation in northern Ontario remote communities was presented. The planning of RE-based remote community microgrids was discussed and a long-term renewable generation planning model was presented. Finally, an introduction to different types of optimization problems as well as the capabilities and flexibilities offered by GAMS for solving these problems was presented.

Chapter 3

Optimal Microgrid Planning Platform

This Chapter presents a novel optimal planning platform for integration of RE resources and energy storage systems in the microgrids of remote communities. The proposed planning platform incorporates the requirements for frequency and voltage regulations of the power system in the planning problem of an isolated microgrid. The impact of economic, technical and regulation constraints on renewable energy deployment in remote communities is considered through the proposed planning platform.

The proposed platform enables detailed studies of impact of ESS integration on increasing allowable penetration level of renewable resources and its contribution to reserve resources.

3.1 Introduction

The objective of the optimal planning platform is to determine the optimal combination of RE resources and ESS for integration in diesel fuel-based isolated microgrids of remote communities. This can be achieved through understanding the existing challenges, identification of the planning objectives and evaluation of the results. Some of the challenges are the high costs of RE and ESS technologies, reliable operation of RE and ESS resources and their impact on the operation of the isolated microgrid. The objectives are usually defined to serve the best interest of the project stakeholders. After the planning is completed,

the results are evaluated to assure that the performance of the designed system during its future operation will be satisfactory.

The proposed multi-stage optimal planning platform is developed to account for some of the potential challenges of RE integration in remote community microgrids. The planning problem is decomposed into identification, optimization, evaluation and decision making stages in the suggested platform. The structure of the planning platform is demonstrated in Figure 3.2.

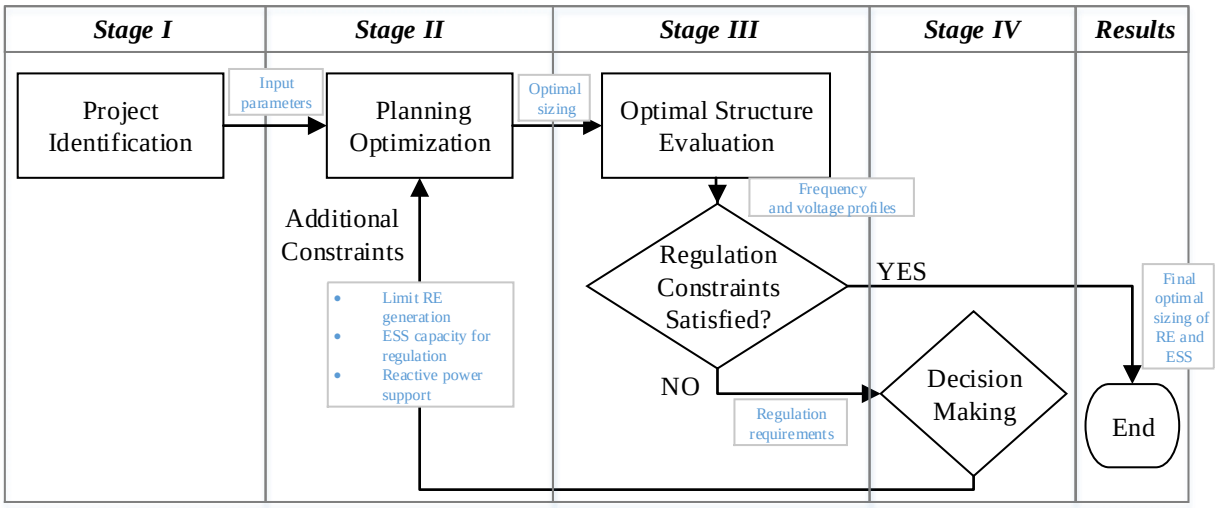

Figure 3.1: The structure of the proposed multi-stage optimal planning platform.

3.2 Proposed Optimal Planning Platform

The multiple stages of the planning platform are: Project identification, Planning optimization, Optimal structure evaluation and Decision making. These stages are explained in detail in the following subsections.

3.2.1 Stage I: Project Identification

The first step in initiating a successful microgrid planning project is a thorough study on various aspects of the isolated microgrid. The many aspects of an isolated microgrid include

objectives and challenges, available resources (energy resources, funding resources), available technologies, incentives, environmental concerns, economic parameters, characteristics of the existing power system and specific operation requirements of the system [54].

In many remote community RE projects, the main objective is to incorporate RE resources into the existing diesel generator-based microgrids to increase the generation capacity while reducing the electricity generation costs, increase the total benefits obtained by the community, improve the reliability of the power network and decrease the environmental impact of electricity generation resources.

Assessment of geographical characteristics of the microgrid location and on-site data collection help to determine the availability of RE resources such as wind, solar, hydro, geothermal and tidal energy for integration in the microgrids of the remote communities.

The availability of funding resources, incentives, cost values, energy prices, discount rates and economic benefits and downsides of carrying out an RE-based microgrid project must be studied by performing financial and economic evaluations.

Engaging the residents of the community in the RE deployment projects and raising awareness towards potential benefits of microgrid planning project are critical concerns that need to be addressed before beginning of the project. Providing relevant information on different aspects of RE-based microgrids, their characteristics and advantages, conducting surveys to collect residents' opinion and concerns on evolvement of such projects, developing skill sets and experience among local residents of the community for future operation and maintenance requirements of the microgrid, would help to better facilitate the process of integration of RE technologies in remote community microgrids.

Planning a well-designed and properly-manageable RE-based microgrid requires careful investigations on specific requirements of the microgrid operation (e.g., reserve capacity and regulation requirements), positive/negative environmental impacts (e.g., GHG emissions, added noise level, cutting trees or making changes to the environment), positive/negative social impacts (e.g., creating/limiting job opportunities) and potential challenges and barriers (e.g., community engagement and scarcity of resources) that have to be completed in the first stage of the planning project. The first stage requires contribution of various groups on different aspects of identification of the planning problem and entails multidisciplinary effort to identify the broad range of microgrid planning activities.

3.2.2 Stage II: Planning Optimization

The core component of the proposed planning platform is the mathematical model of the planning problem that embodies the identified objectives and constraints of the planning

project in terms of mathematical formulations.

Any optimization problem can be defined to minimize (or maximize) one or a set of objectives. In the case of a microgrid planning project, the set of objectives may include cost, environmental pollution, reliability and project's total benefits. Depending on the project's scope, one or more of these objectives can be selected.

In the proposed microgrid planning platform, maximizing community's social welfare is taken as the optimization objective. The optimization model presented in [19] is adapted to take the integration of ESS into account. The detailed description of the objective function and its components are presented in section 2.3.

In developing the mathematical optimization model, the structure of remote community microgrid is divided based on customer types, as described in subsection 2.2.1. It is assumed that the microgrid is divided into several subsidized and unsubsidized customer groups, each having the option to integrate RE resources and ESS and gain benefits by doing so. The customer groups also have the option to inject their excess generated power to the microgrid and receive power from the rest of the microgrid. Integration of a dump load may also be considered to avoid RE curtailment, in cases where ESS integration is not feasible. Figure 3.2 demonstrates the microgrid structure subdivided based on customer types.

The modifications made to the model presented in section 2.3 to comply with the subdivided structure of the microgrid, shown in Figure 3.2, and accommodate integration of ESS are as follows:

The savings component of the social welfare, given by (3.1), has an additional term taking the injection of power to the rest of the microgrid by each customer group into account. An incentive rate is assumed to encourage the RE generation and injection to the microgrid.

$$IS_{i,t} = [C_{d_i} \cdot (1 + r_i)^t + INC_i] \cdot \sum_{h=1}^{H} Preu_{i,t,h} + EXP_i \cdot \sum_{h=1}^{H} Pex_{i,t,h} \tag{3.1}$$

In (3.1), $Pex_{i,t,h}$ is the amount of energy injected by each customer group in a one-hour period and EXP_i the corresponding incentive in \$/kWh.

In order to address the replacement cost of the equipment, a cost component is added to the total project costs, as indicated in (3.2). The additional cost is equal to the cost of purchasing the same type and amount of equipment, L_k years after their first purchase, considering their future value at the time of replacement. L_k is the lifetime of the k^{th} equipment, in years. Although equipment lifetime depends on their operation and maintenance during their lifetime, it is assumed to be a pre-specified constant value.

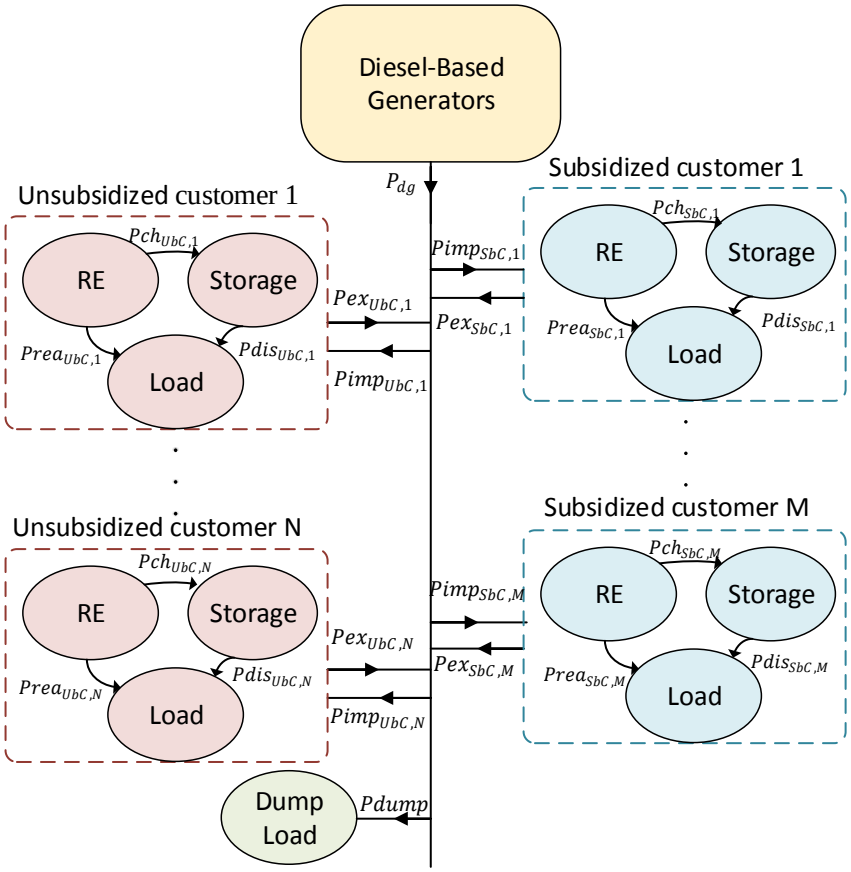

Figure 3.2: Microgrid structure subdivided based on customer types.

$$C_{i,t} = \sum_{k=1}^{K} C_{ce_{i,k,t}} + C_{bpmt_{i,k,t}} + C_{om_{i,k,t}} + C_{rep._{i,k,t}} \tag{3.2}$$

where $C_{rep._{i,k,t}}$ is the equipment replacement cost.

$$C_{rep._{i,k,t}} = [rc_{cap_k}.rp_k \cdot x_{i,k,t} \cdot CB_{i,k,t}] \cdot (1 - cc_d\% \cdot (t + L_k)) \cdot b_{cep} \cdot (1 - b_{efp}) \tag{3.3}$$

The capital cost of ESS has also an additional component proportional to its energy rating, $Esize_{i,t}$, added to the term proportional to its power rating, as given by (3.4). It

is also assumed that the costs of ESS decrease by $cce_d\%$ each year.

$$C_{cap_{i,ESS,t}} = [rc_{cap_{ESS}}.rp_{ESS} \cdot x_{i,ESS,t} \cdot CB_{i,ESS,t} + C_{energy_i} \cdot Esize_{i,t}] \cdot (1 - cce_d\% \cdot t) \quad (3.4)$$

In (3.4), C_{energy_i} is the ESS energy cost per kWh. The O&M cost of ESS also comprises two components, as given by (3.5): an annual fixed cost which depends on the power rating of the ESS and a variable cost which is proportional to the energy supplied/withdrawn to/from the ESS.

$$C_{om_{i,ESS,t}} = rc_{om_{ESS}} \cdot rp_{ESS} \cdot (1 + b_{om_t}) \cdot EOS_{i,ESS,t} + VarOMC_i \cdot \sum_{h=1}^{H} (Pch_{i,t,h} + Pdis_{i,t,h}) \quad (3.5)$$

In (3.5), $VarOMC_i$ is the ESS variable O&M cost in \$/kWh. $Pch_{i,t,h}$ and $Pdis_{i,t,h}$ are the power charged/discharged to/from ESS, respectively.

The constraints of the optimization problem are derived based on the scheme shown in Figure 3.2 and are presented in the following.

In (3.6), the power provided by the diesel generator units, $P_{dg_{t,h}}$, is represented by the difference between the power received from the microgrid, $Pimp_{i,t,h}$, and the power injected to the microgrid, $Pex_{i,t,h}$, summed over all customer groups. At each hour, only one of the variables $Pimp_{i,t,h}$ and $Pex_{i,t,h}$ can take a value, this constraint is represented by complementary symbol "$\perp$". A dump load is also considered to make sure the minimum diesel generation level is met at all times, especially when ESS is not integrated to the microgrid.

$$P_{dg_{t,h}} = \sum_{i=1}^{I} (Pimp_{i,t,h} - Pex_{i,t,h}) + Pdump_{t,h} \qquad ,\forall i,t,h \qquad Pimp_{i,t,h} \perp Pex_{i,t,h} \quad (3.6)$$

Equation (3.7) represents the demand-supply balance equation for each customer group. The load demand of each customer type, $PD_{i,t,h}$, is provided by the deployed RE resources, $Prea_{i,k,t,h}$. The excess power is injected into and the power deficit is imported from the rest of the microgrid. The ESS can also provide or absorb power, $Pstorage_{i,t,h}$, depending on the microgrid operational requirements.

$$Pimp_{i,t,h} + Prea_{i,k,t,h} + Pstorage_{i,t,h} - Pex_{i,t,h} - PD_{i,t,h} = 0 \quad (3.7)$$

The lower limit of diesel generator operation should not be violated, as described as a constraint in (2.61). The detail of operation of the diesel generators is not included in this

model. However, it is assumed that operation of single or multiple diesel generators takes the operation constraints of the diesel generators into account, as presented in [19]. These constraints include: minimum loading constraint, spinning reserve constraint, maximum power constraint and minimum operating time of each unit [15].

Operation of ESS also has specific conditions and constraints which are described in (3.8)-(3.13)

The power supplied/withdrawn to/from ESS, $Pstorage_{i,t,h}$, takes positive or negative values. Hence, it is defined in (3.8) as the difference of two positive variables, $Pdis_{i,t,h}$ and $Pch_{i,t,h}$, which represent the power withdrawn from the ESS and power supplied to the ESS, respectively. Note that, at each hour, only one of the variables $Pdis_{i,t,h}$ and $Pch_{i,t,h}$ can take a value.

$$Pstorage_{i,t,h} = Pdis_{i,t,h} - Pch_{i,t,h} \quad ,\forall i,t,h \quad Pch_{i,t,h} \perp Pdis_{i,t,h} \tag{3.8}$$

The energy stored in the ESS and the power supplied/withdrawn to/from it are related by (3.9).

$$Energy_{i,t,h+1} = [Pch_{i,t,h} \cdot \eta_{ch} - \frac{Pdis_{i,t,h}}{\eta_{dis}}] + Energy_{i,t,h} \tag{3.9}$$

where $Energy_{i,t,h}$ is the available energy stored in the ESS and η_{ch} and η_{dis} are the charging and discharging efficiencies of the ESS.

The ESS power and energy values are bounded within their minimum and maximum limits:

$$|Pstorage_{i,t,h}| \leq EOS_{ESS_{i,t}} \cdot rp_{ESS} \tag{3.10}$$

$$SOC^{min} \cdot EES_{i,t} \leq Energy_{i,t,h} \leq SOC^{max} \cdot EES_{i,t} \tag{3.11}$$

In (3.11), SOC^{min} and SOC^{max} are the allowable minimum and maximum values for state of charge of the ESS. $EES_{i,t}$ represents the cumulative number of ESS energy rating at investment year t, given by (3.12).

$$EES_{i,t} = \begin{cases} Esize_{i,t} & t \leq 1 \\ EES_{i,t-1} + Esize_{i,t} & t > 1 \end{cases} \tag{3.12}$$

Equation (3.13) formulates the relation between the energy size and the power size of the ESS, as different types of ESS have particular ranges of energy to power ratio [55].

EPR^{min} and EPR^{max} are the minimum and maximum energy to power ratios of the ESS, respectively.

$$EPR^{min} \cdot x_{ESS_{i,t}} \cdot rp_{ESS} \leq Esize_{i,t} \leq EPR^{max} \cdot x_{ESS_{i,t}} \cdot rp_{ESS} \tag{3.13}$$

The renewable energy used to supply the load demand, $Preu_{i,t,h}$, is calculated in (3.14) based on the amount of load power demand that has been provided by customers' RE resources and has not been received from the rest of the microgrid.

$$Preu_{i,t,h} = PD_{i,t,h} - Pimp_{i,t,h} \tag{3.14}$$

Equations (2.66) and (2.67) are the remaining constraints to calculate the available power from RE resources and limit deploying the same equipment types.

The mathematical model of the planning optimization problem can be solved using an optimization solver engine. The results of the optimization problem determine the numbers and ratings of RE resources and ESSs for integration in the microgrid, as well as their respective hourly dispatch scheme.

3.2.3 Stage III: Optimal Structure Evaluation

The optimal sizes of the RE resources and ESSs, determined in the previous stage, are obtained through maximizing or minimizing a certain set of objectives. However, the performance of the system in real-time operation depends on many control and management actions. Although these actions take place in a time frame much different than that in the project planning phase, which is usually much before the system operation is started, they are eminently affected by the selected system structure.

In the proposed planning platform, in order to evaluate the system performance after integration of RE and ESS, frequency and voltages are obtained through simulation to investigate whether the regulation requirements are met. The impact of system sizing and structure on the frequency and voltages of the system is investigated in this stage.

Frequency Regulation

The most significant impact of integration of RE on frequency of an isolated microgrid is causing notable frequency deviations through introducing fluctuations with rapid ramp rates to the generated power in the microgrid. In many isolated microgrids where the

penetration level of RE is low or medium and RE resources are mainly operating in grid-supporting mode, RE generation can be considered as negative load. Hence, RE integration contributes in building a fast fluctuating load profile that must be compensated by dispatchable generation units such as fuel-based generators and ESS. However, generators and ESSs have limited capacity to compensate for all those fluctuations, depending on their size, characteristics and operating condition.

The frequency block diagram of an isolated microgrid, shown in Figure 2.9, is used in this stage to simulate the frequency profile of the system in the presence of RE generation. The results of optimization problem in the previous stage, which determine the optimal RE and ESS sizes, are used to define the amount of RE generation and form the load profile, considering actual load demand and RE negative load. High-resolution data (one-second resolution) is used in this stage to simulate the system frequency. Evaluation of the system frequency and its comparison with desired regulation range for the microgrid, determine whether extra decisions for revising the structure of the microgrid are required or there is no need for further actions.

Voltage Regulation

One of the main features of connection of DERs to the distribution networks is the reverse power flow possibility. In traditional distribution networks, the power flows from a main distribution substation to the end users, whereas in the networks with interconnected distributed generation the power flow direction may be reversed. As a result, this may cause over voltages in a distribution network. The voltage rise due to injection of power at a network feeder is calculated as follows [56]:

$$\Delta V = \frac{PR + QX}{V} \tag{3.15}$$

In (3.15), ΔV is the change in voltage at the DG connection point due to injection of active and reactive powers, P and Q by the DG. X and R are the reactance and resistance of the feeder connecting the DG to the microgrid. V represents the nominal voltage of the DG at its terminals.

In distribution networks, the ratio of X/R is relatively low and changes in the injected active power by the DG unit cause voltage variations on the distribution network. Furthermore, in long distribution feeders with considerable line resistances, the voltages at the end of the feeder may face under voltages that need to be taken care of. Thus, to investigate the impact of RE integration on voltage levels at different buses in an isolated

microgrid, a power flow analysis model, such as the one presented in subsection 2.1.4, is used to simulate the voltage profile of the system, for various instances during system's operation. The simulated voltage profile is compared with the accepted voltage ranges for the system and further actions and decisions to revise the system structure are taken accordingly.

At the end of this stage, the frequency and voltage profiles of the system, after inclusion of RE resources, are simulated and evaluated to determine whether the system's regulation constraints are satisfied. It should be noted that, the simulated voltage and frequency profiles cover most of the conditions that can happen in the system during various time periods with different loading and available generation conditions, and due to the existing trends and patterns in the load demand and RE generation profiles, it can be inferred that most of the possible frequency and voltage events are covered. The regulation constraints are determined based on the purpose the microgrid is serving (e.g., military, mining or remote community) and the requirements imposed by the system operator. Such constraints for isolated microgrids are often more flexible than those for grid-connected microgrids. However, it is required to assure the delivered power to the customers meets certain criteria.

3.2.4 Stage IV: Decision Making/ Structure Revising

In this stage, the results of the stage III are used to decide whether changes have to be made to the optimization model constraints in stage II based on satisfaction of the frequency and voltage regulation constraints.

Frequency Regulation Constraints

If the frequency profile of the system after addition of RE resources, derived in previous stage, does not meet the regulation requirements of the system, one or a combination of the following actions can be implemented.

1. *Limiting RE penetration level:* In this case, the power generated by RE resources is limited to reduce the share of fluctuating power injected to the microgrid. To implement this option, the maximum allowed RE penetration level, $M_{pen.}$, should be identified by studying the effect of RE penetration level on frequency deviations using (2.9) and the block diagram of Figure 2.9.

The relationship between frequency deviations and RE generation fluctuations, given by (2.9), can be simplified into a linear relationship between RE power fluctuations and

deviations in frequency, where the absolute value of frequency deviations increases by increasing the fluctuations in RE power, as shown in Figure 3.3. $\Delta\omega_{max}$ and $\Delta P_{RE,max}$ are the maximum frequency deviation and maximum RE power fluctuations of optimal RE generation, determined by the results of planning optimization model (Stage II). $\Delta\omega_{allowed}$ and $\Delta P_{RE,allowed}$ are the accepted frequency deviation range and its corresponding RE power fluctuations, respectively. The maximum allowed RE penetration level, $M_{pen.}$, is defined as the ratio of the allowed RE power fluctuations to the maximum RE fluctuations.

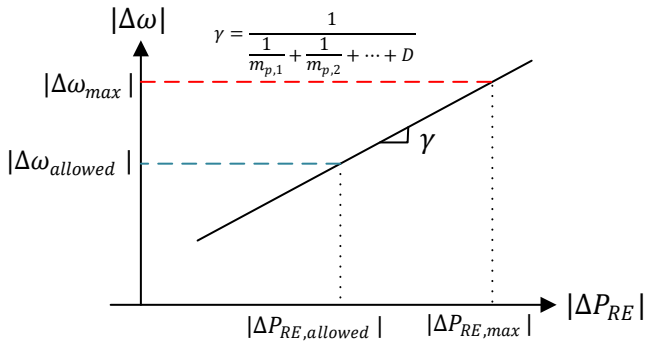

Figure 3.3: The relationship between frequency deviation and the corresponding RE power fluctuation.

$$M_{pen.} = \frac{|\Delta P_{RE,allowed}|}{|\Delta P_{RE,max}|} \tag{3.16}$$

The revised optimization model should include a constraint to enforce the maximum allowed RE penetration limit. Therefore, an additional constraint, given by (3.17), is added to the optimization problem to define the maximum limit of RE penetration level.

$$\sum_{i=1}^{I}\sum_{k=1}^{K} Prea_{i,k,t,h} \leq M_{pen.} \cdot \sum_{i=1}^{I}\sum_{k=1}^{K} Prea^{*}_{i,k,t,h} \qquad \forall\, t,h \tag{3.17}$$

In (3.17), $Prea^{*}_{i,k,t,h}$ is the available renewable resource power, determined from the solution of the optimization problem in Stage II, according to:

$$Prea^{*}_{i,k,t,h} = P_{rem_{k,t,h}} \cdot EOS^{*}_{i,k,t} \qquad k : RE\ resources \tag{3.18}$$

where $EOS^{*}_{i,k,t}$ is the optimal sizes of the RE resources obtained in Stage II.

2. *Allocating ESS capacity for frequency reserve:* Utilization of an energy storage system is a robust solution for providing regulation and load following services to the microgrid. Integration of an ESS allows maximum optimal RE penetration, while satisfying the regulation constraints. However, proper sizing of an ESS, contributing to frequency control reserves requires a thorough investigation leading to a relation between the required primary and secondary control reserve capacities and regulation specifications of the microgrid.

According to Figure 2.9 and (2.10)-(2.18), the slope of droop characteristic, m_p, and the participation factor of the ESS, α, are the main factors affecting the power and energy requirements of the ESS for primary and secondary control actions. The droop characteristic affects the amount of primary frequency reserve capacity in terms of available instantaneous power that should be provided by the ESS upon occurrence of a mismatch between load and generation as presented in (2.10)-(2.12). The secondary frequency control reserve capacity allocated by the ESS to contribute in secondary control actions is proportional to the participation factor of the ESS, as presented in (2.16)-(2.18). However, the primary frequency reserve is part of ESS power capacity, while the secondary reserve capacity is allocated from ESS energy capacity. Hence, the expected reserve capacity of the ESS to participate in primary and secondary frequency control must be recognized and incorporated in the planning optimization problem. It is also reasonable to devise incentives to account for the power and energy capacity of the ESS that is reserved for primary and secondary frequency control actions.

The profile of the ESS primary control reserve capacity normalized by ESS rated power capacity versus frequency deviations, which is derived by changing the value of $m_{p,ESS}$ and recording the values of frequency deviations and power variations (according to (2.10)-(2.12)), determines the percentage of the power capacity that should be reserved for primary control actions (β_{fP}). Also, the profile of the ESS secondary control reserve capacity normalized by ESS rated energy capacity versus participation factor of ESS in secondary control, which is derived by changing the value of α_{ESS} and recording the energy requirements, defines the percentage of the energy capacity to be reserved for secondary frequency control (β_{fE}). The values of β_{fP} and β_{fE} are selected according to the desired tolerance band for frequency deviation and extent of participation of ESS, defined by system operator, as illustrated in Figure 3.4.

The revision of the planning optimization problem includes extra terms added to the existing equations to take into account the incentives and the allocated capacities of ESS for its contribution in the frequency control actions, defined in (3.19)-(3.21). The incentives

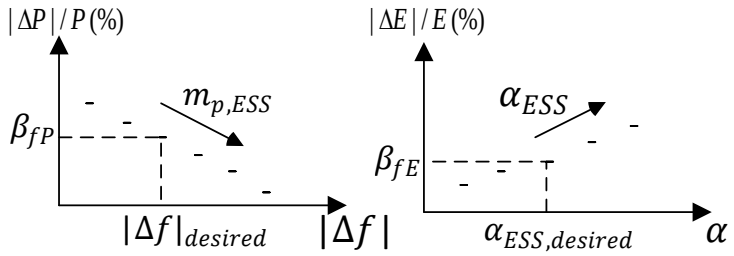

Figure 3.4: Profiles of reserved power capacity of ESS for primary frequency control vs. frequency; and reserved energy capacity of ESS for secondary frequency control vs. participation factor.

are included in the savings component of the social welfare, as indicated by (3.19).

$$IS_{i,t} = [C_{d_i} \cdot (1+r_i)^t + INC_i] \cdot \sum_{h=1}^{H} Preu_{i,t,h} + EXP_i \cdot \sum_{h=1}^{H} Pex_{i,t,h} \\ + PINC_i \cdot \beta_{fP}\% \cdot EOS_{i,ESS,t} \cdot rp_{ESS} + EINC_i \cdot \beta_{fE}\% \cdot EES_{i,t} \tag{3.19}$$

In (3.19), $PINC_i$ and $EINC_i$ are the incentives for the reserved power and energy capacities of ESS for frequency control. Also, β_{fP} and β_{fE} are the percentages of the power and energy capacities of the ESS to be allocated for frequency control.

The modified constraints take the extra capacity required for frequency reserve allocation into account, as demonstrated in Figure 3.5 and described by (3.20) and (3.21).

$$|Pstorage_{i,t,h}| \leq EOS_{i,ESS,t} \cdot rp_{ESS} \cdot (1 - \beta_{fP}\%) \tag{3.20}$$

$$SOC^{min} \cdot EES_{i,t} \leq Energy_{i,t,h} \leq (SOC^{max} \cdot EES_{i,t}) - (\beta_{fE}\% \cdot EES_{i,t}) \tag{3.21}$$

Voltage Regulation Constraints

The voltage profile of the system, derived in Stage III, determines whether there is a need for additional actions to keep the voltages regulated. If it is required to make extra decisions for allocating more resources or revising the structure of the system, there are two possible courses of action.

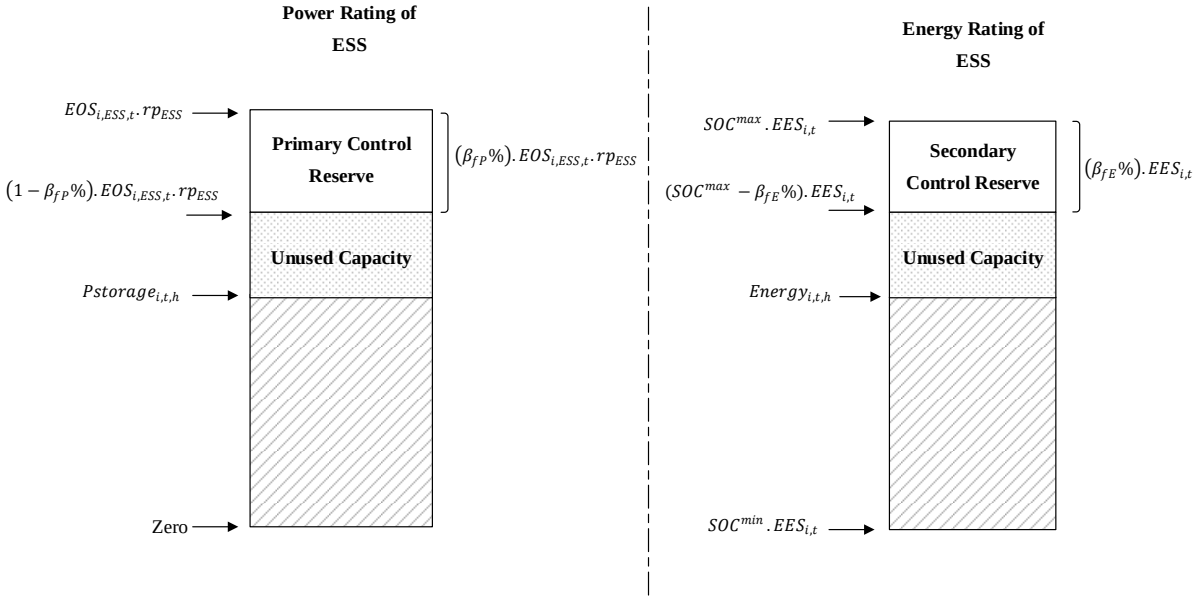

Figure 3.5: The ESS power and energy ratings, capacities allocated for frequency control and the remaining capacity for energy management.

1. *Limiting RE generation:* Similar to the case where frequency regulation limits are not met, in this case the RE generation level can be limited in order to make sure the voltage regulation requirements are satisfied. Limiting the RE generation level is one of the feasible ways to avoid the problem of over voltages, especially when utilizing ESS for storage of extra active power is not economically beneficial [57]. In many remote community isolated microgrids, inverters interfacing RE resources to the microgrid operate at unity power factor to maximize the utilization of the installed capacity. Thus, if the injected power to the microgrid increases the voltage deviation at the connection point beyond specified limit, the active power injection should be limited or the over voltage should be compensated for with reactive power absorption. For the case where the inverter operates at unity power factor, the maximum allowed voltage deviation determines the corresponding maximum allowable power to be injected to the microgrid [57], as given by (3.22).

$$\Delta V_{max,allowed} = \frac{R \cdot P_{max,allowed}}{V_{max}} \tag{3.22}$$

In (3.22), $P_{max,allowed}$ is the maximum power at unity power factor and V_{max} the maximum voltage at inverter terminals. $\Delta V_{max,allowed}$ is the maximum voltage deviation at the

microgrid connection point. R is the resistance of the feeder connecting the DG to the microgrid

If injection of more active power without increasing the voltage at the connection point is desired, reactive power must be absorbed. Assuming the same voltage for the grid connection point, the amount of reactive power to be absorbed can be calculated as [57]:

$$Q = -\Delta P \frac{R}{X} \tag{3.23}$$

where ΔP is the difference between the amount of injected active power for the case where inverter operates at unity power factor and the case with increased amount of active power. However, this increased active power injection requires an inverter with higher power capacity.

If the installed RE resource is to be operated at unity power factor and there is no storage mechanism available, the amount of active power injected at the point of connection to the microgrid should be limited to the maximum value that keeps the voltage deviation within acceptable limits. Implementing generation curtailment control algorithms is an effective way of avoiding over voltages at DG connection buses. However, incorporation of RE resources with high installation costs at remote communities is only reasonable if the use of available resources is maximized and curtailing the power generation might not allow making the most use of available resources. In this case, a guideline can be provided by the system operator to determine the maximum allowable active power injection for interconnecting DGs, and the sizing of DG resources can take that maximum generation level into account. Such constraints for limiting the maximum RE active power at the point of connection to the microgrid can be implemented as follows:

$$\sum_{k=1}^{K} Prea^{n}_{i,k,t,h} \leq N^{n}_{pen.} \cdot \sum_{k=1}^{K} Prea^{n*}_{i,k,t,h} \qquad \forall\ i,t,h,n \tag{3.24}$$

where $N^{n}_{pen.}$ is the ratio of the maximum allowable injected power at the point of connection to the microgrid to the maximum active power injected at each network bus to the microgrid, determined from optimization solution, for every point of connection of RE resources, n.

$$N^{n}_{pen.} = \frac{P^{n}_{max,allowed}}{\sum_{k=1}^{K} Prea^{n*}_{i,k,t,h}} \tag{3.25}$$

2. *Providing reactive power support to the microgrid:* Another solution for assuring the acceptable regulation of voltages at all network buses is to incorporate reactive power

compensation devices in the network and/or use the available resources such as ESS units for providing reactive power support for voltage regulation. Both cases can be considered by running an ORPP in order to minimize a certain objective function such as the amount/cost of reactive power required for keeping the voltages regulated. The results of the ORPP determine the sizes and locations of required reactive power support.

Defining the ORPP problem depends on many parameters including the microgrid structure and locations, sizes and operating conditions of generation resources. However, the general guideline is to determine the candidate buses requiring reactive power support and define the objective function accordingly. The constraints of the ORPP problem can vary, but the main constraints include minimum and maximum limits of voltage at network buses, power flow equations and minimum and maximum reactive power capacities of Var compensation devices. For the case where ESS unit is selected to participate in Var support, the sizing of the inverter unit should be performed accordingly to accommodate both active power and reactive power transfer. In this case the inverter should be oversized by a specific percentage with respect to the size of ESS in order to be able to support reactive power exchange while maintaining the required active power exchange capability.

Algorithm 1 summarizes the decision making procedure leading to revising constraints of the optimal planning problem according to operation simulation results and their comparison with the regulation constraints. These extra constraints enforce one or a combination of the following actions: (i) set a limit on the penetration level of RE resources, (ii) determine the additional ESS capacity to be allocated for regulation actions, (iii) allocate reactive power compensation devices.

At the end of this stage, the planning optimization problem of Stage II is solved again to reach a new optimal solution which makes sure that the frequency and voltage regulation requirements of the system are satisfied.

In order to demonstrate the effectiveness of the proposed multi-stage planning platform, a case study is developed for planning of the isolated microgrid of the northern Ontario remote community of Kasabonika Lake First Nation (KLFN). The next section describes the multiple stages of carrying out a microgrid planning project for KLFN.

3.3 Case Study: Kasabonika Lake First Nation Community (KLFN)

Kasabonika lake first nation is a northern Ontario community located approximately 500 km north of Thunder Bay (Ontario, Canada), with a population of about 1,100 people. The

Algorithm 1 Decision Making Algorithm

INPUT: Frequency and Voltage Profiles

procedure
  while $|\Delta f| > \Delta f_{max}$ **do**
    if ESS participation in frequency control is not feasible **then**
      Determine Maximum Allowed RE Generation Level
    else
      Allocate ESS Reserve Capacity for Frequency Regulation Services
    end if
  end while
  while $|\Delta V| > \Delta V_{max}$ **do**
    if Reactive power support is not feasible **then**
      Limit the RE Generation Level
    else
      Allocate Var Compensation Devices and/or ESS Capacity Participation in Voltage Regulation
    end if
  end while
end procedure

access to the community is by plane all-year-round or through winter roads, when seasonal conditions permit. In 2014, KLFN community possessed three installed diesel generators rated at 400 kW, 600 kW and 1 MW to supply the electric demand of the community which was about 12.9 MWh/day, with a peak demand of 900 kW in winter. A 1.6 MW diesel generator is added to the diesel generation station while the 400 kW generator is removed and is not operating anymore. Three 10 kW Bergey wind turbines [58] and a 30 kW Wenvor wind turbine [59] have been installed at KLFN by Hydro One Remote Communities Inc. (HORCI), and measurement equipment has been deployed for data collection to be used for studying the impact of integration of RE in northern communities. Table 3.1 summarizes the data related to the power generation and consumption at KLFN.

The three existing diesel generators in KLFN are run based on a simple dispatch strategy which allows running only one diesel generator at a time, except for a very short overlap period when one generator turns on and the other one shuts down. Based on the dispatch strategy, once a generator reaches 90% of its rated power capacity and continues providing a power higher than 90% of its rated power for 2 minutes, the next larger generator is turned on and the smaller one is shut down. On the other hand, when the load demand

Table 3.1: Summary of KLFN data

Population	Around 1,100
Electricity demand[a]	12.9 MWh/day
Peak demand[b]	900 kW
Existing diesel generation[a]	3 Generators: 400, 600 and 1000 kW
Existing RE resources[a]	3×10 kW Burgey Wind turbine
	30 kW Wenvor Wind Turbine
	10 kW rooftop PV system[c]

[a] Year 2014,[b] Winter Peak, [c] Community Water Treatment Plant

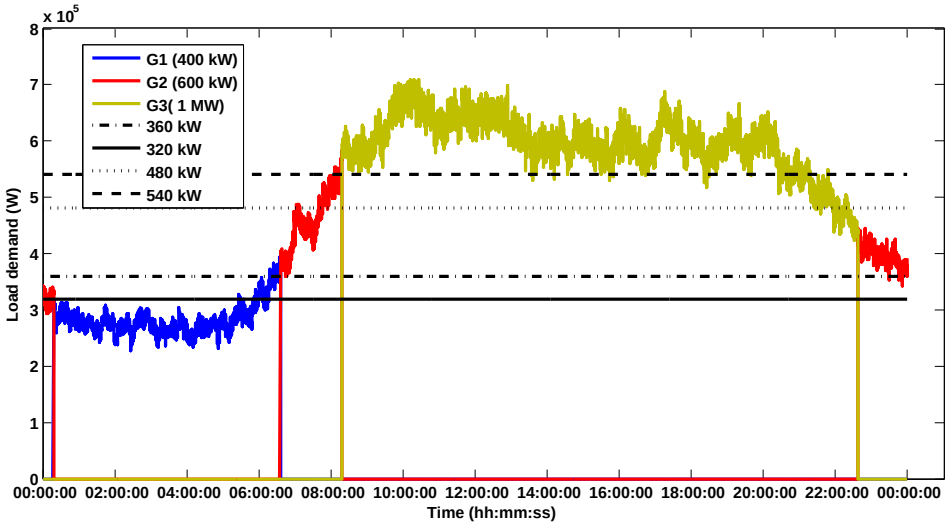

Figure 3.6: The dispatch strategy of the 3 diesel generators at KLFN.

falls below 80% of the rated output of the next smaller generator and stays in that condition for 15 minutes, then the smaller unit will turn on and supply the load, while the larger unit will turn off.

The dispatch of the generators for a typical selected day in KLFN, the frequency profile of the system and the voltage profile at the generation bus for the same selected day are shown in Figures 3.6-3.8, respectively. The major spikes observed in these profiles are related to the transition of power between diesel generator units.

Besides the high cost of fuel, high O&M cost, fuel transportation issues and high carbon emissions, falling into the Load Restriction (LR) status has been the community's main

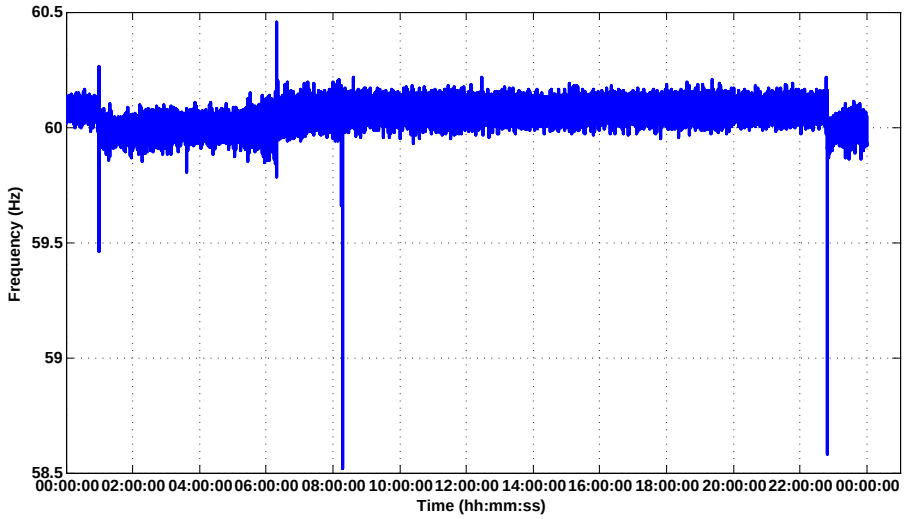

Figure 3.7: Frequency profile of the system for the selected day at KLFN.

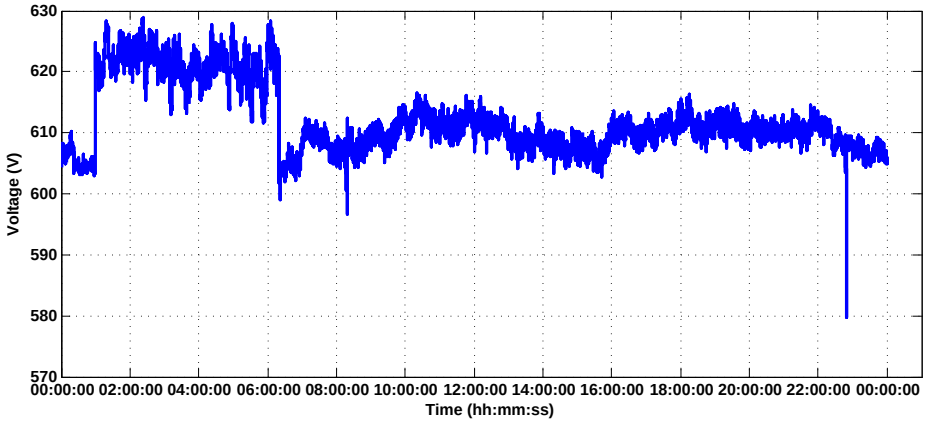

Figure 3.8: Voltage profile (RMS of phase A voltage) at generation bus for the selected day at KLFN.

challenge since 2007; this means that the community has reached a point where the peak load constitutes more than 75% of the diesel generation capacity, according to HORCI. By 2014, the peak demand exceeded 90% of the capacity of the largest diesel generator unit. Consequently, the community was not allowed to connect any new consumption to the distribution system, implying that no new building can be built that will receive electricity supply; as a result, in past few years, the community has been in a no-growth scenario, and has been trying to work with Aboriginal Affairs and Northern Development Canada (AANDC) to get funding to upgrade the plant and increase the power generation capacity; meanwhile, the community is looking for alternatives to provide additional electricity supply to help them deal with growth issues. There are some very short-term and some longer-term development alternatives to deal with the need for power generation capacity expansion. For example as a short-term solution, solar panels have been installed on the roof top of the water treatment plant. Longer-term plan includes integrating renewable energy resources (such as wind and solar) and energy storage, to form an isolated microgrid which certainly requires further studies in different aspects, such as feasibility study, component sizing, and control and management of the microgrid.

The following subsections describe the details of planning an RE-based isolated microgrid for KLFN.

3.3.1 Stage I

Recognizing the available resources is the first step in starting a microgrid planning project. In most remote communities, on-site measured wind speed and solar irradiation data is rarely available. These type of data is usually estimated and might not be a good representative of the real available resources at these locations. In case of KLFN community, a set of on-site measured data (including three phase voltages, currents, active, reactive and apparent powers, power factor and frequency) with one second resolution has been collected by installing measurement equipment at the diesel generation station, three 10 kW Bergey wind turbine terminals, community store, water treatment plant, solar panel terminals, community school, nursing station, police station, sewage and a number of residential households. The measured output powers of installed wind turbines and solar panels is used as the baseline for selecting the ratings of wind turbines and solar panels for integration in KLFN.

The cost analysis of equipment in remote communities is performed differently compared to on-grid installations. Special deployment conditions such as limited local equipment, site remoteness, limited local technical resources, difficulty of transportation and

Table 3.2: Equipment deployment cost at KLFN [60]

	Total Installation Cost	O&M Cost
Small Wind Turbine ($P_{rated} = 50kW$)	13,414 $/kW	0.15 $/kWh
Solar Photovoltaic	8,365 $/kW	0.09 $/kWh
Battery Bank	650 $/kWh	0.08 $/kWh
Diesel Generator	400 $/kW	0.84 $/kWh

short construction season impact the overall cost of equipment at remote communities. Therefore, equipment costs can reach up to 2.5 times of those for on-grid installations [60]. The cost of deployment of wind turbines include the costs of turbine, tower, foundation and crane, as well as cost of installation, logistics, and spare parts. For solar PV, the deployment cost include costs of the panels, converter and connection equipment. The cost of wind turbine at remote communities ranges between $5000 and $7000 per kW for the turbine itself. Including the additional costs, the total cost will be around $13000-$14000 per kW [60]. The installation cost of solar panels is considerably lower compared to that of wind turbines due to their modularity which makes the transportation easier. The total installation cost of solar panels including the cost of the panels, converters and spare parts in remote communities ranges between $8000 and $9000 per kW [60]. The installation cost of battery storage system at KLFN, based on the data available for a Rolls/Surrete battery unit (4KSS21P), 4V, 1104Ah, 4.42kWh, considering the cost of the equipment, inverter, connection and transportation, is estimated at around $650 per kWh. The cost of additional diesel generator units is estimated to range from $200 to $500 per kW. Table 3.2 summarizes the estimated total installation and O&M costs of the RE equipment at KLFN.

In the past few years, various research groups and individuals have been involved with KLFN community in order to identify different aspects of the microgrid planning project, including community engagement, identifying the available resources and existing challenges [61].

3.3.2 Stage II

The optimization model of the planning problem is solved to find the optimal RE combination over a 20-year planning horizon for KLFN. The first five years are considered as the investment period of the project and the investment decisions and operation of the

equipment are assumed to be implemented at the beginning of each year. The community store (with peak consumption of around 70 kW at 2014) and water treatment plant (with peak consumption of around 40 kW at 2014) are considered unsubsidized customers and the rest of the community load falls under subsidized electricity rate category. The loss of opportunity cost, (2.56), is assumed to be zero for KLFN. The equipment lifetime, except for the ESS, is assumed to be 20 years. Thus, it is assumed that the replacement costs of the equipment is out of scope of the current funding mechanisms and is equal to zero in this case. It is also assumed that installation and replacement of diesel generators is not within current funding structure. The funding resources to replace or purchase new diesel generators and other equipment is likely to be provided by different resources. Thus, they are not included in the optimization problem. It is assumed that the community becomes the owner of added RE and ESS equipment; However, operation and maintenance of all the generation units and equipment is the responsibility of the utility, i.e., HORCI. Incentive mechanisms are devised to encourage the integration of RE resources; they include allocation of extra funding for integration of ESS and providing incentives to subsidized customers for deployment of RE resources. Table 3.3 lists the parameter values used for optimizing the microgrid structure for KLFN.

The optimization problem is formulated as a mixed integer linear programming (MILP) problem, where the variables are the number of wind turbine and solar PV units, the power and energy capacities of ESS units and the dispatch of power among generation units and the loads for 20 years. The optimization problem is solved for two cases, with and without considering ESS units, as there might be conditions where incorporating ESS is not feasible. The problem is solved using GAMS/CPLEX solver on a desktop PC. The proposed planning platform is used during the planning process of a remote microgrid rather than the real-time operation. Hence, the simulation time is not a concern in this work and is not measured.

A summary of the results of the planning optimization problem is presented in Table 3.4. Two different cases, with and without considering ESS integration, are illustrated.

Inclusion of ESS helps to increase the penetration level of RE by almost 100% for both customer groups. The social welfare is almost doubled after inclusion of ESS. However, the project's initial capital cost increases from \$1.79M to \$3.27M. Thus, higher initial investments are required when considering ESS integration in the planning project.

The unsubsidized customers make the most benefit by integrating RE resources, while RE integration for subsidized customers is hardly justified considering the low income obtained as a result of paying already lower electricity rates.

The diesel generator power generation over the 20-year planning horizon decreases by

Table 3.3: Parameter values of case study [19]

Parameter		Value	Parameter		Value
b_{cep}		0.1	EXP_i	(\$/kWh)	0
b_{efp}		$0.5^{a,b}$ 0.7^{c}	EPR_{max}		5
b_{omt}	(%)	0	EPR_{min}		1
C_{d_i}	(\$/kWh)	0.926^{d} 0.394^{e}	INC_i	(\$/kWh)	0^{d} 0.3^{e}
C_{energy}	(\$/kWh)	600	r_b	(%)	5
$d_{gs_{min}}$		0.4	r_{d_i}	(%)	6
blt_k	(years)	15	r_i	(%)	1
η_{ch}	(%)	95	RP_t^{min}	(kW)	400
η_{dis}	(%)	95	SOC_{max}	(%)	80
cc_d	(%)	1.5	cce_d	(%)	3
rp_k	(kW)	5^{a} 20^{b} 5^{c}	SOC_{min}	(%)	20
rc_{om}	(\$/kW.year)	130^{a} 250^{b} 25^{c}	rc_{cap}	(\$/W)	9^{a} 12^{b} 2^{c}
$VarOMC_i$	(\$/kWh)	0.0011			
[a]PV,[b] Wind,[c] ESS, [d]Unsubsidized customer,[e] Subsidized customer					

almost 2% when considering ESS integration compared to the case without ESS. The total diesel fuel consumption over 20 years for the case without ESS is 97% of the base case without any RE integration. Integration of ESS and RE can reduce the fuel consumption to 95% of the base case with zero RE penetration. The low capacity factors of RE resources at KLFN and high costs of RE equipment deployment are the main factors limiting the penetration level of RE resources at KLFN. In remote communities with larger capacity factors for RE resources and lower cost of transportation, the planning problem's solution allows higher RE penetration level, resulting in lower diesel fuel consumption. Further decrease in cost of RE integration will also lead to solutions suggesting higher RE penetration level. These will become more clear with the sensitivity analysis in Chapter 5.

Table 3.4: Summary of the results of the multiple-year planning problem

	Unit	Without ESS			With ESS		
		Store	WTP	SbC	Store	WTP	SbC
Solar PV size	kW	50[a]	30[a]	100[b]	240[b]	125[b]	150[b]
Wind turbine size	kW	60[b]	20[b]	-	-	-	-
ESS power size	kW	-	-	-	145[b]	100[b]	-
ESS energy size	kWh	-	-	-	725[b]	495[b]	-
Percentage of load demand provided by RE[c]	%	20.99	19.95	1.35	38.45	43.53	2.02
Capital Cost (discounted value)	M$		1.79			3.27	
Solar	M$	0.4	0.25	0.66	1.6	0.83	0.99
Wind	M$	0.65	0.22	-	-	-	-
ESS	M$	-	-	-	0.57	0.39	-
Total income (discounted value)	M$	0.758	0.348	0.384	1.208	0.630	0.575
Total cost (discounted value)	M$	0.665	0.307	0.360	1.024	0.560	0.540
Welfare over 20-year horizon	M$	0.093	0.041	0.024	0.184	0.07	0.035
Total Welfare	M$		0.158			0.287	
Average diesel power generation	GWh/year		5.86			5.75	

WTP: Water Treatment Plant, SbC: Subsidized Customer, [a]1st year,[b] 5th year,[c] 6th year
Average diesel power generation for the case with no RE integration: 6.017 GWh/year

3.3.3 Stage III

The optimal unit sizes, obtained in Stage II, are used to evaluate the impact of optimally selected sizes of generation units on the frequency and voltage profile of the system. In these evaluation studies, the RE output power is considered as negative load since the penetration level of RE resources is low.

Frequency Profile Simulation

The AGC block of the system, presented in Figure 2.9, is modeled in MATLAB/SIMULINK to derive the frequency profile. The parameters used in the AGC block are obtained based on the range of values given in literature and trial and error to get the closest frequency profile compared to the measured data. The diesel generator and ESS are modeled as first order transfer functions where ESS response is ten times faster than the diesel generator's. The on-site measured data at KLFN with 1-second time resolution including load demand, wind turbine output power and solar panel output power are used to simulate the frequency of the system before and after RE integration. The results for a sample of 2-hour period

are demonstrated in Figure 3.9.

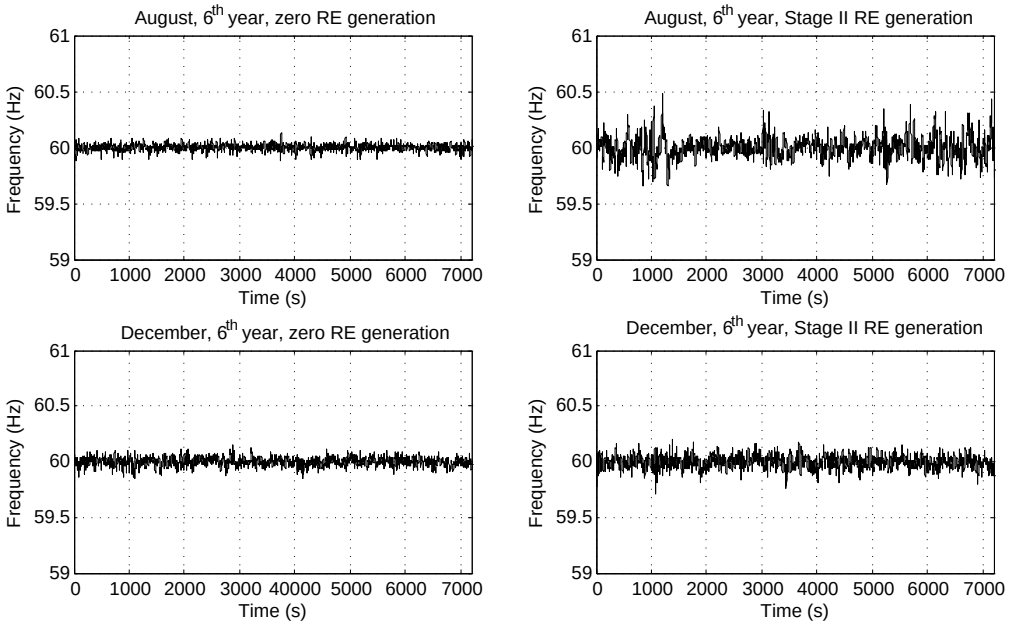

Figure 3.9: Comparison between frequency profiles of the system before and after RE integration for a sample 2-hour period in 6^{th} year, for these sample periods: $PD^{max}_{Aug.} = 506kW$, $PD^{min}_{Aug.} = 417kW$, $PD^{max}_{Dec.} = 774kW$, $PD^{min}_{Dec.} = 700kW$, $Prea^{max}_{Aug.} = 195kW$, $Prea^{min}_{Aug.} = 35kW$, $Prea^{max}_{Dec.} = 18kW$, $Prea^{min}_{Dec.} = 9kW$.

As it is seen from Figure 3.9, the frequency deviations after the addition of RE resources are considerably larger than those with zero RE penetration. Hence, if the system operator decides that the frequency is not regulated tightly enough, in order to limit the frequency deviation of the system ($|\Delta f| = |f - f_{nom.}|$), the penetration level of RE resources should be decreased or ESS contribution in frequency regulation must be considered.

Voltage Profile Simulation

The voltage profile of the system after addition of RE resources is studied in order to consider the inclusion of additional components for voltage regulation purposes, if required.

The power network structure of KLFN community that was identified using available maps and drawings, is shown in Figure 3.10, where the locations of diesel generation station, existing wind turbines, community store and water treatment plant are pinpointed.

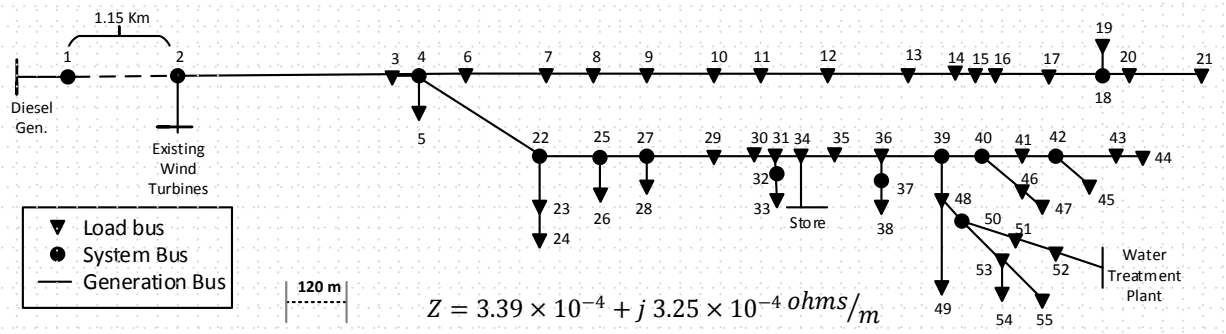

Figure 3.10: The network structure of KLFN.

Power flow analysis, presented in section 2.1.4, is performed on the KLFN network for many instances during planning horizon, to cover most of the possible voltage events, in order to investigate the profile of system voltages after the addition of RE resources. The distribution voltage level at KLFN network is 25 kV, and three-phase and single-phase transformers are installed at load buses. Because of the KLFN network configuration, proper selection of the feeder impedances and load profile, the power losses are very low and the voltage drops are almost negligible. Figure 3.11 demonstrates the simulated voltage profile at KLFN network buses over a 24-hour period, after inclusion of RE resources. As it can be seen, the voltage levels at all buses are very close to the nominal value. Thus, it can be inferred that integration of RE resources has no considerable adverse effect on the voltage profile of the system in KLFN network.

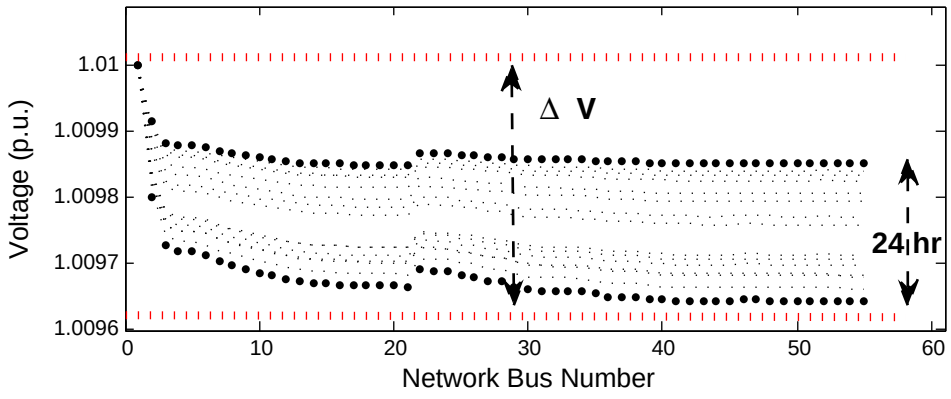

Figure 3.11: Voltage profiles at different buses over a sample 24-hour period, for this sample period: $PD = 740kW$ and $Prea = 4kW$.

3.3.4 Stage IV

The comprehensive study of the frequency and voltage profiles of the system, in stage III, determines the need for taking complementary actions. In the case of KLFN system, frequency deviations are not within the desired tolerance band of ±1.4% around the nominal value. Thus, extra constraints have to be incorporated to ensure tighter regulation of frequency. If ESS integration is not a feasible option for KLFN network, the maximum allowed RE fluctuation rate should be determined based on the desired frequency deviation limit. Then, an additional constraint, (3.17), is added to the optimization problem to enforce upper limit of RE generation. The maximum fluctuation limit of the RE resources is determined based on (2.9) and the dynamic model of the system, as illustrated in Figure 2.9. Figure 3.12 presents the minimum and maximum frequencies for each percentage of optimal RE generation level, determined by the solution of the optimization problem in stage II.

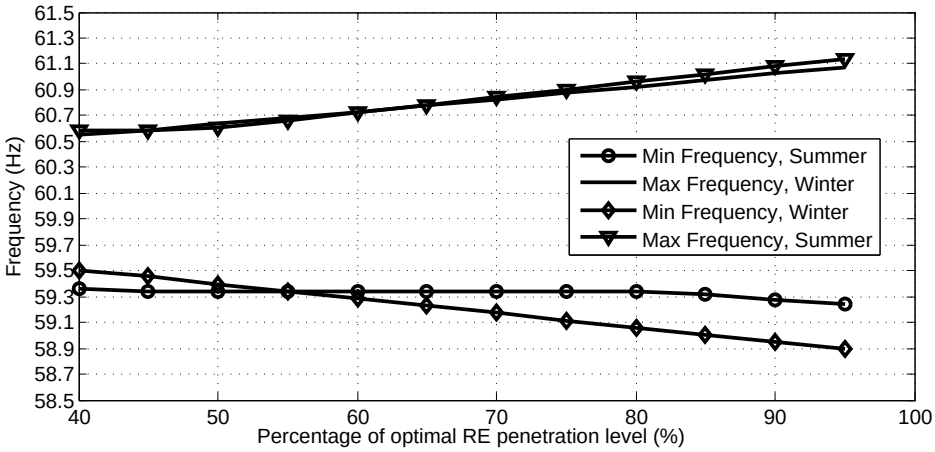

Figure 3.12: Maximum and minimum frequencies of the system vs. percentage of optimal RE generation level, determined in stage II.

As it is observed and anticipated, frequency deviations decrease by reducing the RE generation. In order to obtain frequency deviations within ±1.4% of the nominal frequency, the fluctuations introduced to the system should be limited to 65% of the value determined by the result of the optimization problem in stage II (i.e., $M_{pen.} = 0.65$). The penetration level constraint is added to the optimization problem in stage II and the new optimal solution is obtained. Table 3.5 summarizes the results of the optimization problem before and after considering the penetration level constraint, for the case where integration of ESS is not considered.

Table 3.5: Summary of the results of the multiple-year planning problem, without ESS integration, before and after inclusion of frequency regulation constraints

		Stage II results			Stage III included ($M_{pen.} = 0.65$)		
	Unit	Store	WTP	SbC	Store	WTP	SbC
Solar PV size	kW	50[a]	30[a]	100[b]	100[b]	-	-
Wind Turbine size	kW	60[b]	20[b]	-	20[b]	20[b]	-
ESS power size	kW	-	-	-	-	-	-
ESS Energy Size	kWh	-	-	-	-	-	-
Percentage of load demand provided by RE[c]	%	20.99	19.95	1.35	16.7	9.17	0
Capital Cost (discounted value)	M$		1.79			0.82	
Solar	M$	0.4	0.25	0.66	0.66	-	-
Wind	M$	0.65	0.22	-	0.22	0.22	-
ESS	M$	-	-	-	-	-	-
Total Welfare	M$		0.159			0.144	

WTP: Water Treatment Plant, SbC: Subsidized Customer, [a]1st year,[b] 5th year,[c] 6th year

It is apparent that the RE generation level decreases by introducing the additional penetration level constraint to the system. Note that, in this case, the subsidized customer's RE penetration is reduced to zero. The unsubsidized customers' RE penetrations are also decreased to take into account the limit on total RE output power fluctuations injected to the microgrid. Figure 3.13 shows the impact of limiting RE generation on frequency profile of the system for a selected 2-hour period, where the difference is more noticeable during the summer due to low RE power generation in winter.

In a different case, where ESS integration is regarded as a viable option for KLFN community and funding resources are available to cover the costs of ESS, the ESS reserve capacity can be used to help mitigate the frequency deviations. In this case, the power and energy sizing of the ESS not only depends on the distribution of dispatch of the power between ESS and diesel generator, but also on the level of participation of ESS in frequency control services. An incentive mechanism is also considered to remunerate the power and energy capacity of the ESS that is allocated for frequency control actions, taking the available price range in the literature into account [62], and making assumptions accordingly.

The reserve capacity requirements of the ESS for participation in frequency control are determined based on (2.10)-(2.18), according to the block diagram shown in Figure 3.14.

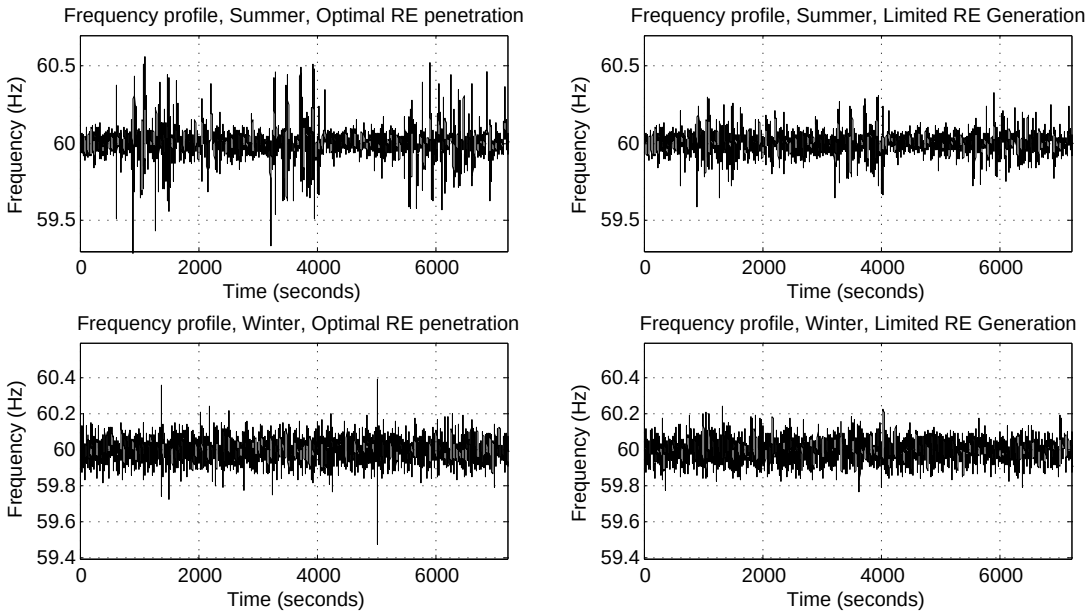

Figure 3.13: The comparison between frequency profiles of the system before and after limiting the RE generation.

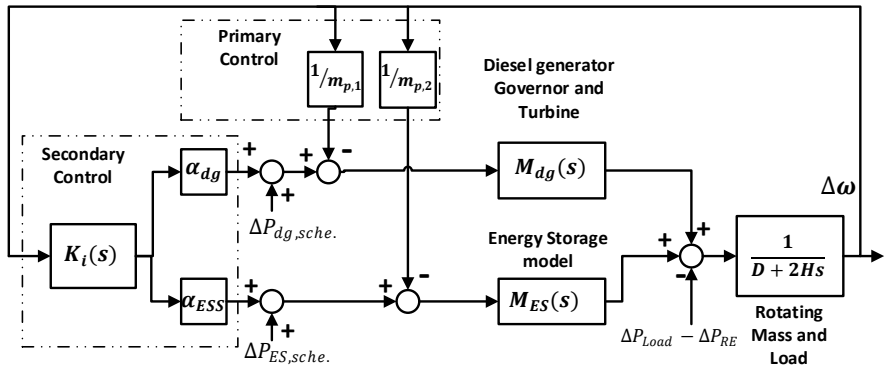

Figure 3.14: Joint contribution of ESS and diesel generator to frequency control.

The percentages of the energy and power capacities of the ESS to be reserved for regulation services (β_{fE} and β_{fP}) are determined by deriving the profile of the required energy versus participation factor and the required power versus frequency deviations, respectively, as shown in Figure 3.15.

The values of β_{fP} and β_{fE} are determined based on the specific requirements of the

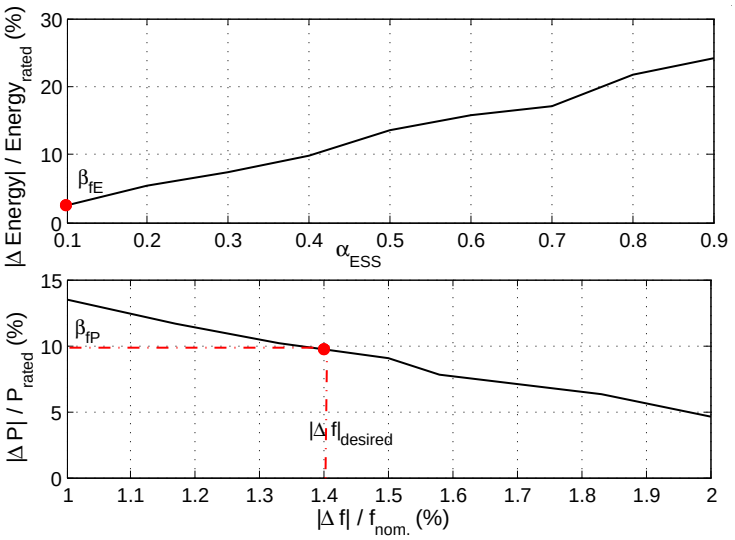

Figure 3.15: The required energy and power capacities for control actions versus participation factor of ESS and frequency deviations, respectively.

system operation. In this case, it is assumed that the desired frequency deviation range is $\pm 1.4\%$ of the nominal frequency and the participation factor of ESS is 0.1. These values are introduced to the optimization problem as the additional required power and energy capacities of the ESS. The optimization problem is solved again to revise the results by considering the regulation constraints, (3.19)-(3.21). The ESS unit at the community store is selected as the candidate unit for participation in frequency control reserve. β_{fP} and β_{fE} values are equivalent to 10% and 3%, respectively, and the corresponding incentives for primary and secondary frequency reserves are $PINC = 300\$/kW.year$ and $EINC = 350\$/kWh.year$. A summary of the results are presented in Table 3.6.

The results summarized in Table 3.6 demonstrate that the RE penetration level is increased after inclusion of stage III, due to added ESS power and energy available for control actions, encouraged by frequency regulation incentives. The total welfare, after inclusion of stage III results, is increased by almost 45% in this case, due to the additional savings and income obtained by added RE unit sizes and incentive mechanisms; however, the initial capital costs are increased from \$3.27 M to \$4.16 M which is a 27% increase in the initial capital costs. Figure 3.16 illustrates the impact of ESS contribution to frequency regulation on frequency profile of the system for a selected 2-hour period. The improvements in frequency profile are noticed in both winter and summer.

Table 3.6: Summary of the results of the multiple-year planning problem, considering ESS integration, before and after inclusion of frequency regulation constraints

		Stage II results			Stage III included ($\beta_{fE} = 3\%$, $\beta_{fP} = 10\%$)		
	Unit	Store	WTP	SbC	Store	WTP	SbC
Solar PV size	kW	240[b]	125[b]	150[b]	300[b]	135[b]	190[b]
Wind Turbine size	kW	-	-	-	-	-	-
ESS power size	kW	145[b]	100[b]	-	265[b]	105[b]	-
ESS Energy Size	kWh	725[b]	495[b]	-	1325[b]	515[b]	-
Percentage of load demand provided by RE[c]	%	38.45	43.53	2.02	47.15	46.03	2.56
Capital Cost (discounted value)	M$		3.27			4.16	
Solar	M$	1.6	0.83	0.99	1.99	0.89	1.26
Wind	M$	-	-	-	-	-	-
ESS	M$	0.57	0.39	-	1.03	0.40	-
Total Welfare	M$		0.289			0.416	

WTP: Water Treatment Plant, SbC: Subsidized Customer, [a]1st year,[b] 5th year,[c] 6th year

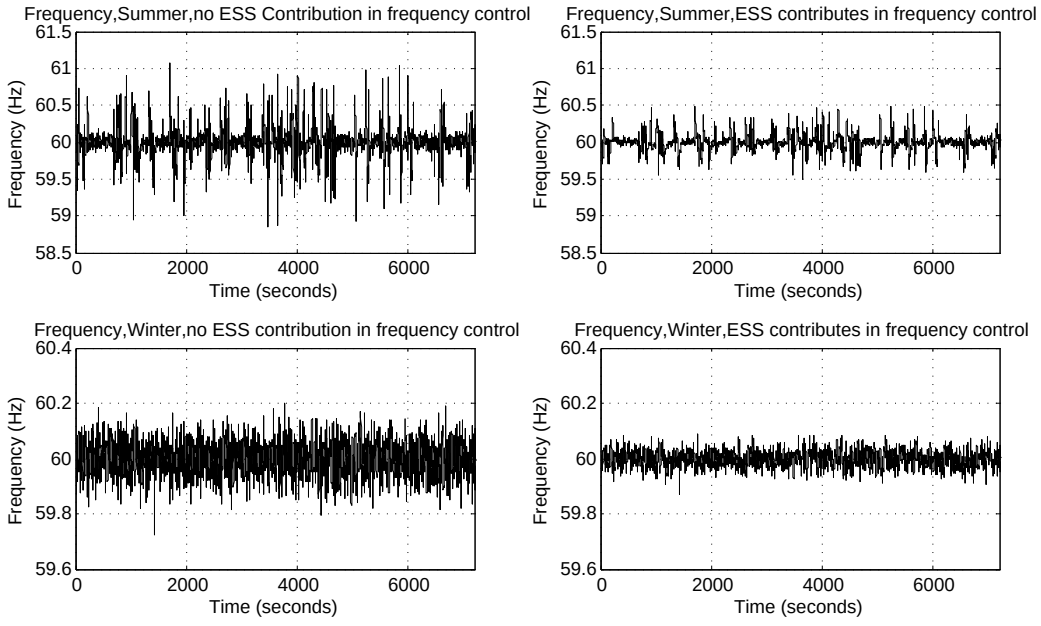

Figure 3.16: The comparison between frequency profile of the system before and after ESS participation in frequency control.

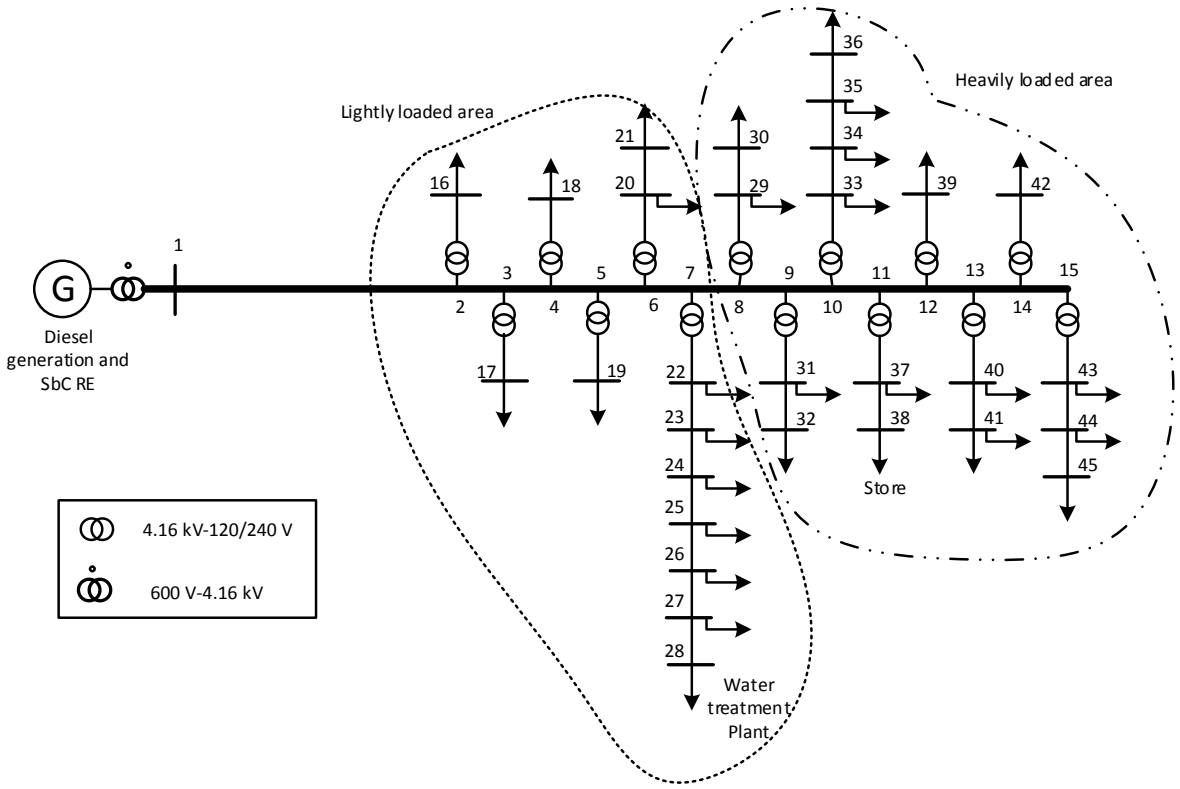

Figure 3.17: Developed structure for the case study.

3.4 Case Study for Voltage Regulation

In order to demonstrate the impact of RE integration on voltage regulation, a network structure is developed to make it possible to observe voltage events such as over voltage and under voltages, using the load and generation data of KLFN. Thus, the structure shown in Figure 3.17 is adopted to investigate the impact of voltage regulation constraints on the sizing of the system. The developed network parameters are summarized in Table 3.7 and Table 3.8.

Power flow analysis, presented in subsection 2.1.4, is performed on the developed network for different loading conditions. With a constant increase in load demand in the planning horizon and during heavy load periods, which basically happen in winter time and when the generation level of RE resources is very low, the voltage level at the end of the distribution feeder can drop to values lower than those allowed by system operation

Table 3.7: Line connectivity of the network

from	to	type	length(m)	from	to	type	length(m)
1	2	2	3000	23	24	1	50
2	3	2	500	24	25	1	50
3	4	2	500	25	26	1	50
4	5	2	500	26	27	1	50
5	6	2	500	27	28	1	50
6	7	2	500	8	29	1	50
7	8	2	500	29	30	1	50
8	9	2	500	9	31	1	50
9	10	2	500	31	32	1	50
10	11	2	500	10	33	1	50
11	12	2	500	33	34	1	50
12	13	2	500	34	35	1	50
13	14	2	500	35	36	1	50
14	15	2	500	11	37	1	50
2	16	1	50	37	38	1	50
3	17	1	50	12	39	1	50
4	18	1	50	13	40	1	50
5	19	1	50	40	41	1	50
6	20	1	50	14	42	1	50
20	21	1	50	15	43	1	50
7	22	1	50	43	44	1	50
22	23	1	50	44	45	1	50

Table 3.8: Impedance for different conductors

		Impedance (ohm/m)		
type	Phase	a	b	c
1	a	0.632+j0.218	0.033+j0.303	0.033+j0.303
	b	0.033+j0.303	0.632+j0.218	0.033+j0.303
	c	0.033+j0.303	0.033+j0.303	0.632+j0.218
2	a	0.458+j0.851	0.0021+j0.188	0.0021+j0.188
	b	0.0021+j0.188	0.458+j0.851	0.0021+j0.188
	c	0.0021+j0.188	0.0021+j0.188	0.458+j0.851

regulations, such as ±6% for hydro one networks [63]. These under voltage events are not resulted from integration of RE resources; however, integration of RE and ESS units introduces additional equipment to the network which can help to mitigate those problems. During light load periods in summer time where RE generation can reach its maximum levels, over voltages can occur at the DG interconnection point and nearby buses.

The voltage profile of the developed network is simulated, for a typical winter day with very low RE generation level, during a 24-hour period and the results are demonstrated in Figure 3.18. It can be seen that, under voltage events can happen at the end of the line, considering a ±6% voltage regulation standard.

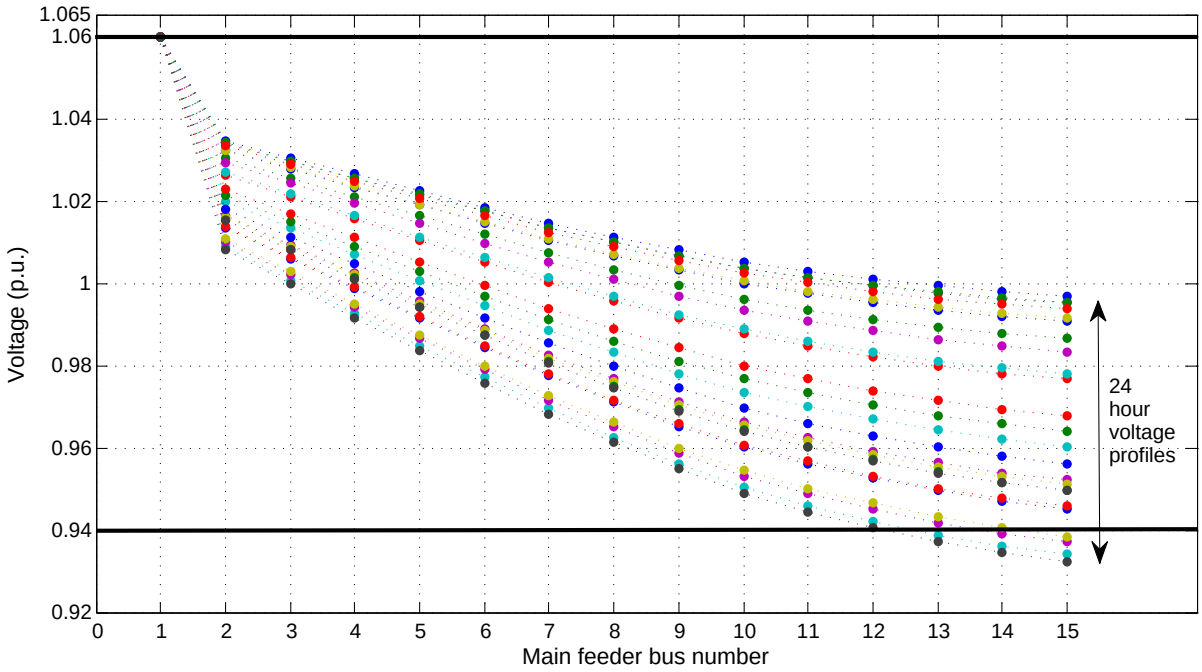

Figure 3.18: Voltage profiles at the main feeder buses for a typical winter day over a 24-hour period.

The voltage profile at the distribution line connecting the water treatment plant to the main feeder for a 24-hour period in a typical day in summer where the RE generation level is high is shown in Figure 3.19. This is for the case where ESS integration is not feasible. The voltage level at the DG interconnection point increases when the RE generation levels increase and there are time periods where the DG interconnection voltage level exceed the 6% voltage limit.

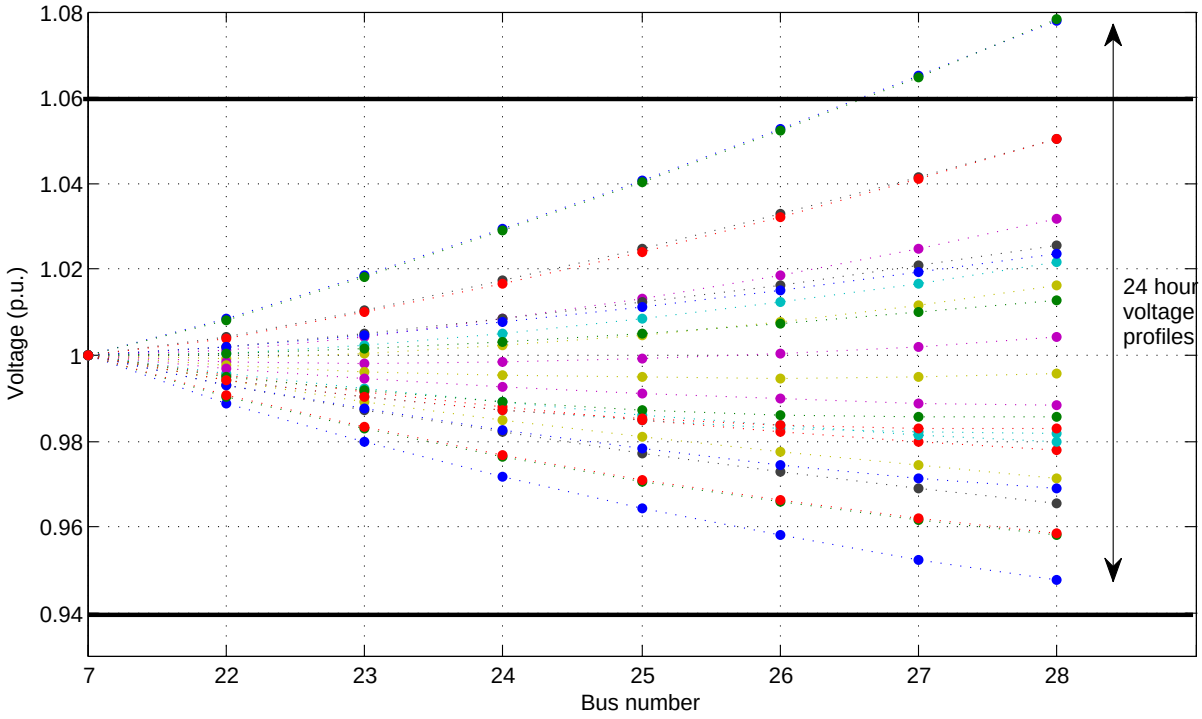

Figure 3.19: Voltage profiles at distribution buses for a typical summer day over a 24-hour period.

In order to mitigate the impact of RE integration on over voltages and help mitigate under voltage problems there are a set of actions that can be taken:

1. Limiting RE generation level: This option can be considered where ESS integration to absorb the extra RE generation is not feasible and the inverters interfacing the RE resources to the microgrid are required to operate at unity power factor; hence, they can not absorb reactive power. Thus, the maximum feeder capacity for RE integration must be determined and a constraint should be added to the optimization problem to impose this limit, as presented in (3.25). This can be done by reducing the amount of RE generation at the network bus with over voltage problem and observing the maximum threshold for keeping the voltages within limits. In this network, the maximum RE generation at bus number 28 should be limited to 85% of the optimal RE generation obtained in Stage II. The additional constraint is introduced to the optimization problem and a new set of optimal results are obtained. The results are summarized in Table 3.9. Another scenario by inclusion of both frequency and voltage regulation constraints is also investigated and

Table 3.9: Comparison of the results after inclusion of frequency and/or voltage regulation constraints

		Stage II results			Voltage regulation constraint ($N^{wtp}_{pen.} = 0.85\%$)			Frequency regulation constraint ($M_{pen.} = 0.65\%$)			Frequency regulation and voltage regulation constraints included ($M_{pen.} = 0.65\%$, $N^{wtp}_{pen.} = 0.85\%$)		
	Unit	Store	WTP	SbC	Store	WTP	SbC	Store	WTP	SbC	Store	WTP	SbC
Solar PV size	kW	50[a]	30[a]	100[b]	50[a]	25[a]	105[c]	100[b]	-	-	110[c]	-	-
Wind Turbine size	kW	60[b]	20[b]	-	80[c]	-	-	20[b]	20[b]	-	-	-	-
ESS power size	kW	-	-	-	-	-	-	-	-	-	-	-	-
ESS Energy Size	kWh	-	-	-	-	-	-	-	-	-	-	-	-
Percentage of load demand provided by RE[d]	%	20.99	19.95	1.35	24.56	9.38	1.42	16.7	9.17	0	16.69	0	0
Capital Cost													
Solar	M$	0.40	0.25	0.66	0.40	0.21	0.69	0.66	-	-	0.73	-	-
Wind	M$	0.65	0.22	-	0.86	-	-	0.22	0.22	-	-	-	-
ESS	M$	-	-	-	-	-	-	-	-	-	-	-	-
Total Welfare	M$	0.159			0.148			0.144			0.139		

WTP: Water Treatment Plant, SbC: Subsidized Customer, [a]1st year,[b] 4th year,[c] 5th year,[d] 6th year

the optimal solution is presented in Table 3.9.

It can be seen from the results that including the voltage regulation constraint, limits the penetration level of RE for community water treatment plant, located at bus number 28, while the RE penetration level increases for the community store and slightly for subsidized customers, to maximize the community welfare. Including frequency and voltage regulation constraints together, further decreases the RE penetration level for all customer types, making it only feasible for community store to incorporate RE resources. It should be noted that, frequency regulation constraint, limits the total amount of RE generation for the entire microgrid, while voltage regulation constraint, restricts the RE generation only for the buses with over voltage problem. As can bee seen from the results shown in Table 3.9, frequency regulation constraint has more impact on limiting the RE generation compared to voltage regulation constraint. Figure 3.20 shows the voltage profiles after including the voltage regulation constraint for the same summer day considered in Figure 3.19. The impact of limiting the RE generation level at bus number 28 on solving the over voltage problem can be observed.

2. Providing reactive power support: To determine the amount and location of Var support devices such as shunt capacitors for installation in the network, an ORPP program is run to obtain the required amount of reactive power for injection to the microgrid to avoid under voltage problems. The ORPP program objective is to minimize the amount of required reactive resources at candidate buses. In this case, buses number 13, 14, and 15 are selected as candidate buses for Var device installation. The constraints of the ORPP problem are the active and reactive power balance equations, active and reactive power generation

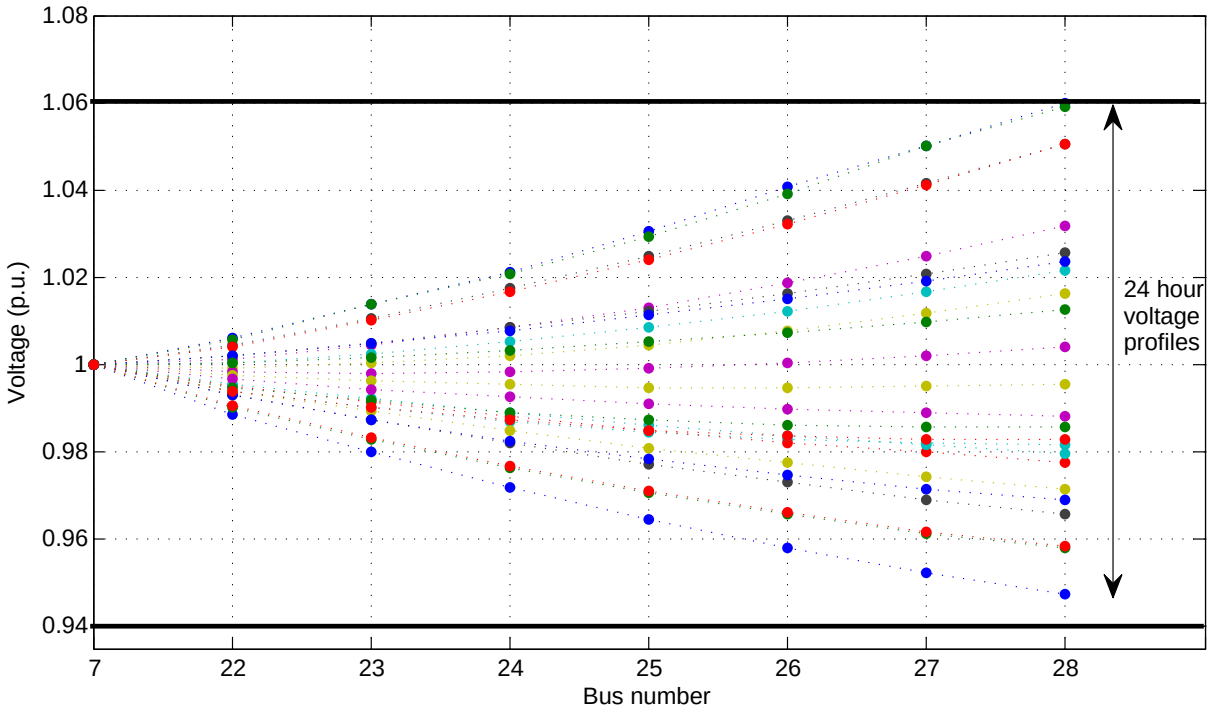

Figure 3.20: Voltage profiles at distribution buses after limiting the RE generation at bus 28.

limits, bus voltage limits and Var source sizing limit. An alternative for installation of Var support devices is to make use of the available power inverters interfacing the RE and ESS units to the microgrid. In this case, the rating of the inverter is determined by taking the reactive power transfer capability into account, while maintaining the full active power transfer capability. However, this option is restricted by the location of installed RE and ESS resources. A summary of the possible actions to mitigate the under voltage voltage problem by reactive power support is as follows:

- Installation of a capacitor bank at bus 15 to compensate the losses: during the 20-year planning horizon the load growth can push the microgrid towards under voltage occurrences; thus, to compensate for the losses a capacity of 65 kVar (three-phase) can be installed to support the microgrid during under voltage events in the 20-year planning horizon, as suggested by ORPP problem. This installation can happen anytime during planning horizon where the under voltage problems arise as a result of load growth. In the studied case, the under voltage problems mainly begin and

continue to happen in the 18^{th} year. Thus, it is required to look into options to mitigate these problems in 18^{th} year of the planning horizon.

The capacitor bank cost in $\$/Kvar$ depends on many factors including the voltage level of the bank, number of switched stages and control requirements [64]. As an example, the capacitor bank equipment costs can vary between $2\$/Kvar$ and $10\$/Kvar$ for standard two bushing capacitors, where higher costs are associated with the lower capacitor $Kvar$ ratings [64]. This cost estimate does not take the unique nature of northern community projects and the installation cost of equipment into account. In the case of KLFN the cost estimate for equipment and installations can reach up to 2.5 times on-grid installations [19]. The assumption is that the cost of the capacitor bank is provided by the utility which takes care of the operation and maintenance of the system. Hence, it is not included in the planning optimization problem which takes the costs paid for by the community into account.

- Allocation of inverter capacity at bus 38 to accommodate reactive power transfer: Inverters are power electronic devices capable of participating in active and reactive power transfers. However, their capability is restricted by the ability of their switches to withstand voltages and currents. In order for inverters to be able to participate in reactive power transfer and to provide the full amount of required active power, their total rating must be selected according to the total required apparent power capacity. In this case, up to 75 kVar (three-phase) capacity participation from the inverters located at bus number 38 can prevent the occurrence of under voltages after the 18^{th} year of the 20-years planning horizon, as suggested by ORPP problem. This option is more expensive compared to the case where capacitor banks are installed (up to 5 times the cost of capacitor banks); However, the flexibility and rapid response provided by power electronic converters is notably superior [65, 66]. ESS can be utilized as a reactive power compensation device while making use of its active power exchange capability [66, 67].

Figure 3.21 presents the voltage profiles after inclusion of reactive power support to the microgrid for the same winter day considered in Figure 3.18. As it is seen, the under voltage problem is solved as a result of providing reactive power support to the microgrid.

3.5 Summary

A novel multi-stage, multiple-year planning platform is presented in this chapter that considers the frequency and voltage regulation constraints in the planning and sizing of

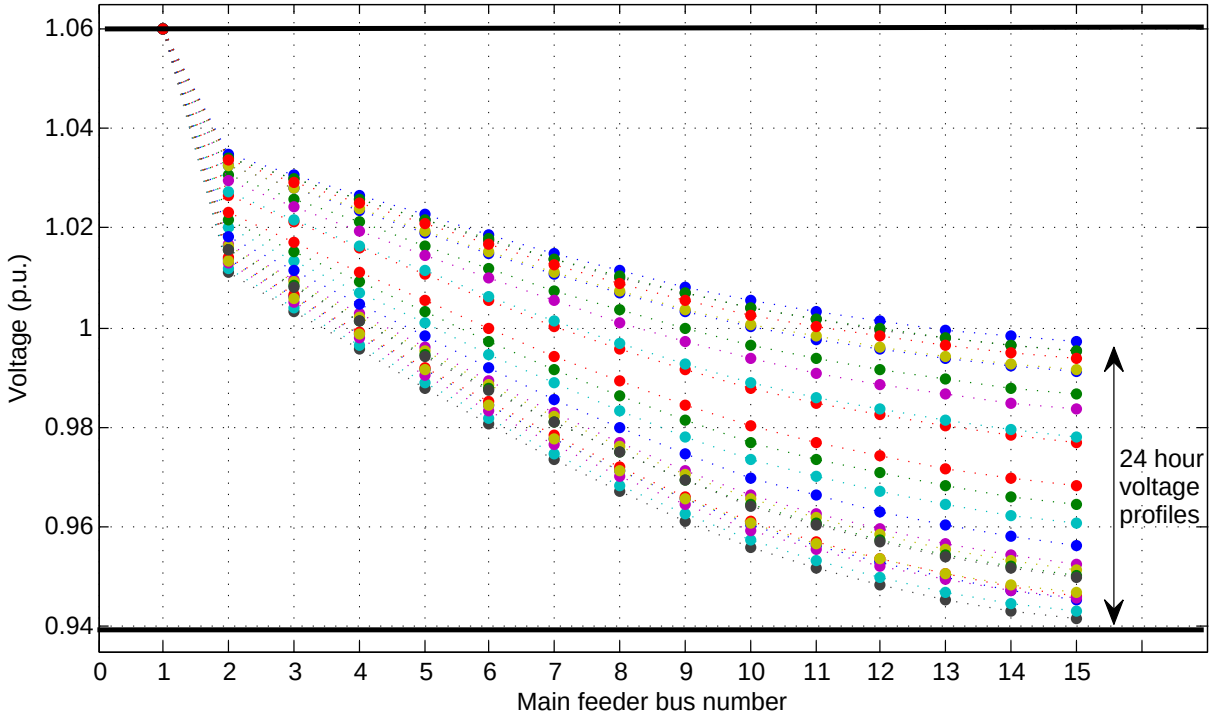

Figure 3.21: Voltage profiles at the main feeder buses for a typical winter day over a 24-hour period after addition of reactive power support.

a remote microgrid. The proposed framework optimizes the system sizing and structure, while taking the frequency and voltage regulation constraints of the system into account. The isolated microgrid planning project for remote communities is identified, optimized and evaluated during multiple stages. Frequency and voltage regulations, as two of the most important power system operation requirements, are used to investigate the effect of inclusion of regulation constraints in optimal planning on system sizing. Frequency and voltage are simulated for the proposed unit sizes and according to the frequency and voltage regulation limits, decisions are made to limit RE penetration level, dedicate extra ESS capacity to frequency/voltage regulation or add Var compensation devices in order to keep the frequency and voltage within acceptable limits. Additional constraints are added to the optimization problem to address the decisions made. The performance of the proposed platform is put to test by conducting a case study for planning an isolated microgrid for Kasabonika Lake First Nation community and the results are compared and evaluated.

Chapter 4

Selection of the Energy Storage Systems

In this Chapter the different aspects of selecting a proper energy storage system for isolated microgrids of remote communities are discussed. Several ESS types are reviewed and their main features are explained and compared. Selection of an ESS system for KLFN community is investigated, considering integration of a battery ESS or combination of a battery and a flywheel ESS. The results of the planning optimization problem that considers ESS integration for energy management and regulation tasks are presented.

4.1 Energy Storage Systems

Nowadays, energy storage plays a significant role in the power grid by providing numerous services including load leveling, asset deferral, ramping and regulation. Load leveling is the act of storing energy during off-peak periods and delivering it back to the grid when the demand is high. Asset deferral is to address the peak load growth by deferring large investments on generation, transmission and distribution via storage to make the best use of available assets. Ramping/capacity firming is to make up for the low ramp rates of conventional power generation units to keep up with highly intermittent and fluctuating nature of RE resources. ESS can provide much higher ramp rates compared to the traditional generation units. ESS can also provide fast response to the changes in system frequency and voltage by injecting or absorbing power very quickly.

Various types of energy storage systems are capable of enabling one or more of the above-mentioned services. However, there is no single ESS that can provide all required

services for all applications. Thus, selecting the proper type and size of ESS for each application requires a thorough investigation of the power system characteristics and requirements to determine the best available ESS options that can satisfy the needs to the highest extent.

4.2 ESS in Microgrids of Remote Communities

In remote communities, ESS can be utilized to enable/facilitate the incorporation RE resources into the microgrid and improve service quality. Considering the fact that most microgrids of remote communities are isolated (i.e., operating independent of the main power grid), ESS can be of great significance in providing uninterruptible electricity service to the customers. However, specific requirements have to be met by the ESS in order to be considered a suitable option for operation in microgrids of remote communities.

Considering the remoteness of the locations and lack of easy access to experienced technicians and other resources on-site, one of the most desired characteristics of a remote community ESS is high level of technology maturity. Moreover, similar to any other investment project, an ESS technology with relatively low capital, operation and maintenance costs is preferred for remote community microgrids. Other important factors to consider when looking for ESS options for remote community microgrids are the geographical, environmental and climate-related aspects. Some ESS technologies, such as pumped hydro, require specific geography to be available for their implementation. There are also technologies that use toxic material, including batteries that contain lead or cadmium, and require proper handling and care to avoid hazards. Manufacturing and recycling of these technologies increase the risk of exposure of these materials [68]; thus, they are not the most preferred choices from environmental impact point of view. Furthermore, many remote communities are located in areas where harsh weather conditions make it difficult or impossible for operation of some ESS technologies without taking extra measures. Technologies such as Sodium-Sulfur battery operate efficiently in high temperature ranges (300-350°C) and require proper thermal management for their operation which eventually could increase their size and decrease their efficiency [69].

In addition to the above-mentioned factors affecting selection of ESS for remote community microgrids, the role of the ESS in the microgrid (e.g., energy management or regulation) is a key factor in selecting the type and size of ESS. Batteries, fuel cells, pumped hydro and compressed air energy storage are examples of ESS types that can be used for long-term energy management tasks, including load leveling. On the other hand, flywheel,

batteries, Superconducting Magnetic Energy Storage (SMES), capacitor and super capacitor are best suited for short-term power management purposes, such as regulation and stabilization. Furthermore, in microgrids with high RE penetration levels, there is a need for fast-acting ESS, with high ramping rates and high speed of response, to compensate for the rapidly-varying generation.

4.3 Kasabonika Lake First Nation Community

The optimal RE and ESS unit sizes for KLFN community are obtained by solving a planning optimization problem, where the goal is to maximize community's social welfare. The results are presented in Table 3.4. The ESS sizing suggested by Stage II results considers only the long-term energy management role of the ESS in the microgrid, including load leveling. However, if ESS were to participate in regulation tasks, there should be extra capacity allocated for short-term regulation services provided by ESS, as suggested by Stage III results. Hence, the technology selected for this application should be capable of providing both long-term and short-term services to the grid or a hybrid ESS should be taken into consideration. Considering the specific geographic condition of the KLFN community and the required maturity level of ESS, among various technologies utilized for both types of services, the followings are the most feasible ESS options:

- Lithium-ion battery
- Flow battery
- Hydrogen Fuel cell
- Flywheel

4.3.1 Lithium-ion Battery

Lithium-ion batteries have been used in portable electronics applications for quite a while and are the main technology for the ESS of EVs; however, their use in stationary power grid applications is still under development compared to other well-established technologies such as lead-acid or nickel-cadmium batteries. Nevertheless, they are finding their ways into stationary applications due to their superior features compared to their competitors. With nickel-cadmium batteries being slowly eliminated from market due to environmental

concerns and cost-related factors [70], lead-acid batteries, which have been around for more than a century, are the main contenders for lithium-ion batteries.

Although high cost of lithium-ion technology and its lower level of technology maturity compared to lead-acid are still some of the shortcomings of this technology, higher energy density and specific energy, longer cycle life, better discharge rate and lower sensitivity to temperature make lithium-ion a more favorable choice for power grid applications [71]. The increase in the number of Electric Vehicles (EVs) and the possibility of reusing the EV batteries in stationary applications, after their energy storage capacity and efficiency degrade to levels below those required for EVs, can also contribute to decreasing the overall cost of lithium-ion batteries for stationary grid-scale applications [72], leading to further integration of ESS in remote communities. It should also be mentioned that, lead is a hazardous material and considering the lower energy density of lead-acid batteries, their manufacturing and recycling leads to greater amounts of environmental impacts. Additionally, since lead-acid batteries have shorter cycle life and require regular maintenance, they are not a good choice for long term energy management applications [70].

With development of innovative technologies that enable the integration of ESS in communities such as KLFN, where extremely low temperatures limit the use of some ESS types, lithium-ion battery is becoming a more interesting option for integration in such applications. The installation of SAFT's "Cold Temperature Package" lithium-ion technology in Kotzebue (Alaska) [73] and Colville Lake (NWT, Canada) [74], shows a promising future for utilization of lithium-ion batteries in remote communities with extreme climate conditions.

4.3.2 Flow Battery

Flow batteries are electrochemical energy storage systems, featuring independent power and energy ratings. This desirable feature makes them flexible to operate in both short-term and long-term applications. However, their low energy density is a disadvantage that limits their use for some applications. Flow batteries have lower efficiency compared to lithium-ion battery. Even though they have a wider range of SOC operation compared to lithium-ion batteries, the difference in efficiency still makes lithium-ion battery a better option [75] in terms of the savings that can be obtained. The energy costs ($/kWh) of flow battery are lower than those of lithium-ion, while the power costs ($/kW) are rather higher [75]. Utilization of this type of battery in cold temperatures requires appropriate temperature control mechanisms or proper insulation to prevent performance deterioration and battery damage [76].

There are a few cases of flow battery application in remote areas [77, 78], but there is no clear evidence of possibility of successful operation of this battery type in northern Canada remote communities.

4.3.3 Hydrogen Fuel cell

Hydrogen Fuel cell is an electrochemical energy conversion device that together with an electrolyzer and hydrogen storage tanks makes a complete energy storage system. Fuel cell uses hydrogen and oxygen to generate electricity. The reverse reaction takes place in an electrolyzer, releasing oxygen and hydrogen by using electricity and water. The main features of fuel cell are high energy density, scalability, modular structure and low energy efficiency. The charging rate, discharging rate and storage capacity of this ESS type are independent of one another. This ESS also creates less environmental impacts compared to batteries. However, fuel cell has relatively higher power and energy costs compared to batteries [79].

With integration and operation of this technology in remote communities such as Bella Coola (BC, Canada) [80] and Ramea Island (NFL, Canada) [81], the interest in integration of Hydrogen technologies in remote communities can potentially grow noticeably.

4.3.4 Flywheel

Flywheel is a high-inertia mechanical system, comprising a rotor, a stator and bearings, that stores energy in the form of kinetic energy. Storing energy increases the speed of the rotor and discharging it decreases the speed. This ESS type can only deliver or absorb power for very short durations (5-30 seconds), thus it is suitable for short-term high-power applications such as regulation. Flywheel is a quite mature technology, with main features including long lifetime and cycle stability, little maintenance requirement, high power density, high efficiency and being environmentally benign [79]. Flywheels can also operate in a wide range of temperatures and have lower failure rate compared to batteries. However, their major shortcoming is high level of self-discharge due to losses resulting from moving parts [82]. This ESS type has low power cost ($/kW) compared to battery types, while its energy cost ($/kWh) is relatively high [69].

Because flywheels are not capable of providing energy for long durations, their combination with other ESSs that are suitable for energy applications, is a good choice for providing both long-term and short-term services to the microgrids.

Table 4.1: Comparison of different ESS technologies [79], [85]

Technology	Maturity	Cost		Lifetime (cycles)	Efficiency	Response Time	Application
		$/kW	$/kWh				
Li-ion Battery	Developed	1200-4000	600-2500	1000-10000	up to 95%	<1/4 cycle	Short/long term
Flow Battery	Developed	600-1500	150-1000	12000	up to 75%	<1/4 cycle	Long term
Hydrogen Fuel cell	Developing	10000		1000	up to 40%	<1/4 cycle	Long term
Flywheel	Developed	250-350	1000-5000	20000	up to 95%	<1 cycle	Short term/high power

Two flywheel units operating in parallel in Kodiak Island(Alasaka,USA) [83] and the flywheel unit installed on St. Paul Island (Alaska,USA) [84], are examples of successful deployment of flywheel energy storage systems to increase RE penetration in isolated microgrids.

Table 4.1 provides a comparison of the ESS technologies that are suitable for remote community microgrid application [79], [85].

4.4 ESS Sizing for KLFN Community

Optimal ESS sizing for KLFN is obtained using the multi-stage optimal planning platform that considers regulation constraints. The assumption is that ESS participates in frequency control actions as well as energy management tasks. The ESS type and size selected for this application should be able to meet system's specific requirements. One of these requirements is the ramping rate of the RE output power. Figures 4.1 and 4.2 present the output powers of PV system and wind turbines in KLFN, respectively, based on on-site measured data for a selected day in summer. The maximum ramping rate for the 10 kW PV system is more than 20% of the capacity per minute. The ramping rate for wind turbine output power can reach 50% of the capacity per minute.

Even though the increased number of RE units and their dispersed installations can have impact on smoothing the overall ramping rate [86], dealing with highly variable generation can still be challenging. The fast-increasing generation can be curtailed using control algorithms, while the decreasing ramp is more troublesome to control, as there should be available resources to compensate for the decreasing generation [86]. Utilizing energy storage to control the ramp rate of RE units is an effective approach which requires ESS to be capable of providing high amounts of power during short time intervals. Therefore, the selected ESS involved in such services should be suitable for power management applications.

Simulation results for the terminal power of the ESS for KLFN system for a 2-hour

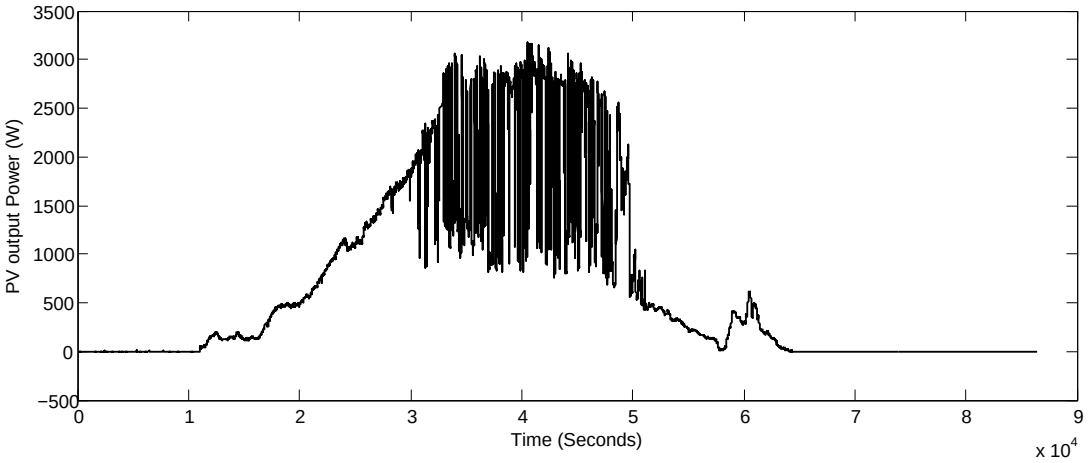

Figure 4.1: The output power of 10 KW rooftop PV solar system at KLFN.

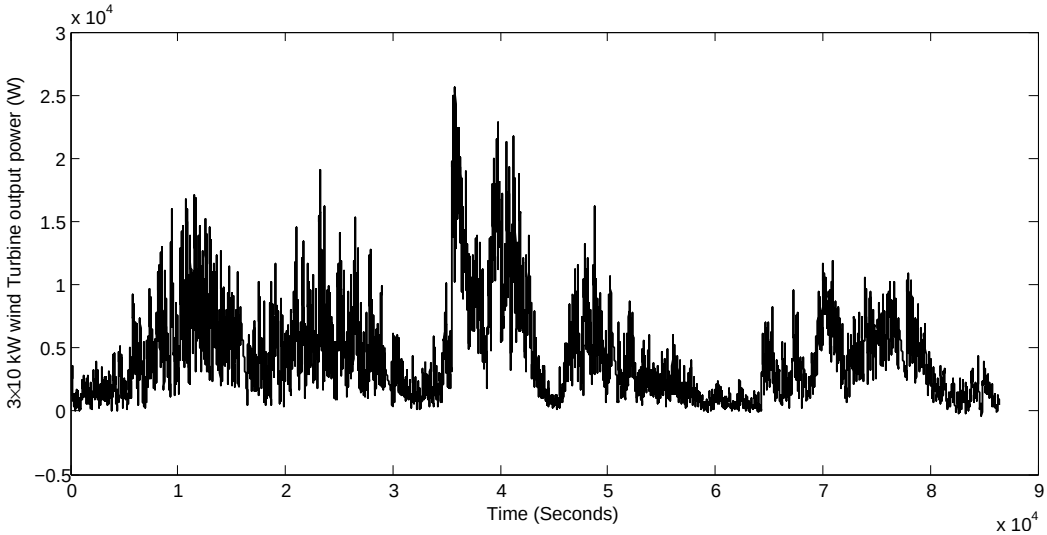

Figure 4.2: The output power of 3×10 KW wind turbines at KLFN.

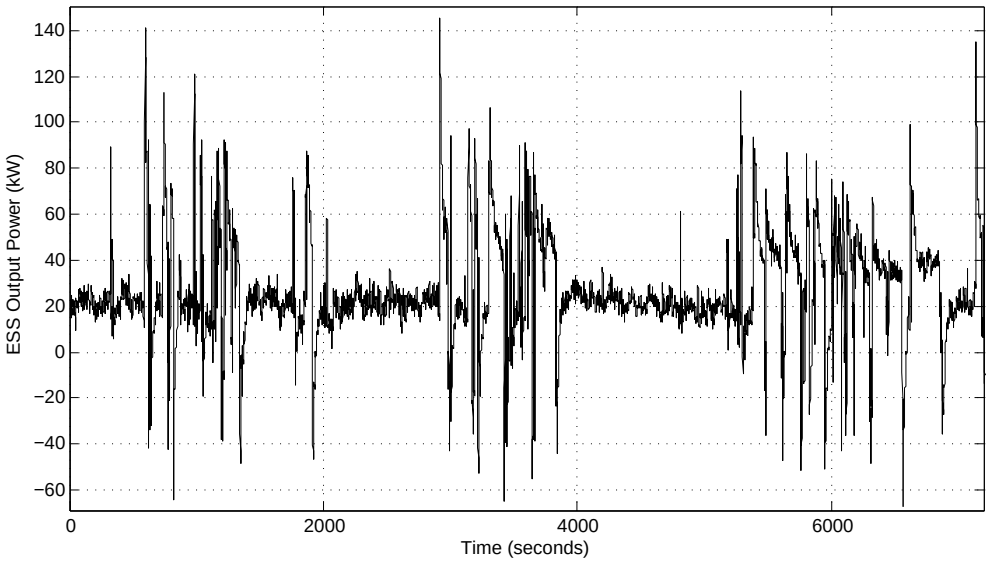

Figure 4.3: The simulated profile of terminal power of ESS for KLFN system.

period, considering the optimal sizing of the RE and ESS units determined in the optimization problem, are presented in Figure 4.3. It is shown that the fluctuations of the power and the ramping rates are significant and the ESS should be capable of participating in the energy management as well as providing ramping rate support to the system. Thus, it should have fast response to the variations in power and also should provide high amounts of power in very short time intervals.

4.4.1 Hybrid ESS

Hybrid Energy Storage Systems (HESS) for microgrid applications are receiving increasing attention, as combining the advantageous features of two or more ESS types enables both energy management and power quality improvement. ESS hybridization decreases the costs of the system, increases the efficiency and lifetime of the system and enables optimal operation of the ESS in the microgrid [87]. In this type of arrangement, the ESS with high energy rating, low self-discharge rate and low cost of energy ($/kWh), such as a battery, can be used to participate in the generation dispatch to supply the load of the system or to store the extra energy generated by RE resources, whereas the ESS with high power capability, short response time and low cost of power ($/kW), such as a flywheel, can be used to support the grid for stabilization and providing regulation services, and to cover

Table 4.2: Comparison of the results for different ESS usage

		Baseline: ESS for Energy management			Scenario I: Battery for primary and secondary frequency control ($\beta_{fE} = 3\%$, $\beta_{fP} = 10\%$)			Scenario II: Flywheel for primary and Battery for secondary frequency control ($\beta_{fE} = 3\%$, $\beta_{fP} = 10\%$)		
	Unit	Store	WTP	SbC	Store	WTP	SbC	Store	WTP	SbC
Solar PV size	kW	240[b]	125[b]	150[b]	300[b]	135[b]	190[b]	280[b]	100[a]	150[b]
Wind Turbine size	kW	-	-	-	-	-	-	-	-	-
ESS power size	kW	145[b]	100[b]	-	265[b]	105[b]	-	220[b]	50[b]	-
ESS Energy Size	kWh	725[b]	495[b]	-	1325[b]	515[b]	-	1100[b]	250[b]	-
Percentage of load demand provided by RE[c]	%	38.45	43.53	2.02	47.15	46.03	2.56	44.62	33.86	2.02
Capital Cost										
Solar	M$	1.6	0.83	0.99	1.99	0.89	1.26	1.86	0.66	0.99
Wind	M$	-	-	-	-	-	-	-	-	-
ESS	M$	0.57	0.39	-	1.03	0.40	-	0.86	0.2	-
Total Welfare	M$		0.289			0.416			0.360	

WTP: Water Treatment Plant, SbC: Subsidized Customer, [a]4th year,[b] 5th year,[c] 6th year

the fast fluctuations in generation and load. This will consequently reduce the need for frequent battery replacements and also provide support to the frequency regulation of the system. Thus, two different scenarios for ESS selection for KLFN are considered, besides the basic application of ESS only for energy management purpose. In the first scenario, a battery storage system is selected to participate in energy management actions, as well as to contribute in primary and secondary frequency control tasks. In the second scenario, a battery and a flywheel are incorporated. The battery participates in energy management and secondary control actions, while flywheel takes care of the primary frequency control task. The optimization results are presented in Table 4.2.

- Scenario I: In this case, the ESS unit installed at the store is selected to participate in frequency control tasks. A battery storage is assumed to participate in energy management and take care of primary and secondary control actions, with primary and secondary reserves of 10% and 3% of the rated power and energy capacities of the battery, respectively. The reserved capacity for frequency control tasks is rewarded through proper incentives. Hence, the total penetration level of the RE and the total community welfare are increased due to available incentive rates. The main disadvantage of this scenario is the reduced lifetime of the battery due to frequent charging and discharging for primary frequency control actions. The lifetime of ESS can be reduced in a wide range depending on many factors, including the energy management strategy and SOC range of the ESS [88]. The performance

of the battery is impacted significantly due to increased number of cycles and cell temperature [88]. In this case, replacement of the batteries requires funding resources and further decreases the total welfare.

In order to demonstrate the impact of replacing the ESS on social welfare and system costs, the replacement cost of the ESS is considered as a component in the total project costs and the optimal solution is obtained. It is assumed that the required funding for ESS replacement is preserved form the beginning of the project. The ESS lifetime is assumed to be 10 years, where the same amount and type of ESS should be purchased and installed 10 years after their first installment. It should be noted that the amount of preserved funding for equipment replacement is equal to their future value at the time of their replacement. The results, summarized in Table 4.3, confirm that ESS replacement imposes higher costs on the system which can further decrease the RE and ESS optimal sizing due to higher costs. The social welfare can accordingly decrease as a result of higher equipment cost.

Table 4.3: Summary of the results for including replacement cost of ESS

		No replacement cost			Replacement cost included ($L_{ESS} = 10$)		
	Unit	Store	WTP	SbC	Store	WTP	SbC
Solar PV size	kW	300[c]	135[c]	190[c]	225[c]	135[c]	140[c]
Wind turbine size	kW	-	-	-	-	-	-
ESS power size	kW	265[c]	105[c]	-	145[c]	100[c]	-
ESS energy size	kWh	1325[c]	515[c]	-	725[c]	500[c]	-
Percentage of load demand provided by RE[c]	%	47.15	46.3	2.56	36.49	45.90	1.88
Capital Cost							
Solar	M$	1.99	0.89	1.26	1.498	0.899	0.932
Wind	M$	-	-	-	-	-	-
ESS	M$	1.03	0.4	-	0.933	0.391	-
Total income (discounted value)	M$	1.675	0.670	0.729	1.239	0.669	0.537
Total cost (discounted value)	M$	1.375	0.601	0.684	1.055	0.597	0.504
Welfare over 20-year horizon	M$	0.302	0.069	0.044	0.184	0.072	0.033
Total Welfare	M$		0.416			0.289	

WTP: Water Treatment Plant, SbC: Subsidized Customer, [a]1st year,[b] 4th year,[c] 5th year,[d] 6th year

- Scenario II: The second option is to incorporate a flywheel storage alongside a battery system. The battery system (installed at store) participates in energy management and also secondary frequency control with secondary reserve capacity of

3% of its rated capacity. The flywheel system is responsible to contribute in primary frequency control to provide primary reserve capacity. In this scenario, the contribution of battery in secondary frequency control is rewarded through incentives, whereas no incentives are considered for primary control reserve capacity. In this case the assumption is that the capital cost for installation of flywheel is not provided by community; thus, no income is obtained through providing this service. The main advantage of this scenario over the first scenario is preserving the lifetime of the battery and reducing the need for battery replacement. The results of the optimization problem are presented in Table 4.2, where a flywheel unit with capacity range of 20-50 kW (depending to the available commercial unit sizing) should also be considered for taking care of the primary frequency reserve requirements. Although, the welfare is decreased compared to Scenario I due to lack of incentives allocated for primary frequency reserve, the additional cost for battery replacement in Scenario I would decrease the total welfare to values lower than those for Scenario II. Thus, the advantage of this Scenario over Scenario I is performance improvement and lifetime preservation of battery units.

4.5 Discussion

Integration of ESS in microgrids of remote communities is still restricted due to limited confidence and experience in successful operation of such systems. High installation, operation and maintenance costs of ESS are also an important barrier in development of ESS projects in remote communities. The advances in ESS technologies, ESS price reduction, financial support from governments and industry and further studies on different aspect of ESS technology integration can lead to increased number of ESS projects in remote communities. However, communities such as KLFN can still benefit from ESS technologies such as lithium-ion battery and flywheel to extend their microgrid and embrace the addition of RE resources in their power generation portfolio. Considering geographic specifications of the community, the maturity and availability of the ESS technologies, the installation and operation costs, the efficiency and lifetime of different ESS technologies and their environmental impacts, combining lithium-ion battery and flywheel makes a reliable and reasonable hybrid ESS for integration in KLFN to provide energy management and regulation services.

4.6 Summary

This Chapter provided an overview of different ESS technologies for integration in isolated microgrids of remote communities. The main criteria for selecting the most feasible ESS options are discussed. Major advantages and shortcomings of various technologies, including lithium ion battery, flow battery, hydrogen fuel cell and flywheel, are compared. The methodology of sizing an ESS for KLFN remote community and the possibility of considering a HESS are introduced. The results of the planning optimization problem for two cases where a battery ESS and a hybrid ESS comprising a battery and a flywheel are presented and discussed.

Chapter 5

Demand Response, Carbon Footprint, and Sensitivity Analysis

In this Chapter, first the impact of demand response on the optimal sizing of RE and ESS units for integration in isolated microgrids of remote communities is investigated. It is assumed that a certain percentage of load demand can be shifted to a different time during a day and the impact of load shifting on the solution of the planning optimization problem is evaluated. Next, the impact of integrating RE and ESS on carbon footprint reduction in remote communities is addressed and studied. Finally, sensitivity analysis is conducted to assess the effect of varying some of the optimization model parameters on the solution of optimal microgrid planning problem.

5.1 Demand Response

Electric power generation in remote communities is often characterized by use of expensive resources, such as diesel fuel. Deploying RE resources in remote locations can also be costly due to high costs of equipment transportation to remote areas and installation. Thus, exploring different options for reducing the power generation costs and making the best use of the available resources is of great importance. Demand Response (DR) can play an important role in matching the profile of the load demand to that of the generated power, especially in microgrids with RE integration, where a fraction of the generated power is intermittent and fluctuating. Implementation of DRM techniques in the control and management of microgrids can help to increase the benefits obtained by the customers through improved utilization of the available resources [89–92].

Implementing DRM includes adjusting the customers' consumption patterns through voluntary or automatic processes [89]. The decisions made by customers and the actions taken by them toward changing the electricity consumption behavior, in response to signals such as variable electricity pricing, are part of voluntary DRM. Automatic DRM entails direct control of loads such as heating or cooling systems [89], based on an agreement between the customers and utility.

The flexibility in consumption patterns can be achieved by rescheduling a specific portion of the total load demand to another time period within a specified time window. The types of loads that can be considered as flexible/controllable loads include thermostatically-controllable loads such as water heaters, space heaters and air conditioning units, as well as appliances that are not necessarily required to operate at a specific time, such as dishwashers, cloth washers and dryers. These flexible loads constitute about 70% of the total residential loads [91], that can be managed to contribute to DRM.

Flexible loads can be considered as virtual storage as they can change the energy consumption patterns by delaying or advancing the energy consumption [89]. They can also be managed to follow the generation of RE resources; thus, allowing higher RE penetration levels [90].

In order to implement DRM in remote communities, the composition of loads must be recognized first. The subsidized customer category mainly includes the residential loads. The management of these loads can be done automatically by adjusting the thermostats or voluntarily through a pre-specified schedule provided to the customers. For unsubsidized customer category which include mostly government and business buildings, depending on type of loads, a similar management strategy can be used. It should be noted that residents of remote communities are usually aware of the electric power restrictions in their community and are often willing to cooperate to overcome the related issues. Their participation does not necessarily need to be compensated for by incentives. The main incentive is for the utility which benefits by reducing its costs through efficient utilization of its resources [89]. In some Canadian remote communities, demand management strategies including energy efficiency improvements and energy conservation awareness education and training programs are deployed to reduce fuel consumption and GHG emissions [93].

In order to consider flexible loads in the planning optimization problem, extra set of constraints are added to the mathematical formulation of the planning problem, as presented in subsection 3.2.2. The load profile of the system is rescheduled by adding a flexible load component to the original load profile; hence the rescheduled profile of the system is derived according to 5.1:

$$PDresch._{i,t,h} = PD_{i,t,h} - PDflex._{i,t,h} \tag{5.1}$$

In (5.1), $PD_{i,t,h}$ is the load profile of the system with no flexible loads and $PDresch._{i,t,h}$ is the new load profile after considering flexible loads that must be supplied through demand-supply balance equation, presented in 3.7. $PDflex._{i,t,h}$, which is the flexible load component, can be positive/negative depending on whether a portion of the load is being shifted from/to another time within a 24-hour time window. Hence, the total load shifted from/to another time in each 24-hour period should be zero, as expressed by (5.2). $PDflex._{i,t,h}$ is an optimization variable and is determined in the result of the optimization problem. It is also assumed that hourly flexible load can be no more than a certain percentage ($RSCH$) of the hourly load demand, as expressed by (5.3).

$$\sum_{h=24(n-1)+1}^{24n} PDflex._{i,t,h} = 0 \qquad \forall i, t, n = 1 : 365 \tag{5.2}$$

$$|PDflex._{i,t,h}| \leq RSCH \cdot PD_{i,t,h} \tag{5.3}$$

5.1.1 Case Study: KLFN Community

The optimization problem is solved to evaluate the impact of flexible loads on the solution of optimal planning problem of KLFN community, using the parameters listed in Table 3.3. Multiple cases assuming maximum 15% ($RSCH = 15\%$) and 30% ($RSCH = 30\%$) flexibility in total load, with and without integration of ESS, are considered. A summary of the results of the multiple-year planning problem considering the flexible demand is presented in Table 5.1.

Figure 5.1 demonstrates the implementation of DRM for an arbitrary 24-hr period in KLFN's subsidized customer group considering maximum 15% flexible load ($RSCH = 15\%$). The total load demand, reschedulable and non-reschedulable portions of the total load and the maximum permissible flexible demand are shown.

As the results of Table 5.1 show, implementing DRM in remote community microgrids can increase the potential benefits provided by integration of RE by decreasing the mismatch between generation and the load profile.

For the case with 15% flexible load, the RE penetration level decreases compared to the case with 0% flexible load; however, the total welfare increases due to increased utilization of resources.

The 30% flexible load, allows for higher penetration of RE compared to the case with 15% flexible load and the total welfare increases as well. The total community welfare

Table 5.1: Summary of the results of the planning optimization problem considering flexible load demand

			Solar PV Size	Wind Turbine Size	ESS Power Size	ESS Energy Size	Percentage of load demand provided by RE[f]	Capital Cost			Total Welfare
		Unit	kW	kW	kW	kWh	%	Solar M$	Wind M$	ESS M$	M$
Without ESS	RSCH=0%	WTP	30[a]	20[e]	-	-	19.95	0.25	0.22	-	0.158
		Store	50[a]	60[e]	-	-	20.99	0.40	0.65	-	
		SbC	100[e]	-	-	-	1.35	0.6	-	-	
	RSCH=15%	WTP	25[e]	20[e]	-	-	18.5	0.2	0.22	-	0.204
		Store	100[b]	-	-	-	16.22	0.7	-	-	
		SbC	-	-	-	-	~ 0	-	-	-	
	RSCH=30%	WTP	30[d]	20[e]	-	-	20.35	0.24	0.22	-	0.236
		Store	100[b]	60[e]	-	-	28.8	0.7	0.65	-	
		SbC	-	-	-	-	~ 0	-	-	-	
With ESS	RSCH=0%	WTP	125[e]	-	100[e]	495[e]	43.53	0.83	-	0.39	0.287
		Store	240[e]	-	145[e]	725[e]	38.45	1.6	-	0.57	
		SbC	150[e]	-	-	-	2.02	0.99	-	-	
	RSCH=15%	WTP	100[e]	-	50[e]	250[e]	34.77	0.66	-	0.20	0.317
		Store	240[e]	-	140[e]	700[e]	39.05	1.6	-	0.55	
		SbC	100[e]	-	-	-	1.35	0.66	-	-	
	RSCH=30%	WTP	100[e]	-	100[e]	270[e]	35.73	0.66	-	0.28	0.339
		Store	270[e]	-	150[e]	750[e]	43.45	1.8	-	0.58	
		SbC	145[e]	-	-	-	1.96	0.96	-	-	

WTP: Water Treatment Plant, SbC: Subsidized Customer, [a]1st year,[b] 2nd year,[c] 3rd year,[d] 4th year,[e] 5th year,[f] 6th year

can increase by almost 28% where 15% of the hourly demand can be rescheduled, and the increase in welfare can rise by 48% where 30% of the demand is reschedulable, for the case without considering ESS.

For the condition where integration of ESS is considered, implementing demand response can increase the welfare by up to 18% which is more than twice the welfare for the condition where no ESS and DRM are considered. Implementing DRM can replace a fraction of the required ESS capacity, confirming the role of virtual storage, by shifting the power demand to different time frames, and decrease the total capital cost of the project.

5.2 Carbon Footprint

There are about 300 remote communities in Canada, and more than 80% of these communities are electrified by fossil fuel-based generation [94]. These generators consume more than 215 million liters of fuel per year to generate electricity, which corresponds to more than 600 kilo-tonnes of CO_2 emissions [95]. It is estimated that province of Ontario's remote first nation communities produce about 65 kilo-tonnes of GHG emissions annually, to supply their current electricity demands [96]. Relying on fossil fuel for electricity

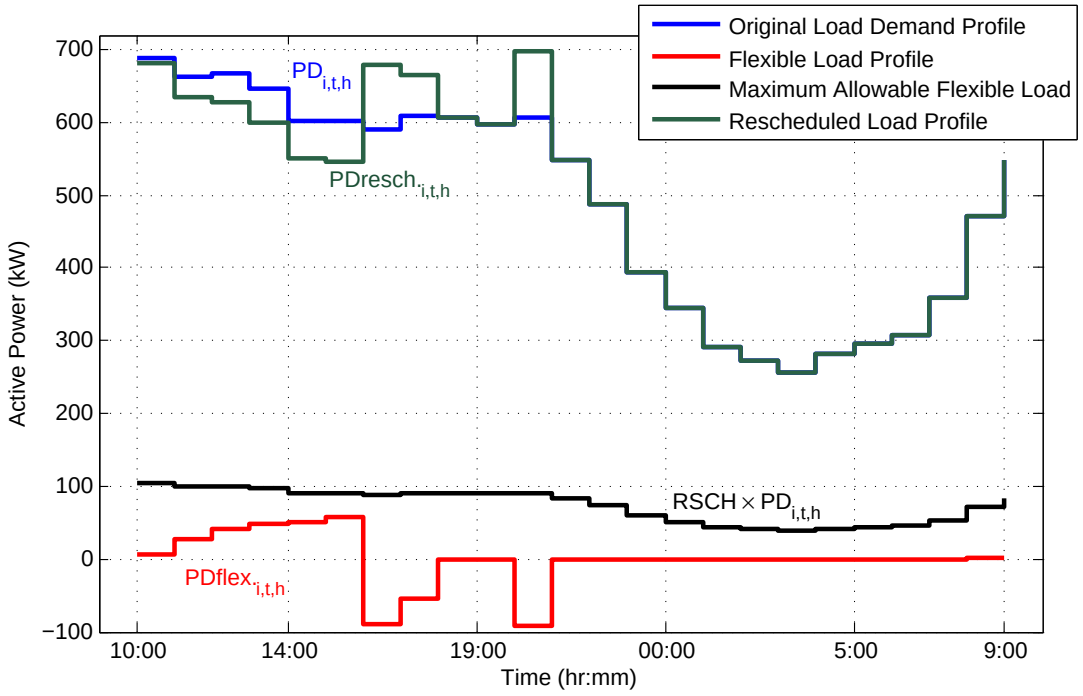

Figure 5.1: Implementation of DRM for an arbitrary 24-hr period in KLFN's subsidized customer group considering 15% flexible load.

generation increases the contribution of these communities to GreenHouse Gas (GHG) emissions as their electric power demand grows. Furthermore, fuel transportation to these communities which in many cases entails shipment over long distances either by plane or via winter roads, is another source of GHG emissions. Fuel spills on generation sites and during transportation also contribute to the total pollution created by fuel-based electricity generation. Figure 5.2 shows the composition of GHG emission sources for HORCI's communities [93], where indirect GHG emissions, including fuel transportation, constitute more than 40% of the total emissions.

In order to reduce dependency on fuel and limit the adverse environmental impacts of fuel-based power generation, RE integration as well as connection to provincial transmission grids are being considered by federal and provincial governments in Canada, to promote sustainable power supply to remote communities and decrease GHG emissions. As an example, the Wataynikaneyap Power project aims to connect the northern Ontario remote communities to the Ontario's transmission network. It is estimated that this project will contribute to more than 1 million dollars in Canada's gross domestic product

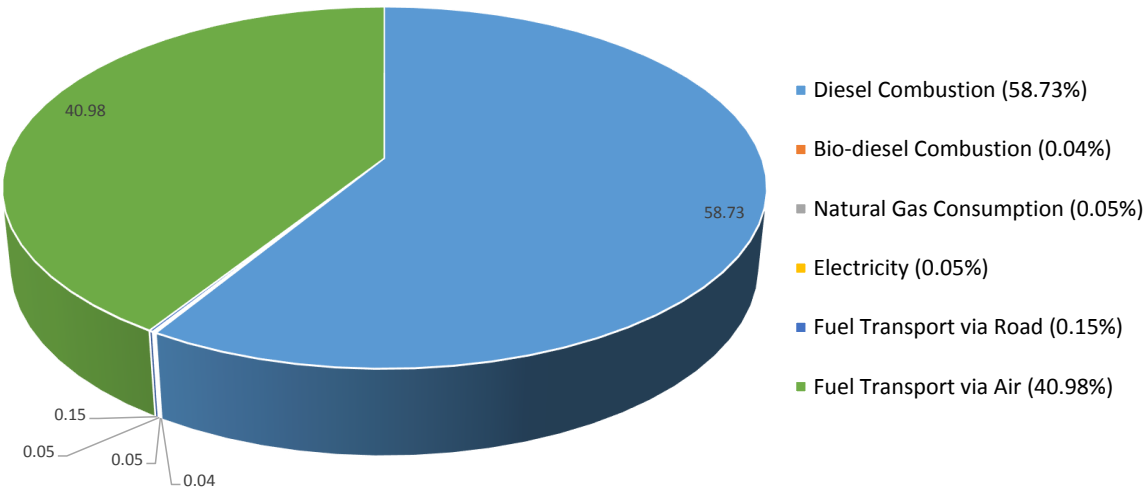

Figure 5.2: Composition of GHG emission sources for HORCI's communities [93].

(GDP) and will create numerous job opportunities in northern Ontario and Canada [97]. Consequently, it will have a considerable impact on GHG emissions reduction. Furthermore, participation of communities in renewable energy projects has been facilitated by providing financial assistance and loan mechanisms and establishing regulatory acts and agreements. Through Ontario's Green Energy and Green Economy Act, price incentives, reduced security payments and price adders are offered and loan guarantee and energy partnership programs are developed to increase the engagement of the remote communities in RE projects [98]. Furthermore, there have been direct actions taken towards reducing GHG emissions, including equipment upgrade, fuel switching and implementing demand management programs [93]. As an example, deploying direct actions in HORCI's communities, have decreased the CO_2 emission by 277 tonnes in 2011 [93].

In Canada, provinces of British Columbia in 2008 and Alberta in 2017 have developed carbon tax mechanisms, while provinces of Quebec in 2014 and Ontario in 2017 have chosen to implement cap-and-trade systems to participate in government's plan on GHG emission reduction. The carbon tax mechanism puts a price on each tonne of emitted GHG to encourage reduction of fuel consumption, increase in fuel efficiency and adaption of new technologies. The cap-and-trade program puts a limit on GHG emissions, while adding the flexibility to the way the cap limit is being met. The other provinces and the federal government of Canada are also planning to take or have started taking similar approaches towards enforcing actions for reaching the federal government's goal of GHG emission reduction by 30% with respect to 2005 levels by 2030 [99].

5.2.1 Case Study: KLFN Community

The total direct GHG emissions of KLFN community in 2011 has been around 3,200 tonnes per year which is equal to 7.30% of the total CO_2 emissions by HORCI's communities [93]. Fuel transportation to KLFN, by road and air, also contributed to GHG emissions of almost 14 and 1,200 tonnes per year in 2011, respectively [93].

As part of emission reduction activities at KLFN, two engines were replaced in 2009 that has increased the generation efficiency by around 0.15 kWh per Liter and reduced the CO_2 emissions by almost 150 tonnes per year [93]. Renewable energy integration projects at KLFN have also been taking place to investigate the feasibility of integration of RE resources in order to reduce the fuel dependency and GHG emissions [19].

The RE integration projects involve determining the optimal RE and possibly ESS unit sizes to meet certain objectives and requirements, as presented in subsection 3.2.2. In the case of KLFN community, the optimal sizes of RE and ESS units, as determined in subsection 3.3.2 and illustrated in Table 3.4, are obtained by the objective of maximizing the total welfare to the community. As a consequence, the GHG emissions are reduced compared to the base case with no RE included in the microgrid of the community.

Table 5.2 shows the impact of RE and ESS integration on carbon footprint reduction in KLFN's microgrid. The diesel consumption is estimated using the fuel consumption curves for different generator sizes. Figure 5.3 shows the fuel consumption curves at different load percentages for various generator sizes. It is worth noting that fuel consumption at idling could be approximately up to 25 to 30% of the consumption at nominal rated power [100].

The results demonstrate that integration of RE resources can reduce the GHG emissions by almost 3.5% for the case without ESS. If ESS is considered as a feasible option for integration in KLFN network, GHG emissions can be reduced by more than 6%.

Increasing the penetration levels of RE resources beyond optimal values, to increase the carbon footprint reduction, can impose higher costs and decrease the total welfare. In order to investigate the impact of further decreasing the carbon footprint on optimal unit sizes and associated costs, an additional constraint is added to the optimization problem to enforce the minimum diesel generation reduction limit. The additional constraint, as given by (5.4), limits the generated power by diesel generators at each year to a percentage of the total load demand, specified by $PDG_{red.}$. According to this constraint, the maximum

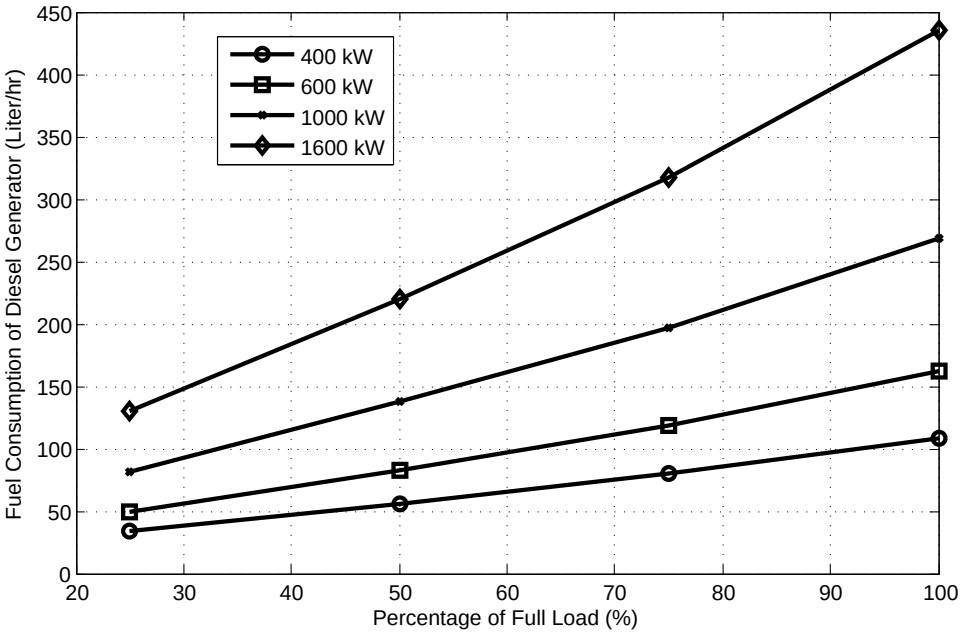

Figure 5.3: Fuel consumption of a diesel generator based on the generator size and percentage of full load [101].

Table 5.2: Impact of RE and ESS integration on carbon footprint reduction in KLFN

	Unit	No RE	Without ESS			With ESS		
			Store	WTP	SbC	Store	WTP	SbC
Solar PV size	kW	-	50^a	30^a	100^b	240^b	125^b	150^b
Wind Turbine size	kW	-	60^b	20^b	-	-	-	-
ESS power size	kW	-	-	-	-	145^b	100^b	-
ESS Energy Size	kWh	-	-	-	-	725^b	495^b	-
Percentage of load demand provided by RE[c]	%	0	20.99	19.95	1.35	38.45	43.53	2.02
Diesel Power Generation[c]	GWh/year	5.33	5.15			5.00		
Diesel fuel Consumption[c]	M liters/year	1.423	1.375			1.338		
Direct GHG Emission[c]	tonnes/year	$4,264^+$	$4,120^+$			$4,000^+$		

WTP: Water Treatment Plant, SbC: Subsidized Customer, [a]1st year,[b] 5th year,[c] 6th year
[+]Direct GHG emission (diesel combustion) is assumed to be 0.0008 $tonnes/kWh$ [50]

diesel power generation in each year is restrained.

$$\sum_{h=1}^{H} Pdg_{t,h} \leq PDG_{red.} \times \sum_{i=1}^{I} \sum_{h=1}^{H} PD_{i,t,h} \quad \forall\, t = 1, .., T \tag{5.4}$$

The results of the optimization problem, including (5.4), for two values of $PDG_{red.}$ are summarized in Table 5.3.

Table 5.3: Summary of the results of the planning optimization problem, considering carbon footprint reduction constraint

		$PDG_{red.} = 0.9$			$PDG_{red.} = 0.8$		
	Unit	Store	WTP	SbC	Store	WTP	SbC
Solar PV size	kW	235^a	150^c	500^a	330^c	130^b	500^a
Wind turbine size	kW	120^c	40^b	80^c	180^c	40^a	900^a
ESS power size	kW	155^c	100^c	-	190^c	100^c	-
ESS energy size	kWh	725^c	500^c	-	950^c	500^c	-
Percentage of load demand provided by RE[d]	%	58.14	61.53	8.06	72.17	58.87	20.93
Capital Cost (discounted value)	M$		8.37			16.51	
Solar	M$	1.66	0.99	3.54	2.23	0.90	3.45
Wind	M$	1.26	0.46	0.86	1.83	0.46	8.51
ESS	M$	0.56	0.39	-	0.74	0.39	-
Total income (discounted value)	M$	2.132	0.993	3.079	2.344	1.038	8.42
Total cost (discounted value)	M$	2.145	0.987	3.167	2.483	1.113	9.890
Welfare over 20-year horizon	M$	-0.013	0.006	-0.088	-0.139	-0.075	-1.465
Total Welfare	M$		-0.095			-1.679	
Diesel Power Generation[d]	GWh/year		4.57			3.89	
Diesel Consumption[d]	M liters/year		1.22			1.04	
Direct GHG Emission[d]	tonnes/year		$3,656$			$3,112$	

WTP: Water Treatment Plant, SbC: Subsidized Customer, [a]1st year,[b] 2nd year,[c] 5th year,[d] 6th year

The results confirm that in order to increase the penetration level of RE to reduce the GHG emissions, the project costs increase significantly. Furthermore, the income obtained by the project is not enough to cover all the costs, thus resulting in negative welfare. Decreasing the maximum diesel power generation from 90% of the total demand to 80%, increases the project capital cost by almost 100%. However, the diesel consumption reduces by almost 15% and the GHG emissions decrease accordingly.

Reaching lower diesel consumption with current conditions, further increases the costs and decreases the total welfare; thus, at the current rates and prices achieving higher RE

penetration levels is not economically feasible. In order for high RE penetration levels to become feasible, extra incentives and funding resources must be allocated. Decreasing the capital cost of RE equipment which is likely to happen in the coming years can also help to increase the share of RE in electric power generation portfolio of remote communities. Also, implementing carbon tax pricing schemes or cap-and-trade programs can promote the integration of RE resources by increasing the savings obtained by incorporation of RE.

5.3 Sensitivity Analysis

The mathematical model of the planning optimization problem, presented in subsection 3.2.2, employs various parameters, such as cost values, discount rates and incentives, which influence the results of the optimal planning problem. Each one of these parameters can be dependent on multiple variables and their value can change over time, as a result of technological advances or under certain regulatory acts and programs. Hence, evaluating the effect of variation of some of these parameters on the results of the optimal planning model is invaluable and can provide an insight into economic and technical outlook of RE integration projects. Therefore, a sensitivity analysis is performed in order to determine how the planning model parameters impact the objective and the variables of the optimization model. The following is a discussion on the results of the sensitivity analysis performed on the planning optimization model of the KLFN community:

- *Alternative Funding:* In many RE projects, the project capital costs is funded through contribution of several stakeholders. In the planning model presented in 2.3, these contributions are denoted by parameters b_{cep} and b_{efp} which represent the percentages of capital contribution of the community and available external government funding with respect to the total project cost, respectively. In this thesis, the base case study for KLFN, considers 10% and 50% (70% for ESS) contributions from the community and government funding, respectively, as presented in 3.3.2. However, considering various funding alternatives can lead to different outcomes in terms of project objectives and optimal structure of the microgrid. Thus, multiple cases are considered to investigate the alternative options to fund RE projects in KLFN. A summary of the results are presented in Table 5.4 and Table 5.5.

  Table 5.4 considers different government funding contributions higher than the base case presented in 3.3.2. The results confirm that higher RE generation and higher welfare are achievable at the presence of higher funding resources. Consequently, the diesel power generation is decreased as the RE generation increases. However, the

Table 5.4: Summary of the results for alternative government funding options

		$b_{efp} = 60\%$, $b_{cep} = 10\%$			$b_{efp} = 70\%$, $b_{cep} = 10\%$		
	Unit	Store	WTP	SbC	Store	WTP	SbC
Solar PV size	kW	195[c]	125[c]	155[a]	250[c]	105[c]	500[c]
Wind turbine size	kW	100[c]	40[c]	-	120[b]	80[c]	500[c]
ESS power size	kW	125[c]	100[c]	-	265[c]	125[c]	300[c]
ESS energy size	kWh	625[c]	500[c]	-	1325[c]	625[c]	1500[c]
Percentage of load demand provided by RE[d]	%	50.75	58.02	2.09	61.66	66.16	14.83
Total load demand not provided by RE[d]	GWh/year	0.183	0.072	4.687	0.142	0.058	4.077
Diesel Power Generation[d]	GWh/year		4.92			4.24	
Capital Cost (discounted value)	M$		4.41			11.24	
Solar	M$	1.298	0.832	1.099	1.665	0.699	3.330
Wind	M$	1.065	0.439	-	1.285	0.861	4.440
ESS	M$	0.488	0.389	-	1.036	0.488	1.165
Total income (discounted value)	M$	1.060	0.855	0.839	2.030	0.978	4.237
Total cost (discounted value)	M$	1.306	0.741	0.709	1.526	0.767	3.642
Welfare over 20-year horizon	M$	0.294	0.141	0.129	0.503	0.210	0.595
Total Welfare	M$		0.537			1.309	
Community's contribution	M$		0.306			0.681	
Government funding	M$		1.840			4.769	

WTP: Water Treatment Plant, SbC: Subsidized Customer, [a]1st year,[b] 4th year,[c] 5th year,[d] 6th year

total capital costs and the contributions of the community and the government to the project capital costs at the start of the project must increase significantly.

In different cases, the contribution of the community to the project capital cost at the start of the project is decreased and increased compared to the base case. The results, summarized in Table 5.5, indicate the negative and positive impact of lower and higher community contribution on the welfare and RE generation levels compared to the base case.

The external government funding can play an important role in development of RE projects. Although, higher contribution at the start of the project entails greater amount of available funding resources, the savings obtained as a result of replacing fuel-based generation with RE-based generation during project lifetime, which is subsidized by government for certain customers, can compensate for the costs at the beginning of the project.

- *Power Purchase Agreement:* A Power Purchase Agreement (PPA) contract, which

Table 5.5: Summary of the results for alternative community contribution

		$b_{efp} = 50\%$, $b_{cep} = 0\%$			$b_{efp} = 50\%$, $b_{cep} = 20\%$		
	Unit	Store	WTP	SbC	Store	WTP	SbC
Solar PV size	kW	240[c]	100[c]	115[b]	250[c]	125[c]	155[c]
Wind turbine size	kW	-	-	-	-	-	-
ESS power size	kW	140[c]	50[c]	-	160[c]	100[c]	-
ESS energy size	kWh	700[c]	250[c]	-	800[c]	490[c]	-
Percentage of load demand provided by RE[c]	%	33.86	38.25	1.55	40.09	43.47	2.08
Total load demand not provided by RE[d]	GWh/year	0.229	0.113	4.713	0.222	0.097	4.687
Diesel Power Generation[d]	GWh/year		5.04			4.99	
Capital Cost (discounted value)	M$		2.87			3.39	
Solar	M$	1.598	0.666	0.778	1.665	0.832	1.032
Wind	M$	-	-	-	-	-	-
ESS	M$	0.547	0.204	-	0.625	0.386	-
Total income (discounted value)	M$	1.204	0.493	0.483	1.260	0.629	0.595
Total cost (discounted value)	M$	1.021	0.418	0.461	1.075	0.558	0.557
Welfare over 20-year horizon	M$	0.182	0.075	0.022	0.185	0.071	0.038
Total Welfare	M$		0.279			0.294	
Community's contribution	M$		0			0.415	
Government funding	M$		0.967			1.122	

WTP: Water Treatment Plant, SbC: Subsidized Customer, [a]1st year,[b] 4th year,[c] 5th year,[d] 6th year

is legally binding and supports the independent generation and selling of power by independent power producers [102], can be arranged to reward the generation and selling of the RE power by the community. This can promote the community ownership of RE power generation facilities; however, determining the export rate that benefits all the parties involved can be complicated [19]. Usually, the utilities define the PPA rate based on the avoided cost of diesel (i.e., the cost of buying and transporting fuel and generating electricity using fuel in the remote communities), and in Canada, most PPA rates are around 0.30 $/kWh [102].

Three cases are considered in this study to evaluate the impact of implementing a PPA contract on optimal planning problem objective and variables. The results that are summarized in Table 5.6, indicate slight increase in the total community welfare as the PPA rate increases. Furthermore, the major benefit is obtained by the unsubsidized customers which have the capability to generate more than their load demand and export to the microgrid; the subsidized customer's RE generation level

is barely enough to provide their own demand; thus, they do not get any benefits from exporting power to the microgrid.

Table 5.6: Comparison of the results for various available PPA rates

	Unit	$EXP_i = 0.1$ \$/kWh			$EXP_i = 0.2$ \$/kWh			$EXP_i = 0.3$ \$/kWh		
		Store	WTP	SbC	Store	WTP	SbC	Store	WTP	SbC
Solar PV size	kW	240[b]	100[b]	115[b]	250[b]	100[b]	100[b]	255[b]	145[b]	100[a]
Wind Turbine size	kW	20[b]	-	-	-	20[b]	-	40[b]	-	-
ESS power size	kW	145[b]	50[b]	-	145[b]	50[b]	-	135[b]	105[b]	-
ESS Energy Size	kWh	725[b]	250[b]	-	725[b]	250[b]	-	675[b]	520[b]	-
Percentage of load demand provided by RE[c]	%	42.39	33.86	1.55	39.53	42.22	1.35	47.16	48.04	1.34
Exported Power[c] (Pex_i)	MWh/year	8.087	4.660	0	9.313	5.938	0	15.50	7.44	0
Diesel Power Generation[c]	GWh/year		5.02			5.03			5.03	
Capital Cost										
Solar	M$	1.598	0.666	0.766	1.665	0.666	0.666	1.698	0.965	0.677
Wind	M$	0.222	-	-	-	0.222	-	0.439	-	-
ESS	M$	0.567	0.205	-	0.567	0.204	-	0.528	0.406	-
Total income (discounted value)	M$	1.337	0.496	0.442	1.256	0.622	0.384	1.520	0.717	0.420
Total cost (discounted value)	M$	1.150	0.417	0.414	1.061	0.543	0.360	1.317	0.637	0.399
Welfare over 20-year horizon	M$	0.187	0.078	0.027	0.195	0.079	0.024	0.203	0.080	0.021
Total Welfare	M$		0.293			0.299			0.305	

WTP: Water Treatment Plant, SbC: Subsidized Customer, [a]4th year,[b] 5th year,[c] 6th year

- *Discount Rate:* Several scenarios with different discount rates are considered. The base case considers the discount rate of 6% for the project. Two different cases with 4%, the value used by the Ontario Power Authority (OPA) [19], and 8%, reflecting higher risk of future cash-flow, are considered and the results are presented in Table 5.7.

  The higher discount rate is associated with lower welfare as the total welfare has inverse relationship with the discount rate. The lower discount rate offers higher total RE generation levels, but the difference is minor.

- *Reduced equipment cost:* The capital cost of the equipment for installation in remote communities is relatively high compared to those for non-remote locations, as discussed in subsection 3.3.1. Thus, the cost of equipment installation plays an important role in RE integration projects. The cost of different wind, solar and ESS technologies has been on a declining path in many markets worldwide [103–105], due to many reasons, including more competitive supply chains, increased scale and technology improvements [104]. The rate of decrease in costs can reach up to 20% per year depending on location, technology and the scale of the project. However, for remote community applications, considering the relatively small scale and location

Table 5.7: Comparison of the results for different customer discount rates

	Unit	$r_{d_i} = 4\%$			$r_{d_i} = 6\%$			$r_{d_i} = 8\%$		
		Store	WTP	SbC	Store	WTP	SbC	Store	WTP	SbC
Solar PV size	kW	250[b]	125[b]	155[b]	240[b]	125[b]	150[b]	220[b]	130[b]	155[b]
Wind Turbine size	kW	-	-	-	-	-	-	-	-	-
ESS power size	kW	160[b]	100[b]	-	145[b]	100[b]	-	135[b]	100[b]	-
ESS Energy Size	kWh	800[b]	490[b]	-	725[b]	495[b]	-	675[b]	500[b]	-
Percentage of load demand provided by RE[c]	%	40.09	43.47	2.08	38.45	43.53	2.02	35.80	44.75	2.09
Diesel Power Generation[e]	GWh/year		4.9971			5.0063			5.0121	
Capital Cost										
Solar	M$	1.665	0.932	1.032	1.598	0.832	0.999	1.465	0.865	1.032
Wind	M$	-	-	-	-	-	-	-	-	-
ESS	M$	0.625	0.386	-	0.567	0.388	-	0.527	0.390	-
Total Welfare	M$		0.396			0.289			0.212	

WTP: Water Treatment Plant, SbC: Subsidized Customer, [a]1st year,[b] 5th year,[c] 6th year

Table 5.8: Comparison of the results for reduced equipment costs

	Unit	5% *cost reduction*			10% *cost reduction*			20% *cost reduction*		
		Store	WTP	SbC	Store	WTP	SbC	Store	WTP	SbC
Solar PV size	kW	245[d]	125[d]	150[d]	255[d]	130[d]	165[c]	270[d]	130[d]	150[a]
Wind Turbine size	kW	40[d]	20[d]	-	40[d]	-	-	60[d]	20[b]	-
ESS power size	kW	160[d]	100[d]	-	185[d]	100[d]	-	190[d]	100[d]	-
ESS Energy Size	kWh	800[d]	495[d]	-	925[d]	500[d]	-	950[d]	500[d]	-
Percentage of load demand provided by RE[e]	%	47.24	51.45	2.02	48.93	44.75	2.22	53.74	52.56	2.02
Diesel Power Generation[e]	GWh/year		4.9565			4.9535			4.9225	
Capital Cost										
Solar	M$	1.55	0.79	0.949	1.528	0.779	1.005	1.438	0.692	0.851
Wind	M$	0.417	0.211	-	0.395	-	-	0.522	0.183	-
ESS	M$	0.594	0.366	-	0.651	0.352	-	0.594	0.312	-
Total income (discounted value)	M$	1.486	0.749	0.576	1.541	0.650	0.693	1.541	0.650	0.643
Total cost (discounted value)	M$	1.261	0.660	0.521	1.273	0.536	0.611	1.273	0.536	0.611
Welfare over 20-year horizon	M$	0.224	0.089	0.054	0.268	0.113	0.081	0.268	0.113	0.081
Total Welfare	M$		0.368			0.463			0.669	

WTP: Water Treatment Plant, SbC: Subsidized Customer, [a]1st year,[b] 3rd year,[c] 4th year,[d] 5th year,[e] 6th year

remoteness, which affect the cost components, the cost of installation of RE and ESS equipment can decrease by a much smaller percentage. Nevertheless, in this study several cases are assumed to study the impact of reduced equipment capital costs on the objective and variables of the optimal planning problem. Table 5.8, summarizes the results of the planning optimization problem for different cases of 5%, 10% and 20% cost reduction in RE and ESS equipment capital costs at KLFN.

The results indicate the decreasing cost of equipment increases the social welfare remarkably, while the RE and ESS sizes slightly increase with reduced cost. The

Table 5.9: Comparison of the results for reduced cost of individual equipment

		5% cost reduction in solar installation cost			5% cost reduction in wind installation cost			5% cost reduction in ESS installation cost		
	Unit	Store	WTP	SbC	Store	WTP	SbC	Store	WTP	SbC
Solar PV size	kW	250[c]	135[c]	145[b]	220[c]	100[c]	115[c]	220[c]	130[c]	155[c]
Wind Turbine size	kW	20[c]	-	-	40[c]	-	-	-	-	-
ESS power size	kW	165[c]	100[c]	-	130[c]	50[c]	-	135[c]	100[c]	-
ESS Energy Size	kWh	825[c]	500[c]	-	650[c]	250[c]	-	675[c]	500[c]	-
Percentage of load demand provided by RE[d]	%	44.18	45.90	1.95	43.51	33.86	1.55	35.80	44.76	2.09
Diesel Power Generation[d]	GWh/year		4.98			5.02			5.01	
Capital Cost										
Solar	M$	1.581	0.854	0.932	1.465	0.666	0.766	1.465	0.866	1.032
Wind	M$	0.222	-	-	0.417	-	-	-	-	-
ESS	M$	0.645	0.391	-	0.508	0.205	-	0.501	0.371	-
Total Welfare	M$		0.352			0.293			0.299	

WTP: Water Treatment Plant, SbC: Subsidized Customer, [a]1st year,[b] 4th year,[c] 5th year,[d] 6th year

main reason for slight increase in sizing lies behind the fact that considering the low capacity factors of RE generation, the savings obtained by higher RE generation can not still justify the costs. Hence, the sizing remain almost the same while the objective of the optimization increases for reduced costs.

In three different cases, the capital costs of wind, solar and ESS at KLFN are decreased individually by 5% each to evaluate the impact of capital cost of each one of these components on the results of planning optimization problem. The results, summarized in Table 5.9, suggest that cost reduction of solar equipment has slightly higher impact on RE generation levels compared to wind and ESS units. The improvement in social welfare, with respect to the base case, is also higher for the case where solar equipment cost is reduced. The cases with cost reduction for wind and ESS equipment have very similar results in terms of RE generation levels and social welfare; however, the subsidized customers benefit most from ESS cost reduction, in terms of percentage of load fed from RE.

- *Increased amount of RE resources:* Two cases are studied to address the impact of availability of wind and solar resources on the social welfare of the KLFN community. The results for cases with 5% increase in available solar and wind power, summarized in Table 5.10, indicate a remarkable improvement in social welfare for the case with higher available solar power. However, the increase in wind power has a minor impact on the improvement of total welfare. The results are expected due to lower capital cost of solar installations and higher compatibility of solar generation profile with the load profile of the community.

Table 5.10: Summary of the results for the increased amount of available RE resources

		5% increase in solar resources			5% increase in wind resources		
	Unit	Store	WTP	SbC	Store	WTP	SbC
Solar PV size	kW	250[c]	120[c]	145[b]	225[c]	100[c]	120[c]
Wind turbine size	kW	-	-	-	40[c]	20[c]	-
ESS power size	kW	195[c]	100[c]	-	140[c]	50[c]	-
ESS energy size	kWh	850[c]	500[c]	-	700[c]	250[c]	-
Percentage of load demand provided by RE[c]	%	41.79	43.76	2.05	44.78	42.62	1.61
Diesel Power Generation[d]	GWh/year		4.99			5.00	
Capital Cost (discounted value)	M$		3.40			3.27	
Solar	M$	1.665	0.799	0.981	1.498	0.666	0.799
Wind	M$	-	-	-	0.439	0.222	-
ESS	M$	0.664	0.388	-	0.547	0.205	-
Total income (discounted value)	M$	1.316	0.634	0.639	1.406	0.621	0.461
Total cost (discounted value)	M$	1.088	0.542	0.579	1.214	0.543	0.432
Welfare over 20-year horizon	M$	0.227	0.092	0.061	0.192	0.078	0.028
Total Welfare	M$		0.380			0.299	

WTP: Water Treatment Plant, SbC: Subsidized Customer, [a]1st year,[b] 4th year,[c] 5th year,[d] 6th year

5.4 Summary

This Chapter presented the inclusion of demand response in the microgrid planning problem. The impact of 15% and 30% flexibility in the daily load on the results of the planning optimization problem was investigated. It was shown that implementing demand response strategies can enhance the community welfare and replace a fraction of the ESS size by acting as virtual storage. Carbon footprint reduction as one of the drivers for integration of RE resources was addressed and the impacts of RE and ESS integration on reduction of fuel consumption and GHG emissions were studied. In order to evaluate the effect of variation of planning model parameters, such as equipment costs and discount rate, a sensitivity analysis was performed and the results were discussed.

Chapter 6

Summary, Contributions and Future Work

6.1 Summary and Conclusions

Chapter 1 discussed the motivation and relevance of the thesis, followed by a review on the existing work in the literature on the optimal planning of isolated microgrids. The objectives of the research were introduced and the organization of the thesis was explained in this Chapter.

Chapter 2 presented a background review of different topics relevant to the microgrid planning. A general overview of microgrids, distributed energy resources, microgrid loads, demand management and control of microgrids was presented in this Chapter. Frequency and voltage regulation in isolated microgrids and the control mechanism in synchronous machines and inverter-based generation units were discussed briefly. Frequency regulation and load following as two critical services performed in the microgrids were introduced. A three-phase power flow model was presented and used to determine the status of the voltages in an isolated microgrid comprising of inverter-based and conventional generation units. Optimal reactive power planning as a common practice to determine the required reactive support was explained. An introduction to Canadian remote community microgrids and electricity generation scheme in northern Ontario remote communities was presented. Planning of RE-based remote community microgrids as well as a mathematical planning model were explained. Finally, GAMS platform and some of its solvers were introduced as an optimization problem solving tool.

Chapter 3 presented the proposed optimal planning platform for integration of RE and ESS in microgrids of remote communities. The multi-stage multiple-year planning platform subdivides the planning problem into various stages including: project identification, planning optimization, optimal structure evaluation and decision making. Various aspects of planning an isolated microgrid for remote communities, including available resources, objectives and challenges, economic parameters and the characteristics of existing power system, are identified in the project identification stage. In the planning optimization stage, the mathematical model of the planning problem is derived and solved. The optimal unit sizes determined in the optimization stage are used to evaluate the impact of integration of RE and ESS on the frequency and voltage regulation of the microgrid. According to the simulated frequency and voltage profiles and considering the desired regulation limits of the microgrid, a decision to revise the structure of the microgrid is made in the final stage. The planning optimization model is solved again with the additional constraints to include the operation regulation limits. A case study on Kasabonika Lake First Nation (KLFN) community was developed to demonstrate the performance of the multi-stage, multiple-year planning platform. The frequency and voltage profile of the system after integration of RE resources were simulated. The results showed that the voltage regulation in KLFN community was not considerably impacted by integration of RE, whereas the frequency profile was affected and needed to be considered for further evaluation. The structure of the microgrid was revised according to the desired frequency regulation constraint and the new optimal structure was determined. The proposed optimal planning platform is general and can be used in planning of isolated microgrids with different applications and in various locations.

Chapter 4 discussed the criteria for selection of an energy storage system for isolated microgrids of remote communities. Different ESS types and their main features were reviewed and compared. The proper selection of type and size of the ESS for integration in KLFN community was discussed and explained, and sizing of an ESS considering various roles it can play in the microgrid was presented. Finally, the feasibility of integration of hybrid ESS was considered and discussed.

Chapter 5 studied the several subjects associated with microgrid planning projects. The impact of demand response management on the planning and sizing of an isolated microgrid was evaluated. The flexible demand concept was used to study the impact of demand flexibility on the optimal sizing of a microgrid. The case study of KLFN microgrid confirmed the positive impact of implementing DRM schemes on the welfare of the community. It was also shown that DRM could perform as a virtual storage system and replace part of the required capacity for ESS. The impact of RE and ESS integration in microgrid of remote communities on carbon footprint reduction was assessed. The optimal

microgrid sizing was obtained by enforcing a constraint to limit the maximum diesel power generation. The results indicated that limiting the GHG emissions would entail higher costs and reduced welfare while reducing the fuel consumption and GHG emissions. At the end of Chapter 5, a sensitivity analysis was conducted to address the impact of varying optimization model parameters on the objective and variables of the planning optimization problem.

6.2 Main Contributions

The main contributions of this research are:

- Developing a multi-stage, multiple-year optimal planning platform for planning remote community microgrids, considering frequency and voltage regulation constraints in the planning problem. The proposed platform intends to determine the optimal component sizes of the isolated microgrid while taking into account the impact of integration of RE and ESS on the operation and regulation of the frequency and voltage.
- Evaluating the possibility of integration of various ESS types and assessment of the main concerns related to the selection of the type and size of an ESS for isolated microgrids of remote communities.
- Investigating various issues relevant to planning of remote community microgrids, such as implementing demand response management strategies and carbon footprint reduction as a result of RE and ESS integration in remote communities.
- Creating various case studies based on real on-site measured data for KLFN community microgrid. The case studies can be used as a guideline to provide the remote communities with relevant studies on various aspects of planning RE-based microgrids and feasibility and viability of RE integration projects considering some of the existing challenges.

6.3 Future Work

The optimal planning platform can be extended to include the following work:

- Investigating the impact of ESS capacity degradation and cycle life reduction on planning of a microgrid and sizing of the units.
- Considering the impact of diesel generator size, efficiency and optimal operation in the planning of an isolated microgrid.
- Including thermal loads and heat management in the remote communities alongside electrical loads.
- Including the unbalanced load conditions and its impact on the optimal sizing.
- Considering different case studies to include various applications such as mining and military.

References

[1] J. Royer, "Status of remote/off-grid communities in Canada," tech. rep., Natural Resources Canada, August 2011. Available: https://www.nrcan.gc.ca/sites/www.nrcan.gc.ca/files/canmetenergy/files/pubs/2013-118_en.pdf.

[2] A. Mourelatou, "Renewable energies: success stories," tech. rep., Ecotec Research and Consulting Ltd. and European Enviroment Agency, 2001. Available: http://www.seai.ie/Publications/Renewables_Publications_/Energy_RD_D/reportecotec.pdf.

[3] "Tracking the energy revolution- Canada 2015," tech. rep., Clean Energy Canada, September 2015. Available: http://cleanenergycanada.org/trackingtherevolution-canada/2015/assets/pdf/TrackingtheEnergyRevolution-Canada2015.pdf.

[4] "Clean energy Africa-finance guide," tech. rep., Clean Energy Pipeline, VB/Research Ltd., 2015. Available: http://www.cleanenergypipeline.com/Resources/CE/ExpertGuides/CleanEnergyAfricaFinanceGuide%282015Edition%29.pdf.

[5] T. M. Weis and A. Ilinca, "Assessing the potential for a wind power incentive for remote villages in Canada," *Energy Policy*, vol. 38, no. 10, pp. 5504 – 5511, 2010.

[6] T. M. Weis, A. Ilinca, and J.-P. Pinard, "Stakeholders perspectives on barriers to remote wind-diesel power plants in Canada," *Energy Policy*, vol. 36, no. 5, pp. 1611 – 1621, 2008.

[7] "Enabling a clean energy future for Canada's remote communities," tech. rep., Advanced Energy Centre at MaRS Discovery District, December 2015. Available: http://www.marsdd.com/wp-content/uploads/2014/11/Clean-Energy-Future-for-Canada%E2%80%99s-Remote-Communities-.pdf.

[8] J. P. Lopes, N. Hatziargyriou, J. Mutale, P. Djapic, and N. Jenkins, "Integrating distributed generation into electric power systems: A review of drivers, challenges and opportunities," *Electric Power Systems Research*, vol. 77, no. 9, pp. 1189 – 1203, 2007.

[9] E. Koutroulis, D. Kolokotsa, A. Potirakis, and K. Kalaitzakis, "Methodology for optimal sizing of stand-alone photovoltaic/wind-generator systems using genetic algorithms," *Solar Energy*, vol. 80, no. 9, pp. 1072 – 1088, 2006.

[10] K. Sopian, A. Zaharim, Y. Ali, Z. M. Nopiah, J. A. Razak, and N. S. Muhammad, "Optimal operational strategy for hybrid renewable energy system using Genetic Algorithms," *WSEAS Trans. Math.*, vol. 7, pp. 130–140, Apr. 2008.

[11] H. Yang, L. Lu, and W. Zhou, "A novel optimization sizing model for hybrid solar-wind power generation system," *Solar Energy*, vol. 81, no. 1, pp. 76 – 84, 2007.

[12] H. Yang, W. Zhou, L. Lu, and Z. Fang, "Optimal sizing method for stand-alone hybrid solarwind system with LPSP technology by using genetic algorithm," *Solar Energy*, vol. 82, no. 4, pp. 354 – 367, 2008.

[13] H. Yang, Z. Wei, and L. Chengzhi, "Optimal design and techno-economic analysis of a hybrid solarwind power generation system," *Applied Energy*, vol. 86, no. 2, pp. 163 – 169, 2009.

[14] Y. A. Katsigiannis, P. S. Georgilakis, and E. S. Karapidakis, "Hybrid simulated annealing; tabu search method for optimal sizing of autonomous power systems with renewables," *IEEE Transactions on Sustainable Energy*, vol. 3, pp. 330–338, July 2012.

[15] F. Katiraei and C. Abbey, "Diesel plant sizing and performance analysis of a remote wind-diesel microgrid," in *2007 IEEE Power Engineering Society General Meeting*, pp. 1–8, June 2007.

[16] J. Whitefoot, A. Mechtenberg, D. Peters, and P. Papalambros, "Optimal component sizing and forward-looking dispatch of an electrical microgrid for energy storage planning," (Washington, DC, USA), ASME 2011 International Design Engineering Technical Conferences and Computers and Information in Engineering Conference, August 2011.

[17] T. Ersal, C. Ahn, D. L. Peters, J. W. Whitefoot, A. R. Mechtenberg, I. A. Hiskens, H. Peng, A. G. Stefanopoulou, P. Y. Papalambros, and J. L. Stein, "Coupling between

component sizing and regulation capability in microgrids," *IEEE Transactions on Smart Grid*, vol. 4, pp. 1576–1585, September 2013.

[18] J. Xiao, L. Bai, F. Li, H. Liang, and C. Wang, "Sizing of energy storage and diesel generators in an isolated microgrid using Discrete Fourier Transform (DFT)," *IEEE Transactions on Sustainable Energy*, vol. 5, pp. 907–916, July 2014.

[19] M. Arriaga, *Long-term Renewable Energy Generation Planning for Off-grid Remote Communities*. PhD thesis, University of Waterloo, Department of Electrical and Computer Engineering, Waterloo, Ontario, Canada, 2015.

[20] Z. Wang, Y. Chen, S. Mei, S. Huang, and Y. Xu, "Optimal expansion planning of isolated microgrid with renewable energy resources and controllable loads," *IET Renewable Power Generation*, vol. 11, no. 7, pp. 931–940, 2017.

[21] L. Guo, W. Liu, B. Jiao, B. Hong, and C. Wang, "Multi-objective stochastic optimal planning method for stand-alone microgrid system," *IET Generation, Transmission Distribution*, vol. 8, no. 7, pp. 1263–1273, 2014.

[22] B. Zhao, X. Zhang, P. Li, K. Wang, M. Xue, and C. Wang, "Optimal sizing, operating strategy and operational experience of a stand-alone microgrid on Dongfushan Island," *Applied Energy*, vol. 113, pp. 1656 – 1666, 2014.

[23] J. L. Bernal-Agustin, R. Dufo-Lopez, and D. M. Rivas-Ascaso, "Design of isolated hybrid systems minimizing costs and pollutant emissions," *Renewable Energy*, vol. 31, no. 14, pp. 2227 – 2244, 2006.

[24] J. L. Bernal-Agustin and R. Dufo-Lopez, "Multi-objective design and control of hybrid systems minimizing costs and unmet load," *Electric Power Systems Research*, vol. 79, no. 1, pp. 170 – 180, 2009.

[25] J. L. Bernal-Agustin and R. Dufo-Lopez, "Efficient design of hybrid renewable energy systems using Evolutionary Algorithms," *Energy Conversion and Management*, vol. 50, no. 3, pp. 479 – 489, 2009.

[26] Y. Ma, J. Ji, and X. Tang, "Triple-objective optimal sizing based on dynamic strategy for an islanded hybrid energy microgrid," *International Journal of Green Energy*, vol. 14, no. 3, pp. 310–316, 2017.

[27] G. Tina, S. Gagliano, and S. Raiti, "Hybrid solar/wind power system probabilistic modelling for long-term performance assessment," *Solar Energy*, vol. 80, no. 5, pp. 578 – 588, 2006.

[28] A. D. Hawkes, "Optimal selection of generators for a microgrid under uncertainty," in *IEEE PES General Meeting*, pp. 1–8, July 2010.

[29] A. Hawkes and M. Leach, "Modelling high level system design and unit commitment for a microgrid," *Applied Energy*, vol. 86, no. 7, pp. 1253 – 1265, 2009.

[30] A. Khodaei, S. Bahramirad, and M. Shahidehpour, "Microgrid planning under uncertainty," *IEEE Transactions on Power Systems*, vol. 30, pp. 2417–2425, September 2015.

[31] A. Narayan and K. Ponnambalam, "Risk-averse stochastic programming approach for microgrid planning under uncertainty," *Renewable Energy*, vol. 101, pp. 399 – 408, 2017.

[32] R. L. Dohn, "White paper: The business case for microgrids," tech. rep., Siemens, January 2011. Available: https://w3.usa.siemens.com/smartgrid/us/en/microgrid/Documents/The%20business%20case%20for%20microgrids_Siemens%20white%20paper.pdf.

[33] B. Lasseter, "Microgrids [distributed power generation]," in *2001 IEEE Power Engineering Society Winter Meeting. Conference Proceedings (Cat. No.01CH37194)*, vol. 1, pp. 146–149 vol.1, Jan 2001.

[34] M. F. Akorede, H. Hizam, and E. Pouresmaeil, "Distributed energy resources and benefits to the environment," *Renewable and Sustainable Energy Reviews*, vol. 14, pp. 724 – 734, February 2010.

[35] W. Poore, T. Stovall, B. Kirby, D. Rizy, J. Kueck, and J. Stovall, "Connecting distributed energy resources to the grid: Their benefits to the DER owner/customer, other customers, the utility, and society," tech. rep., Oak Ridge National Laboratory, March 2002. Available: https://info.ornl.gov/sites/publications/Files/Pub57447.pdf.

[36] M. H. Albadi and E. F. El-Saadany, "Demand response in electricity markets: An overview," in *2007 IEEE Power Engineering Society General Meeting*, pp. 1–5, June 2007.

[37] A. Safdarian, M. Fotuhi-Firuzabad, and M. Lehtonen, "Benefits of demand response on operation of distribution networks: A case study," *IEEE Systems Journal*, vol. 10, pp. 189–197, March 2016.

[38] D. E. Olivares, A. Mehrizi-Sani, A. H. Etemadi, C. A. Canizares, R. Iravani, M. Kazerani, A. H. Hajimiragha, O. Gomis-Bellmunt, M. Saeedifard, R. Palma-Behnke, G. A. Jimenez-Estevez, and N. D. Hatziargyriou, "Trends in microgrid control," *IEEE Transactions on Smart Grid*, vol. 5, pp. 1905–1919, July 2014.

[39] H. Saadat, *Power System Analysis*. New York, USA: McGraw Hill, 1999. An optional note.

[40] J. Rocabert, A. Luna, F. Blaabjerg, and P. Rodriguez, "Control of power converters in AC microgrids," *IEEE Transactions on Power Electronics*, vol. 27, pp. 4734–4749, November 2012.

[41] B. J. Kirby, "Frequency regulation basics and trends." Available: http://www.consultkirby.com/files/TM2004-291_Frequency_Regulation_Basics_and_Trends.pdf, December 2004.

[42] C. L. DeMarco, C. A. Baone, Y. Han, and B. Lesieutre, "White paper: Primary and secondary control for high penetration renewables," tech. rep., PSERC Publication, May 2012.

[43] M. J. Hossain, H. R. Pota, M. A. Mahmud, and M. Aldeen, "Robust control for power sharing in microgrids with low-inertia wind and PV generators," *IEEE Transactions on Sustainable Energy*, vol. 6, pp. 1067–1077, July 2015.

[44] Y. Rebours and D. Kirschen, "What is spinning reserve?," tech. rep., The University of Manchester, September 2005. Available: https://www2.ee.washington.edu/research/real/Library/Reports/What_is_spinning_reserve.pdf.

[45] F. Daneshfar and H. Bevrani, "Load-frequency control: a GA-based multi-agent reinforcement learning," *IET Generation, Transmission Distribution*, vol. 4, pp. 13–26, January 2010.

[46] Y. Han, P. M. Young, A. Jain, and D. Zimmerle, "Robust control for microgrid frequency deviation reduction with attached storage system," *IEEE Transactions on Smart Grid*, vol. 6, pp. 557–565, March 2015.

[47] M. M. A. Abdelaziz, H. E. Farag, E. F. El-Saadany, and Y. A. R. I. Mohamed, "A novel and generalized three-phase power flow algorithm for islanded microgrids using a newton trust region method," *IEEE Transactions on Power Systems*, vol. 28, pp. 190–201, February 2013.

[48] S. S. Sharif and J. H. Taylor, "MINLP formulation of optimal reactive power flow," in *Proceedings of the 1997 American Control Conference (Cat. No.97CH36041)*, vol. 3, pp. 1974–1978 vol.3, June 1997.

[49] W. Zhang, F. Li, and L. M. Tolbert, "Review of reactive power planning: Objectives, constraints, and algorithms," *IEEE Transactions on Power Systems*, vol. 22, pp. 2177–2186, November 2007.

[50] K. Karanasios and P. Parker, "Recent developments in renewable energy in remote aboriginal communities, Ontario, Canada," *Papers in Canadian Economic Development (PCED)*, vol. 16, pp. 82–97, 2016.

[51] P. Boileau, "Study demonstrates significant socioeconomic benefits from the Wataynikaneyap power project." Available: http://wataypower.ca/node/210, June 2015.

[52] R. E. Rosenthal, *GAMS-A Users Guide*. GAMS Development Corporation, Washington, DC, USA, April 2017. Available: https://www.gams.com/latest/docs/userguides/GAMSUsersGuide.pdf.

[53] GAMS Development Corporation, Washington, DC, USA, *GAMS-The Solver Manuals*, April 2017. Available: https://www.gams.com/latest/docs/solvers/allsolvers.pdf.

[54] N. Izadyar, H. C. Ong, W. Chong, and K. Leong, "Resource assessment of the renewable energy potential for a remote area: A review," *Renewable and Sustainable Energy Reviews*, vol. 62, pp. 908 – 923, 2016.

[55] H. Alharbi and K. Bhattacharya, "Optimal sizing of battery energy storage systems for microgrids," in *2014 IEEE Electrical Power and Energy Conference*, pp. 275–280, November 2014.

[56] T. Xu and P. Taylor, "Voltage control techniques for electrical distribution networks including distributed generation," *IFAC Proceedings Volumes*, vol. 41, no. 2, pp. 11967 – 11971, 2008.

[57] R. Tonkoski, L. A. C. Lopes, and T. H. M. El-Fouly, "Coordinated active power curtailment of grid connected PV inverters for overvoltage prevention," *IEEE Transactions on Sustainable Energy*, vol. 2, pp. 139–147, April 2011.

[58] Information available at: http://bergey.com/products/wind-turbines/10kw-bergey-excel.

[59] Information available at: http://www.wenvortechnologies.com/.

[60] M. Arriaga, C. A. Canizares, and M. Kazerani, "Renewable energy alternatives for remote communities in northern Ontario, Canada," *IEEE Transactions on Sustainable Energy*, vol. 4, pp. 661–670, July 2013.

[61] M. K. Diabo, K. Karanasios, M. Arriaga, and D. Fyfe, "Renewable energy: Current energy status in KLFN, technologies, challenges and project development." Available: http://www.nofnec.ca/PDF/2014/Renewable-Energy-UofWaterloo.pdf, September 2014.

[62] B. Xu, Y. Dvorkin, D. S. Kirschen, C. A. Silva-Monroy, and J. P. Watson, "A comparison of policies on the participation of storage in U.S. frequency regulation markets," in *2016 IEEE Power and Energy Society General Meeting (PESGM)*, pp. 1–5, July 2016.

[63] Hydro One networks Inc., "Distributed generation technical interconnection requirements, interconnections at voltages 50 kV and below," tech. rep., March 2013. Available: https://www.hydroone.com/businessservices_/generators_/Documents/Distributed%20Generation%20Technical%20Interconnection%20Requirements.pdf.

[64] "The fallacy of cost per kvar." Available: https://nepsi.com/resource/Cost%20per%20kvar.pdf.

[65] A. Sode-Yome and N. Mithulananthan, "Comparison of shunt capacitor, SVC and STATCOM in static voltage stability margin enhancement," *International Journal of Electrical Engineering Education*, vol. 41, pp. 158 – 171, October 2012.

[66] J. Machowski, J. Bialek, and J. Bumby, *Power System Dynamics: Stability and Control*. Wiley, 2011.

[67] A. Chakraborty, S. K. Musunuri, A. K. Srivastava, and A. K. Kondabathini, "Integrating STATCOM and battery energy storage system for power system transient stability: A review and application," *Advances in Power Electronics*, vol. 2012, 2012.

[68] "Health & environmental impacts from lead battery manufacturing & recycling in China," tech. rep., Occupational Knowledge International Global Village of Beijing, Institute of Public & Environmental Affairs, August 2012. Available: http://www.okinternational.org/docs/China%20Lead%20Battery%20Report%20IPE%20English%20Revised.pdf.

[69] A. Abele, E. Elkind, J. Intrator, B. Washom, and et al (University of California, Berkeley School of Law; University of California, Los Angeles; and University of California, San Diego), "2020 strategic analysis of energy storage in California," tech. rep., California Energy Commission, 2011.

[70] M. Beaudin, H. Zareipour, A. Schellenberglabe, and W. Rosehart, "Energy storage for mitigating the variability of renewable electricity sources: An updated review," *Energy for Sustainable Development*, vol. 14, no. 4, pp. 302 – 314, 2010.

[71] G. Albright, J. Edie, and S. Al-Hallaj, "A comparison of lead acid to lithium-ion in stationary storage applications," *Published by AllCell Technologies LLC*, 2012.

[72] J. S. Neubauer, A. Pesaran, B. Williams, M. Ferry, and J. Eyer, "A techno-economic analysis of PEV battery second use: repurposed-battery selling price and commercial and industrial end-user value," tech. rep., SAE Technical Paper, 2012.

[73] "Saft delivers innovative cold weather energy storage system in arctic alaska." Available: http://www.saftbatteries.com/press/press-releases/saft-delivers-innovative-cold-weather-energy-storage-system-arctic-\alaska, November 2015.

[74] D. Mall, "Lithium ion battery energy storage for remote microgrids," 2015. Available: https://www.bullfrogpower.com/wp-content/uploads/2015/09/Day1-Part1-SAFT-09-16-2015.pdf.

[75] M. Uhrig, S. Koenig, M. R. Suriyah, and T. Leibfried, "Lithium-based vs. vanadium redox flow batteries- a comparison for home storage systems," *Energy Procedia*, vol. 99, pp. 35–43, 2016.

[76] A. Tang and M. Skyllas-Kazacos, "Simulation analysis of regional temperature effects and battery management schedules for a residential-scale vanadium redox flow battery system," *ChemPlusChem*, vol. 80, pp. 368–375, 2015.

[77] C. Raimann, "Largest flow-battery island grid in Uganda." Available: http://www.ees-magazine.com/largest-flow-battery-island-grid-in-uganda/, 2016.

[78] "ESS Inc's all-iron flow battery to be deployed in microgrid demonstration for U.S. army corps of engineers." Available: http://www.essinc.com/2016/11/16/ess-inc-s-all-iron-flow-battery-to-be-deployed-in-microgrid\-demonstration-for-u-s-army-corps-of-engineers/, November 2016.

[79] H. Chen, T. N. Cong, W. Yang, Y. L. Ch.Tan, and Y. Ding, "Progress in electrical energy storage system: A critical review," *Progress in Natural Science*, vol. 3, pp. 291–312, March 2009.

[80] A. H. Hajimiragha and M. R. D. Zadeh, "Research and development of a microgrid control and monitoring system for the remote community of Bella Coola: Challenges, solutions, achievements and lessons learned," in *2013 IEEE International Conference on Smart Energy Grid Engineering (SEGE)*, (Oshawa, ON), pp. 1–6, 2013.

[81] J. F. Acevedo, "Communication system for the remote hybrid power system in Ramea Newfoundland," Master's thesis, Memorial University of Newfoundland, 2011.

[82] I. Hadjipaschalis, A. Poullikkas, and V. Efthimiou, "Overview of current and future energy storage technologies for electric power applications," *Renewable and Sustainable Energy Reviews*, vol. 13, no. 67, pp. 1513 – 1522, 2009.

[83] W. R. Galton, "Renewables in remote microgrids, stories of success, challenges and perseverance." Available: https://www.bullfrogpower.com/wp-content/uploads/2015/09/Day1-Stories-of-Success-Will-Galton-ABB-09-16-2015.pdf, 2015.

[84] M. A. Stosser and A. Bullwinkel, "Energy storage." Available: http://webcasts.acc.com/handouts/6.4.15-Ene-Webcast-Slides.pdf, 2015.

[85] P. Komarnicki, "Energy storage systems: power grid and energy market use cases," *Archives of Electrical Engineering*, vol. 65, no. 3, pp. 495–511, 2016.

[86] R. van Haaren, M. Morjaria, and V. Fthenakis, "An energy storage algorithm for ramp rate control of utility scale PV (photovoltaics) plants," *Energy*, vol. 91, pp. 894 – 902, 2015.

[87] R. vor dem Esche and R. Tudi, "Benefits of hybrid storage system with flywheels," tech. rep., August 2016. Available: https://www.researchgate.net/publication/309133959_Benefits_of_Hybrid_Storage_System_with_Flywheels.

[88] E. Thorbergsson, V. Knap, M. Swierczynski, D. Stroe, and R. Teodorescu, "Primary frequency regulation with li-ion battery based energy storage system - evaluation and comparison of different control strategies," in *Intelec 2013; 35th International Telecommunications Energy Conference, Smart Power and efficiency*, pp. 1–6, October 2013.

[89] J. Clavier, F. Bouffard, D. Rimorov, and G. Jos, "Generation dispatch techniques for remote communities with flexible demand," *IEEE Transactions on Sustainable Energy*, vol. 6, pp. 720–728, July 2015.

[90] S. M. Hakimi and S. M. Moghaddas-Tafreshi, "Optimal planning of a smart microgrid including demand response and intermittent renewable energy resources," *IEEE Transactions on Smart Grid*, vol. 5, pp. 2889–2900, November 2014.

[91] M. Ahmadi, J. M. Rosenberger, W. J. Lee, and A. Kulvanitchaiyanunt, "Optimizing load control in a collaborative residential microgrid environment," *IEEE Transactions on Smart Grid*, vol. 6, pp. 1196–1207, May 2015.

[92] R. Atia and N. Yamada, "Sizing and analysis of renewable energy and battery systems in residential microgrids," *IEEE Transactions on Smart Grid*, vol. 7, pp. 1204–1213, May 2016.

[93] "2011 greenhouse gas inventory report and action plan." Available: https://www.csaregistries.ca/files/projects/prj_2803_77.pdf, August 2012.

[94] "Status of remote/off-grid communities in canada." Available: http://www.nrcan.gc.ca/energy/publications/sciences-technology/renewable/smart-grid/11916, 2011.

[95] M. Arriaga, C. A. Canizares, and M. Kazerani, "Northern lights: Access to electricity in canada's northern and remote communities," *IEEE Power and Energy Magazine*, vol. 12, pp. 50–59, July 2014.

[96] "Ontario partnering with first nations to address climate change." Available: https://news.ontario.ca/mirr/en/2016/03/ontario-partnering-with-first-nations-to-address-climate-change.html, March 2016.

[97] P. Boileau, "Study demonstrates significant socioeconomic benefits from the wataynikaneyap power project." Available: http://wataypower.ca/node/210, June 2015.

[98] N. Kleer, "Green energy act reforms: Opportunities for promoting aboriginal participation." Available: http://oktlaw.com/drive/uploads/2016/10/njkGreenEnergy.pdf, Nov. 2009.

[99] P. Boothe and F. A. Boudreault, "By the numbers: Canada's GHG emissions." Available: https://www.ivey.uwo.ca/cmsmedia/2112500/4462-ghg-emissions-report-v03f.pdf, 2016.

[100] R. Hunter and G. Elliot, *Wind-Diesel Systems: A Guide to the Technology and its Implementation*. Cambridge University Press, March 1994.

[101] "Approximate diesel fuel consumption chart." Available: http://www.dieselserviceandsupply.com/Diesel_Fuel_Consumption.aspx.

[102] D. Lovekin and B. Dronkers, "Power purchase policies for remote indigenous communities." Available: http://assets.wwf.ca/downloads/arctic_renewable_energy_summit_presentation_11___12___lovekin___dronkers.pdf, September 2016.

[103] E. Lantz, R. Wiser, and M. Hand, "The past and future cost of wind energy." Available: http://www.nrel.gov/docs/fy12osti/54526.pdf, May 2012.

[104] IRENA(2016), "The power to change: Solar and wind cost reduction potential to 2025." Available: http://www.irena.org/DocumentDownloads/Publications/IRENA_Power_to_Change_2016.pdf, May 2016.

[105] K. Ardani, E. O'Shaughnessy, R. Fu, C. McClurg, J. Huneycutt, and R. Margolis, "Installed cost benchmarks and deployment barriers for residential solar photovoltaics with energy storage: Q1 2016," tech. rep., February 2017. Available: http://www.nrel.gov/docs/fy17osti/67474.pdf.